

Copyright  
by  
Aarti Dinesh Punase  
2012

**The Thesis Committee for Aarti Dinesh Punase  
Certifies that this is the approved version of the following thesis:**

**Assessing the effect of reservoir heterogeneity on CO<sub>2</sub> plume migration  
using pressure transient analysis**

**APPROVED BY  
SUPERVISING COMMITTEE:**

**Supervisor:**

---

Sanjay Srinivasan

---

Steven L. Bryant

**Assessing the effect of reservoir heterogeneity on CO<sub>2</sub> plume migration  
using pressure transient analysis**

**by**

**Aarti Dinesh Punase, B.E**

**Thesis**

Presented to the Faculty of the Graduate School of

The University of Texas at Austin

in Partial Fulfillment

of the Requirements

for the Degree of

**Master of Science in Engineering**

**The University of Texas at Austin**

**December 2012**

## **Dedication**

To my parents, brother, family, teachers and friends

## **Acknowledgements**

Foremost, I would like to express my sincere gratitude to my supervisor Dr. Sanjay Srinivasan for the continuous support of my Masters research, for his patience, motivation, enthusiasm, and immense knowledge. His guidance helped me in all the time of research and writing of this thesis. I thank him for the systematic guidance and great effort he put into training me in this field. I could not have imagined having a better advisor and mentor for my research study.

Besides my supervisor, I would also like to express my gratitude to Dr. Steven Bryant for his insightful comments, and hard questions.

I would also like to express my gratitude to Jin Lee for all her help over the duration of this report. Special thanks are also due to Roger Terzian and Joanna Castillo, for their help in matters related to all the software that has been used in my research.

To my fellow graduate research assistants, Selin Erzeybek , Harpreet Singh, Kwangjin Lee, Sayantan Bhowmik, Brandon Henke, Dhananjay Kumar, Young Kim, Hoonyoung Jeong, Nnamdi Azom, Travis Hampton and Hapiz Zulkipli for their loyal friendship, valuable inputs and constant support and encouragement during my study at the University of Texas at Austin.

Finally I would like to give my deep appreciation to the many friends who provided so much support and encouragement throughout my research. In particular I would like to thank Gunja Pandav, Shilpi Goel, Shalini Sahoo, Priya Trg, Saurajit Mukerjee, Bhushan Bhutada, Krupa Kannan and Nikhil Peshave.

Finally, I take this opportunity to express the profound gratitude from my deep heart to my beloved parents, grandparents, and my siblings for their love and continuous support.

## **Abstract**

# **Assessing the effect of reservoir heterogeneity on CO<sub>2</sub> migration using pressure transient analysis**

Aarti Dinesh Punase, M.S.E

The University of Texas at Austin, 2012

Supervisor: Sanjay Srinivasan

The ultimate success of carbon capture and storage project will be ensured only when there is a safe and effective permanent storage of CO<sub>2</sub> for a significant amount of time without any leakages. Credible monitoring and verification is one of the most important aspects of CO<sub>2</sub> sequestration. Accurate reservoir characterization is an important pre-requisite for the design, operation and economic success of processes like CO<sub>2</sub> sequestration. The techniques available include geophysical and geochemical monitoring as well as numerical simulations using models replicating the field. In conducting the numerical simulations, it is required to assess the reservoir heterogeneity correctly.

Previous work has shown that the injection data from wells can be utilized for developing models during CO<sub>2</sub> sequestration to understand the spatial distribution of heterogeneities in the formation. In this research, we first understand and examine the information contained in the injection data for a wide range of reservoir models demonstrating different kinds of heterogeneities and rate fluctuations. We will confirm that the reservoir heterogeneities have an imprint on the injection pressure response and they influence CO<sub>2</sub> plume migration significantly. Later we show that the effect of high or low permeability features along with rate fluctuations

can provide considerable information about permeability heterogeneity in the reservoir. The applicability of this observation is made using field data from In-Salah gas field from central Algeria. Thus we demonstrate the feasibility of developing an inexpensive method of modeling reservoir heterogeneity by employing readily available measurements of injection pressure and rate to track CO<sub>2</sub> migration.

Later we describe method to find out what characteristics of the reservoir heterogeneities can be quantified using injection data (pressure and rate). The injection pressure response during CO<sub>2</sub> sequestration will depend strongly on reservoir, fluid and well properties. A 3-D analytical model with infinite acting boundary is developed in CMG-GEM. Compositional reservoir simulation results from CMG-GEM simulator will be obtained and combined with pressure transient analysis and optimization algorithm for the prediction of reservoir parameters. In case of multiple injection wells in a heterogeneous formation, the analysis yield spatial variations in reservoir parameter groups like transmissibility (kh), permeability to porosity ratio (k/φ) in different part of the reservoir. These parameter groups can subsequently be used to constrain models of reservoir thickness, permeability and porosity. Thus, we imply that multiple reservoir attributes affect migration of CO<sub>2</sub> plume and there is uncertainty associated with the estimation of these attributes. We present an approach to resolve some of that uncertainty using information extracted from injection well response.

## **Table of Contents**

<b>CHAPTER 1 : INTRODUCTION .....</b>	<b>1</b>
1.1 Carbon Capture and Geological Storage: .....	2
1.1.1 What is Geological CO <sub>2</sub> Sequestration?.....	2
1.2 CO <sub>2</sub> Plume migration and monitoring techniques: .....	3
1.3 Research Objectives:.....	4
1.4 Thesis Overview: .....	6
<b>CHAPTER 2: LITERATURE REVIEW.....</b>	<b>7</b>
2.1 Geological CO <sub>2</sub> Storage.....	7
2.2 Trapping Mechanism: .....	10
2.3 CO <sub>2</sub> Phase behavior and Properties .....	12
2.4 CO <sub>2</sub> Monitoring Techniques:.....	13
2.5 Numerical Simulation of CO <sub>2</sub> Sequestration .....	15
2.6 Pressure transient analysis: .....	16
2.7 Pressure transient analysis techniques: .....	18
2.8 Assessment of reservoir heterogeneity through well test analysis: .....	25
2.9 Computer algorithms for pressure transient analysis:.....	26
2.10 Interpretation of well test: .....	27
2.11 Summary:.....	28
<b>CHAPTER 3: ASSESSING THE EFFECT OF RESERVOIR HETEROGENEITY ON CO<sub>2</sub> PLUME MIGRATION .....</b>	<b>30</b>
3.1 Chapter Objective: .....	30
3.2 In- Salah Gas Field description:.....	30
3.3 Krechba Field Geology:.....	35
3.4 Monitoring Techniques:.....	37



3.5 Field Case Study .....	42
3.5.1 Model description: .....	42
3.5.2 Sensitivity Cases .....	50
3.5.2.1 Permeability Sensitivity .....	50
3.5.3 Injection rate Sensitivity .....	55
3.6 Result and analysis:.....	57
3.7 Conclusion: .....	64
<b>CHAPTER 4: ASSESSMENT OF RESERVOIR PARAMETERS USING INJECTION DATA</b>	<b>65</b>
4.1 Chapter Objective: .....	65
4.2 Motivation and Method.....	66
4.3 Dekker Brent Algorithm: .....	68
4.3.1 Iteration method: .....	69
4.4 Objective Function:.....	70
4.5 Model of homogenous reservoir: .....	74
4.6 Results and validation of code: .....	78
4.6.1 Single Well Tests: .....	78
4.6.1.1 Case I: Homogenous isotropic single well reservoir with constant injection: .....	78
4.6.1.2 Case II: Homogenous isotropic single well reservoir with two rate injection: .....	82
4.6.1.3 Case III: Homogenous isotropic single well reservoir with multi-rate injection: .....	85
4.6.2 Multiple well tests:.....	88
4.6.2.1 Case IV: Homogenous isotropic multiple well reservoir with constant rate injection: .....	88
4.6.2.2 Case V: Homogenous isotropic multiple well reservoir with multiple rate injection: .....	94

4.7 Conclusion:	98
<b>CHAPTER 5: UNCERTAINTY ANALYSIS OF RESERVOIR HETEROGENEITY USING INJECTION DATA</b>	<b>100</b>
5.1 Chapter Objective:	100
5.2 Introduction:	100
5.3 Method:	101
5.4 Model Validation using optimization algorithm	103
5.5 Reservoir simulation model	103
5.5.1 Permeability Sensitivity cases:	104
5.5.1.1 Case A: Heterogeneous permeability region around the injection well	105
5.5.1.2 Case B: Presence of high permeability streaks with constant background permeability	105
5.5.1.3 Case C: Presence of high permeability streaks with varying background permeability	106
5.5.2 Injection Rate Sensitivity:	107
5.6 Results and discussion:	109
5.6.1 Single well cases:	109
5.6.1.1 Case I: Single well with heterogeneous block at the centre and multiple rate injection	109
5.6.1.2 Case II: Single well with high permeability streak and constant background	113
5.6.1.3 Case III: Single well with high permeability streak and varying background	115
5.6.2 Multiple Well Tests:	117
5.6.2.1 Case IV: Multiple wells with heterogeneous block and multiple rate injection	118
5.6.2.2 Case V: Multiple wells in a heterogeneous field injecting at multiple rate	121

5.7 Conclusion: .....	124
<b>CHAPTER 6: CONCLUSION AND RECOMMENDATIONS .....</b>	<b>125</b>
6.1 Summary and Conclusions .....	125
6.2 Recommendations:.....	127
<b>APPENDIX .....</b>	<b>129</b>
<b>BIBLIOGRAPHY .....</b>	<b>133</b>

## List of Figures

Figure 1. 1: Increasing trend in the amount of CO <sub>2</sub> emitted over the last two decades .....	2
Figure 2. 1: Overview of CO <sub>2</sub> sequestration project .....	8
Figure 2. 2: Overview of geological CO <sub>2</sub> storage .....	9
Figure 2. 3: Time scale representing geological storage process.....	11
Figure 2. 4: Carbon dioxide pressure-temperature phase diagram .....	13
Figure 2. 5: Pressure build-up rate schedule and pressure response.....	20
Figure 2. 6: Injection test rate schedule and pressure response .....	22
Figure 2. 7: Type curve analysis .....	24
Figure 3. 1: Schematic of CO <sub>2</sub> storage at the Krechba field .....	31
Figure 3. 2: Location of In Salah gas project.....	32
Figure 3. 3: CO <sub>2</sub> injection and monitoring in the Krechba field .....	33
Figure 3. 4: Porosity distribution of Krechba field and the location of wells. ....	34
Figure 3. 5: Krechba stratigraphic structure .....	36
Figure 3. 6: Satellite image of the Krechba field .....	38
Figure 3. 7: Location of Krechba injectors and producers.....	39
Figure 3. 8: Two step process of generating permeability distribution .....	43
Figure 3.9: Permeability distribution of Krechba field.....	44
Figure 3. 10: Porosity distribution map of In Salah field. ....	46
Figure 3. 11: CMG-GEM model showing porosity distribution.....	47
Figure 3. 12: CMG-GEM model showing grid top.....	48
Figure 3. 13: Combined injection rate schedule .....	49
Figure 3. 14: Map showing permeability distribution of the base case .....	51

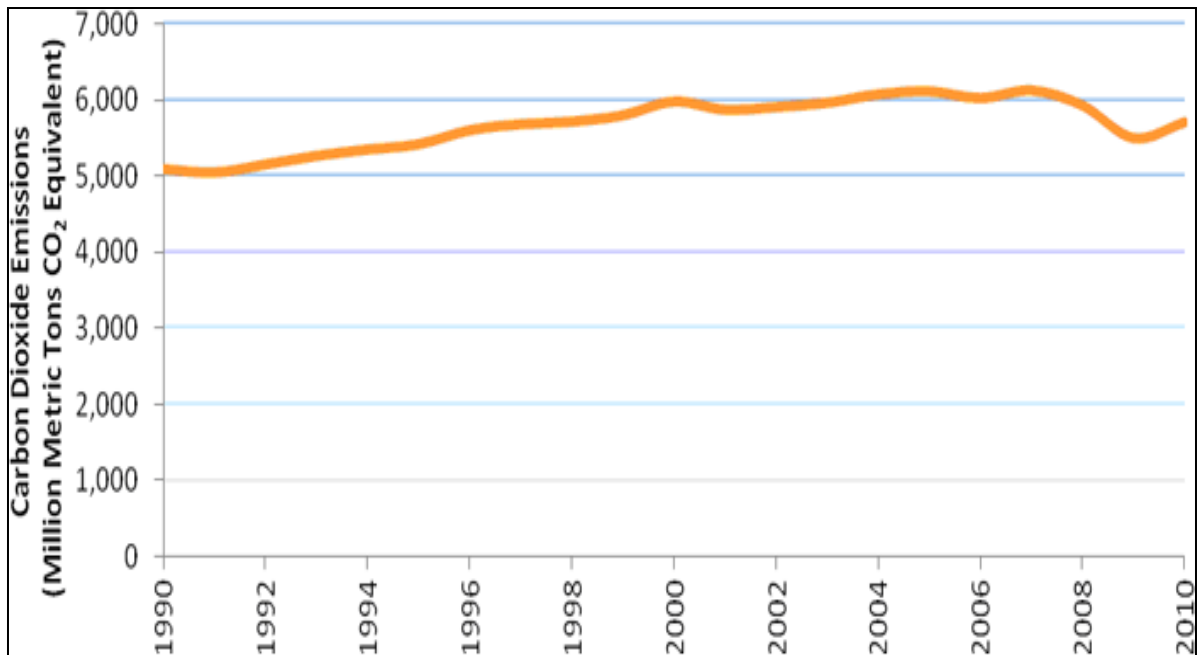
Figure 3.15: Pressure profile for base injection rate at KB-501 .....	51
Figure 3.16: Pressure profile for base injection rate at KB-502 .....	52
Figure 3.17: Pressure profile for base injection rate at KB-503.....	52
Figure 3. 18: Map showing permeability distribution corresponding to the high permeability case .....	53
Figure 3. 19: Map showing permeability distribution of the low permeability case .....	54
Figure 3. 20: Map showing permeability distribution for no streak case .....	55
Figure 3. 21: Injection rate schedule for double injection case .....	56
Figure 3. 22: Injection rate schedule for random injection case .....	57
Figure 3. 23: Pressure profiles for different permeability variations.....	59
Figure 3. 24: Gas saturation profile for 3 different permeability cases .....	60
Figure 3. 25: Pressure profile with 3 different permeability and injection variations .....	63
Figure 4. 1: Process of successive bracketing of a minimum.....	70
Figure 4. 1.1: Flowchart summarising minimization process.....	73
Figure 4. 2: Shows grid top view of the simulator model with single injection well .....	75
Figure 4.3: Permeability distribution map for homogeneous field.....	75
Figure 4.4: Porosity distribution map for homogeneous field.....	76
Figure 4. 5: Injection rate profile for constant rate injection for a single well case .....	78
Figure 4. 6: Generic workflow for estimating reservoir parameter .....	81
Figure 4. 7: Two rate injection profile for single well field.....	83
Figure 4. 8: Multiple rate injection profile for a single well in a homogeneous reservoir. ....	86
Figure 4. 9: Aerial view of grid top model for multiple well field .....	89
Figure 4. 10: Constant and similar injection rate profile at three wells .....	89
Figure 4.11: Gas viscosity map of field at the end of injection period.....	94

Figure 4. 12: Multiple rate injection profile at wells 1, 2 and 3 .....	95
Figure 5. 1: Shows CMG-GEM grid top view of the simulation model .....	103
Figure 5. 2: Permeability distribution of a single well in a heterogeneous block.....	104
Figure 5. 3: Permeability distribution for case with high perm streaks embedded within a constant background .....	105
Figure 5. 4: Map of permeability distribution for the case with high permeability streaks embedded within a heterogeneous background .....	106
Figure 5. 5: Injection profile for single well injection test .....	107
Figure 5. 6: Injection profile for multiple rate well test.....	108
Figure 5. 7: Permeability distribution map of the heterogeneous block .....	110
Figure 5.8: Gas viscosity map for heterogeneous block.....	110
Figure 5. 9: Gas viscosity map for single well with high perm streak and constant background .....	113
Figure 5. 10: Gas viscosity map for single well with high perm streak and varying background .....	116
Figure 5. 11: Permeability distribution of heterogeneous block.....	118
Figure 5. 12: Pressure spread and gas viscosity map for multiple well with heterogeneous block at the centre .....	119
Figure 5. 13: Pressure spread and gas viscosity map for fully heterogeneous field with two injection wells .....	122

## **CHAPTER 1 : INTRODUCTION**

Carbon dioxide is the primary greenhouse gas emitted in large amounts mostly through human activities. Global warming is mainly the result of CO<sub>2</sub> levels rising in the Earth's atmosphere.

Figure 1.1 describes the amount of carbon from anthropogenic CO<sub>2</sub> entering the atmosphere in USA alone. It has grown from 5000 million metric tons per year in 1990 to almost 6000 million metric tons per year in 2010. The increase is approximately 12% in the last two decades. According to EPA article on CO<sub>2</sub> emissions, increase in CO<sub>2</sub> emissions from fossil fuel combustion are influenced by various factors like population growth, economic growth, changing energy prices, new technologies, and seasonal temperatures. Between 1990 and 2010, the increase in CO<sub>2</sub> emissions corresponded with increased energy use by an expanding economy and population, although the economic downturn starting in 2008 influenced the decrease in emissions in 2009. Hence supervision and management of CO<sub>2</sub> becomes a very important issue because the rate at which it is being emitted into the atmosphere can cause huge changes in the climate.



Source: EPA- United States Environment Protection Agency, Inventory of U.S Greenhouse Gas Emission and Sinks (1990-2010)

Figure 1.1- Increasing trend in the amount of CO<sub>2</sub> emitted over the last two decades

## 1.1 Carbon Capture and Geological Storage:

Various studies have been made across the world in order to find an effective way to capture and store CO<sub>2</sub> safely and efficiently. Some of the forms of storage include gaseous storage in various deep geological formations (including saline formations and exhausted gas fields), mineral storage, ocean storage and solid storage by reaction of CO<sub>2</sub> with metal oxides to produce stable carbonates.

### 1.1.1 What is Geological CO<sub>2</sub> Sequestration?

Carbon sequestration means capturing carbon dioxide (CO<sub>2</sub>) from the atmosphere or capturing anthropogenic (human) CO<sub>2</sub> from large-scale sources like power plants and refineries before it is released to the atmosphere. Once captured, CO<sub>2</sub> gas is first compressed and then



transported to a suitable site for long-term storage. Carbon sequestration describes long-term storage of carbon dioxide and as a permanent method to moderate level of CO<sub>2</sub> in the atmosphere. CO<sub>2</sub> sequestration has the potential to significantly reduce the level/amount of carbon that occurs in the atmosphere. Geological sequestration is a process of injecting CO<sub>2</sub> into deep subsurface rock formations like abandoned oil and gas reservoirs or saline aquifers for permanent storage.

## **1.2 CO<sub>2</sub> Plume migration and monitoring techniques:**

What happens to CO<sub>2</sub> once it's injected into the storage reservoir?

In almost all the sequestration projects CO<sub>2</sub> is injected in supercritical state, making it lighter than the resident brine present. After injection, CO<sub>2</sub> will begin to rise up in the formation due to density difference. The flow is governed by buoyancy and it can either rise continuously up in the reservoir or encounter a seal that hinders the vertical movement and that in turn, induces lateral migration. The overall spread of CO<sub>2</sub> plume will depend on the flow channels present inside the formation.

Given the large quantities of anthropogenic CO<sub>2</sub> produced, the ultimate aim of any CO<sub>2</sub> sequestration project is to maximize the injection rate to offset the increased generation rate, assure that the sequestration is safe and there is no possibility of any leakage over the course of time. Many diverse and efficient monitoring techniques have been developed in order to predict correctly the migration of CO<sub>2</sub> and detect any leakages or abnormal migration paths at an early stage before CO<sub>2</sub> has reached the surface.

Some of the methods developed for monitoring and detecting CO<sub>2</sub> leakages/migration are:

- Seismic profiling
- Studying down-hole fluid movement
- Geophysical logs
- Down-hole pressure and temperature analysis
- Micro seismic monitoring
- Sampling for changes in water chemistry in observation wells

However most of the above methods are complex, not efficient in distinguishing minor leaks, sensitive and expensive in application. There is growing research focused on improving these techniques and developing innovative methods with more reliability in predictions.

### **1.3 Research Objectives:**

The success of CO<sub>2</sub> projects in deep abandoned reservoirs or saline aquifers will depend on developing accurate models for the spatial distribution of flow and transport attributes based on geological, engineering and geophysical data and the ability to effectively monitor and predict CO<sub>2</sub> plume migration in order to avoid situations of its leakage at the surface.

A lot of work has been done in developing models that utilize routinely measured injection pressure and injection rate during CO<sub>2</sub> sequestration to model the spatial distribution of heterogeneities in the formation.

One such approach is presented in Mantilla et al. (2009) in which it was demonstrated that dynamic measurement of injection rate and pressure in each well can be used to infer the presence the reservoir heterogeneities large enough to affect the overall plume migration. This idea was then applied in probabilistic history matching software: Pro-HMS (Srinivasan and

Bryant, 2004) to develop reservoir models constrained to both geological and injection data. Bhowmik et. al. (2010) describes an approach for reservoir model selection based on well injection data. This paper demonstrates that the model selection process yields a final set of most probable models used in order to derive a probabilistic estimate of current plume location and for forecasting subsequent migration of the CO<sub>2</sub> plume. The idea was implemented using data for the In Salah gas project.

One of the main objectives for the research presented in this thesis is to understand and examine the information contained in injection data for a range of reservoir models demonstrating different heterogeneities. Here I check how sensitive is the injection data and migration of CO<sub>2</sub> plume to the variability in the reservoir parameters.

Once it is confirmed that reservoir heterogeneities do have an imprint on the well responses, the next objective is to find out what characteristics of these reservoir heterogeneities can be resolved using injection data. The second half of this thesis deals with the method to analyze the well responses with pressure transient analysis in order to infer parameter groups such as transmissibility (kh) and ratio of porosity to permeability ( $\phi/k$ ). We initially infer these quantities for single well exhibiting injection rate fluctuations and later extend it to multiple injection wells. In the case of multiple injection wells, the analysis yields spatial variations in parameter groups in different parts of the reservoir. These parameter groups can subsequently be used to constrain spatial models for reservoir thickness, permeability and porosity. Thus, an important contribution of the thesis is to point out that multiple reservoir attributes (and not only permeability) affect the migration of the CO<sub>2</sub> plume and there is uncertainty associated with the estimation of these attributes. The thesis presents an approach to resolve some of that uncertainty using information extracted from injection well response.

## **1.4 Thesis Overview:**

In Chapter 2 a review of relevant literature investigating the impact of reservoir heterogeneity on CO<sub>2</sub> plume migration will be presented. In order to develop models of reservoir heterogeneity, first a static model is developed constrained to geologic data and then a dynamic model is prepared according to the production/injection data available at the wells. Parameters are history matched during dynamic modeling to match the injection data. A brief review of the various history matching techniques and optimization algorithm will be presented along with drawbacks related to each method.

Chapter 3 presents the details of a study performed for understanding the impact of reservoir heterogeneity on injection pressure measurements. A synthetic case mimicking the In Salah data is presented and local heterogeneities will be introduced in the model manually in order to study the impact on plume migration. A dynamic model is developed in CMG-GEM for modeling the process of CO<sub>2</sub> flow and transport. An analysis of the well bottom-hole pressure profile and gas saturation distribution will be used in order to quantify the presence of reservoir heterogeneity. The key results are summarized in appropriate plots.

Chapter 4 documents the approach for resolving reservoir heterogeneities using injection data. The approach is based on the application of injection well test analysis principles in order to history match the injection data. This chapter explains an optimization algorithm developed to make estimation of reservoir parameters using measurements from the injection well. The algorithm utilizes linear superposition analysis in order to analyze the injection data corresponding to multiple wells exhibiting rate fluctuations. In Chapter 5, the algorithm of history matching injection data is tested on a range of different realistic cases displaying variety of heterogeneities in order to predict estimates values of individual parameters as well as their combinations.

This thesis ends with Chapter 6 discussing the main conclusions and future work.

## **CHAPTER 2: LITERATURE REVIEW**

### **2.1 Geological CO<sub>2</sub> Storage**

The prospect of global warming and increasing level of CO<sub>2</sub> in the atmosphere is a subject of serious concern among researchers, scientist and world leaders. CO<sub>2</sub> concentration in the atmosphere has drastically increased from 280ppm to its current level of 380ppm (Bryant et al, 1997) in the last few decades. It's been widely accepted that human activities plays a major role in contributing towards this increase. The greatest contributor to global warming over the past half century has been the high consumption and combustion of fossil fuels.

One of the techniques proposed by scientists and industry in order to reduce the amount of CO<sub>2</sub> in the atmosphere is geological storage of CO<sub>2</sub> in deep formations. Geological storage of CO<sub>2</sub> has been considered an effective option since it was first proposed in 1990's and has been implemented successfully in many parts of the world since the first large scale project in Norway. In the last decade, a lot of pilot and commercial scale geologic CO<sub>2</sub> sequestration projects have been planned and implemented.

Geological storage of CO<sub>2</sub> can be defined as the method of separating CO<sub>2</sub> from the waste streams of hydrocarbon consuming industrial units (such as power plants), compressing it and then transporting it to a suitable storage sites where it will be injected into deep underground geological formations. The distance between the field and the storage site is an important factor to be considered as it can have significant influence on the economics of the overall sequestration project.

Geological sequestration was first discussed in the 1970s (Baes et al 1980). Geological formations considered for injecting CO<sub>2</sub> include deep saline aquifers, abandoned oil and gas reservoirs and coal seams although other candidates such as basaltic formations have also been proposed by researchers. An estimate of over 35million tones of CO<sub>2</sub> have been injected into the oil reservoirs for the purpose of Enhanced Oil Recovery (EOR) and few more projects are

underway (Ghomian et al, 2008). Figure 2.1 shows an overview of a typical CO<sub>2</sub> sequestration project.

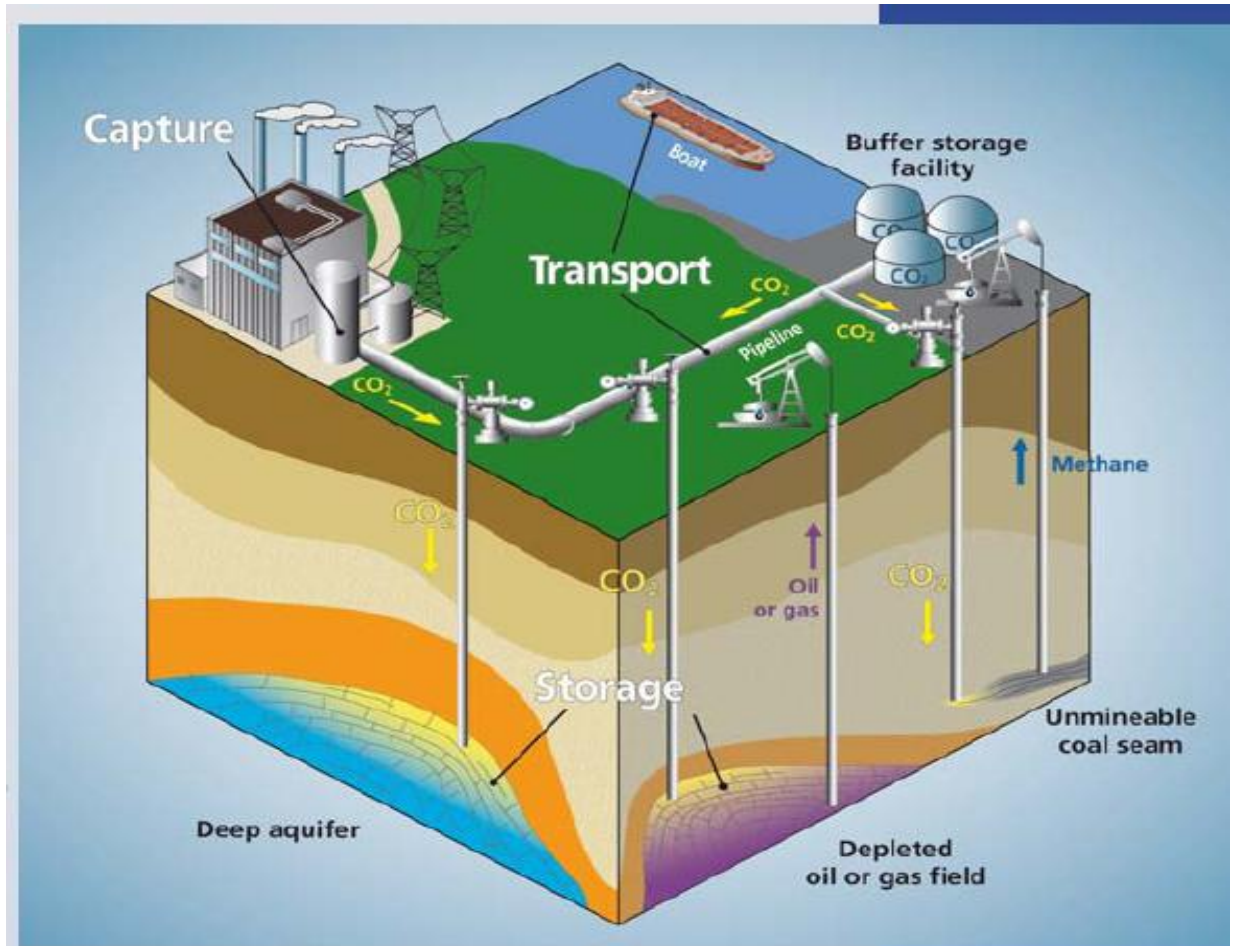


Figure 2.1: Overview of CO<sub>2</sub> sequestration project (BRGM Image, CO<sub>2</sub> GEONet European network of excellence)

Suitable storage sites have to be chosen in order to successfully store CO<sub>2</sub> for a significant period of time. Reservoir properties of depleted natural gas and oil reservoirs are very well known due to hydrocarbon production and therefore the first choice for CO<sub>2</sub> sequestration. Deep saline aquifers offer a larger storage potential but the properties are not very well known.

For successful storage of CO<sub>2</sub>, the host formation should have good porosity, permeability, high storage capacity and even more importantly an effective non-permeable seal

to contain any vertical migration of the injected CO<sub>2</sub>. The presence of this overlying impervious seal ensures that the migrating CO<sub>2</sub> doesn't reach the surface of the earth. Another desired criterion for successful storage is the depth of the formation. The CO<sub>2</sub> is injected under pressure in the host rock as a supercritical fluid. Therefore the depth of formation should be deeper than 800m, where pressure and temperature are high enough to maintain the CO<sub>2</sub> in the supercritical state (Source: Benson et al,2004 ). Figure 2.2 shows overview of geological storage of CO<sub>2</sub>.

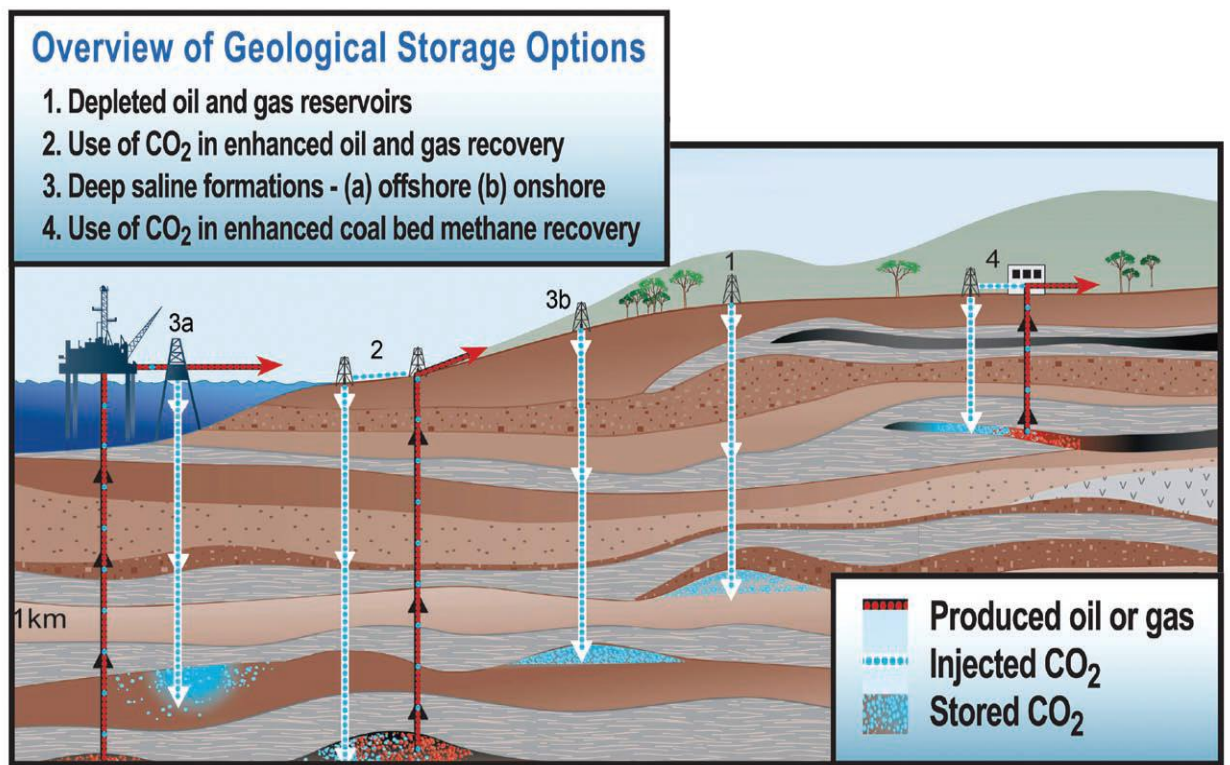


Figure 2.2: Overview of geological CO<sub>2</sub> storage (Source: Benson et al, 2004)

## 2.2 Trapping Mechanism:

Four main trapping mechanisms for CO<sub>2</sub> in a geological structure have been proposed:

- **Stratigraphic/Structural Trapping:** This is the most dominant type of trapping mechanisms that involves either a thick and effective seal that provides an effective barrier to mitigate upward migration or a severe contrast in flow properties of different types of rock that arrest the migration of the CO<sub>2</sub> plume (Sengul et al, 2006).
- **Capillary trapping:** It's a comparatively slow process that occurs mainly in saline formations. The injected CO<sub>2</sub> migrates upwards through the saline formation and dissolves in saline water after its lateral migration has been arrested by changes in stratigraphy. The trailing edge of CO<sub>2</sub> is immobilized by capillary forces, slowing up-dip migration. Studies by Hesse et al (2008) and Ide et al (2007) suggest that eventually all the CO<sub>2</sub> can be immobilized this way.
- **Mineral trapping:** In this process the dissolved CO<sub>2</sub> in a saline aquifer will react directly/indirectly with the minerals of the formation promoting precipitation of carbonate minerals. CO<sub>2</sub> will dissolve in water and decompose into H<sup>+</sup> and HCO<sub>3</sub><sup>-</sup> ions. The weak carbonic acid will in turn react with the reservoir minerals. Mineral trapping is attractive because it could immobilize CO<sub>2</sub> for very period of time (Gunter et al, 1997).
- **Solubility trapping:** The dissolution of CO<sub>2</sub> into water can lead to trapping by solubility. Although the amount of CO<sub>2</sub> that can dissolve into water depends on pressure, temperature and salinity of brine. The principle benefit of solubility trapping is that once the CO<sub>2</sub> is dissolved, there is less CO<sub>2</sub> subject to the buoyant force that drives it upwards. Many experiments show that dissolution of CO<sub>2</sub> is rapid at high pressure when water and CO<sub>2</sub> share the same pore space (Czernichowski-Lauriol et al, 1996).



Figure 2.3 shows the efficiency of different trapping mechanisms with time.

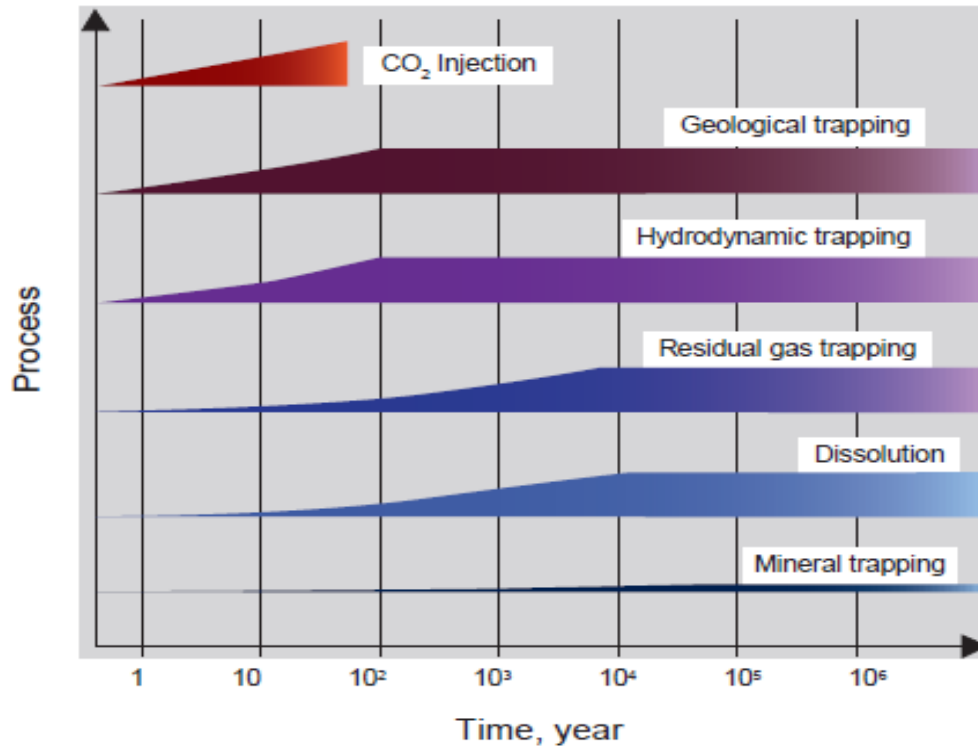


Figure 2.3: Time scale representing geological storage process (Liner et al,2011)

The recent estimate of the storage capacity described in Jasinge et al (2011) states that the estimates are highest for saline aquifers as compare to other options.

Reservoir Type	Lower estimate of storage capacity	Upper estimate of storage capacity
Saline formations	1000	~10000
Oil and gas fields	675	900
Deep coal seams	3-15	200

Table 1: Storage capacity for several geological storage options (IPCC 2005)

The total amount of CO<sub>2</sub> stored and trapped with the above mechanisms will depend on the CO<sub>2</sub> injection rate, total duration of injection and location of the host formation.

### **2.3 CO<sub>2</sub> Phase behavior and Properties**

The supercritical point of CO<sub>2</sub> is 31.1 °C and 72.8 atm. Below the critical point, CO<sub>2</sub> takes the form either of a gas or a liquid depending on the pressure and temperature while at supercritical state CO<sub>2</sub> has liquid like density. It is always advantageous to store CO<sub>2</sub> in supercritical state at deeper depths because that enables the storage of large volume of CO<sub>2</sub> and it is less prone to unwanted migration as would be the case with the gaseous phase. The density of CO<sub>2</sub> varies with temperature and pressure. If we assume the geothermal gradient to be 25°C/ Km and hydrostatic pressure gradient of 0.433psi/ft, we are assured to have supercritical conditions for CO<sub>2</sub> at depths below 800m. Generally the storage site chosen for CO<sub>2</sub> capture are deep (below 800-1000m), which keeps the injected CO<sub>2</sub> in the desired supercritical state. Supercritical CO<sub>2</sub> is 30-40% less dense than the typical formation water (Liner et al 2011). Buoyancy will drive the CO<sub>2</sub> upwards until it meets an impermeable cap rock. Phase behavior diagram of CO<sub>2</sub> is shown in Figure 2.4.

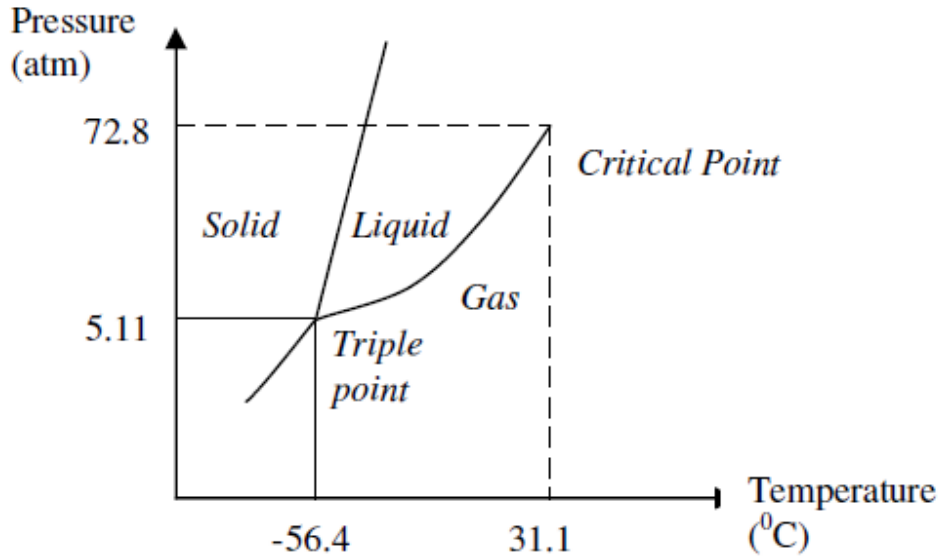


Figure 2.4: Carbon dioxide pressure-temperature phase diagram (Jasinge et al, 2011)

## 2.4 CO<sub>2</sub> Monitoring Techniques:

The ultimate success of a carbon capture and storage project will depend on whether there is safe and effective permanent storage for a significant amount of time without any leakages. Credible monitoring and verification is important to ensure that there are no leakages and to initiate remedial measures in case of unanticipated migration of CO<sub>2</sub>. After CO<sub>2</sub> is injected into the deep geological formations, it displaces the pore fluid. Depending on the rock and fluid properties, CO<sub>2</sub> will either mix with the resident fluid or remain separate in a single phase if it's immiscible. According to Liner et al (2011), under the conventional CO<sub>2</sub> injection procedure, 50% of CO<sub>2</sub> will be trapped either by geological trapping or hydrodynamic trapping. But the risk associated with free phase CO<sub>2</sub> is the highest as CO<sub>2</sub> is mobile and can escape to the atmosphere through a breach in the aquifer seal. Free phase CO<sub>2</sub> can also escape to the atmosphere through corroded well pipes in old and abandoned oil and gas reservoirs (Liner et al, 2011). Various techniques have been developed and combined to monitor the amount of free phase CO<sub>2</sub> after CO<sub>2</sub> injection.

Usually there are five monitoring requirements at the sequestration site; three of which include measurements of CO<sub>2</sub> related behavior and its effect on reservoir and well properties (Monitoring, verification, and accounting of CO<sub>2</sub> stored in deep saline aquifer, NETL). The fourth requirement deals with the measurement taken at the injection and monitoring well. The fifth is the measurement of the location and migration of CO<sub>2</sub> plume in the formation.

Techniques for monitoring plume migration in the subsurface formation are still in the developing stages. Complex geology and petrophysical characteristics of subsurface formations make it difficult to predict the plume behavior accurately. The sensitivity and resolution of current measurement techniques are not adequate for resolving reservoir heterogeneities that affect plume migration. Reservoir heterogeneities can significantly alter the migration path of the CO<sub>2</sub> plume.

The concept of four different categories of monitoring was introduced by Benson et al (2004). He categorized the monitoring activities into four phases, namely

1. **Pre-operation phase:** Here the overall design of project is carried out with selection of appropriate storage site, initial risk involved with geology of the site, overall storage capacity and extent of the formation. Monitoring tools for this phase determines wellhead and formation pressure, gas, groundwater and atmospheric CO<sub>2</sub> concentrations, core and sample analysis and the overall geology. Data is collected through well logs, rate testing and seismic survey.

2. **Operation phase:** During the operation phase, three types of monitoring are initiated. These are: Operational, Verification and Environmental monitoring.

Injection rate, surface casing pressure, bottom-hole pressure and annulus pressure are continuously monitored. Depending on the risk associated with the project, techniques that safeguard against risks to health, safety and environment will be considered here.

3. **Closure phase:** The monitoring in this phase starts after the CO<sub>2</sub> injection has stopped. Post closure monitoring involves recording formation pressure and determining location of the plume front using for example time lapse seismic.

4. **Post- closure phase:** During this phase, monitoring would focus on

- Recording the pressure differential between the pre-operation and anticipated post injection pressure in the injection zone
- Prediction of plume migration and associated pressure front.
- Assuring that vertical leakage to the surface is minimal.

Geophysical measurements techniques such as seismic, electrical and gravity measurements provide regional, cross-well and single well mapping of CO<sub>2</sub> (Nguyen et al 2003). 3-D seismic and instrumented monitoring wells are used to track the movement of CO<sub>2</sub> in the formation. Injection rate and pressure measurements are used to verify the amount of CO<sub>2</sub> injected into the formation and to maintain a safe threshold inside the formation so that it doesn't exceed the formation fracture pressure limit. Samples collected from observation wells are analyzed for changes in brine composition or presence of any tracers (Benson et al, 2004).

## 2.5 Numerical Simulation of CO<sub>2</sub> Sequestration

Academic studies of CO<sub>2</sub> sequestration frequently employ a conceptualized model in which the host formation is considered to be nearly homogenous. However in practice, deep formations are highly heterogeneous in nature. Numerically the effects of these heterogeneities on CO<sub>2</sub> plume migration and total storage can only be studied using numerical simulators.

Shariatipour et al (2012) tested accuracy of current flow simulators for representing flow of CO<sub>2</sub> in saline aquifer reservoirs. A range of 2-D and 3-D models were investigated for black oil and compositional simulators. In Liner et al (2011), several aquifer models were constructed

to study the CO<sub>2</sub> injection rate and storage related safety issues. A full forward simulation was done to predict CO<sub>2</sub> migration after injection. It was also concluded that CMG family of simulators are well suited for analyzing CO<sub>2</sub> sequestration in deep saline aquifers. Similar kind of studies have also been done by many researchers like Bachu et al (1996), Johnson et al (2000), Nghiem et al (2004), Kumar et al (2004), Ozah et al (2005) and Obi and Blunt et al (2006).

Kumar et al (2004), describes reservoir simulation of CO<sub>2</sub> storage in deep saline aquifer using GEM (© CMG) to carry out numerical simulation in order to study the effect of gas migration and storage on reservoir properties. The CO<sub>2</sub> salinity, brine density and brine viscosity models were calibrated against experimental data as a function of density, temperature and pressure. Peng-Robinson equation of state was tuned to fit the experimental data by using the oil phase to model the aqueous phase. The binary interaction parameter between the CO<sub>2</sub> and water was adjusted to fit the CO<sub>2</sub> solubility data. Relative permeability curves for two-phase flow in the reservoir model were generated using the Brooks-Corey correlation. Capillary pressure curves were also adjusted to fit the average permeability using the Leverett J- function (Leverett, 1941). Hurter et al (2007) studied the injection of CO<sub>2</sub> in deep saline aquifers including investigation of complex processes such as dry-out, salting-out and chemical reactions.

In most of the studies mentioned above few assumptions are common:

- Only incompressible fluid was considered, hence considering only supercritical CO<sub>2</sub> flow in the formation.
- The processes during injection and after shut-in were assumed isothermal.

## **2.6 Pressure transient analysis:**

Pressure transient testing of reservoirs was introduced and developed in 1950's and 1960's. There is substantial number of papers written on this subject and numerous methods of interpretation have been developed. Some of the key references are Cinco et al (1985), Raghavan et al (1980), Ramey et al (1968), Smart et al (1988), Ayestaran et al (1989), Daungkaew et al

(2004), Zheng et al (2005). Pressure transient analysis deals with generating and measuring pressure variations with time in wells and subsequently estimating rock, fluid and well properties. A disturbance is created usually by changing the flow rate and its effect on the pressure is monitored. The characteristics of the pressure behavior with respect to time obtained as a result of changes in flow rate reflect reservoir properties.

Well testing has been a core competency of the oil industry for a long time because it provides engineers with valuable information about the reservoir – such as average permeability, type of boundaries etc.. Reservoir engineer must have sufficient information about the reservoir to analyze reservoir performance and predict future performance under various modes of operation. Much of this information can be obtained from pressure transient analysis.

From the early days when the technique was first applied in groundwater hydrology and later quickly adopted to petroleum engineering, pressure transient analysis has been extensively used to determine formation permeability, wellbore conditions and reservoir pressure. Gradually it was also applied to determine fracture length, conductivities and reservoir diagnostics. This information can then be used in drilling, completion, and production and reservoir operations.

The principles of pressure transient analysis were first developed for liquid filled reservoirs with small or negligible compressibility. The differential equation describing fluid flow in a porous media called the diffusivity equation is a combination of the law of conservation of matter, an equation of state and Darcy's law. When expressed in radial coordinates the diffusivity equation for slightly compressible fluid is:

$$\frac{\partial^2 p}{\partial r^2} + \frac{1}{r} \frac{\partial p}{\partial r} = \frac{1}{0.0002637} \frac{\phi \mu c}{k} \frac{\partial p}{\partial t}$$

The diffusivity equation yields the solution for pressure as a function of time at various locations around the well. Specifically, it also yields pressure at the well and it is this pressure vs time plot that is analyzed to determine the reservoir properties.

Transient pressure analysis involves a number of assumptions such as:

- Uniform initial reservoir pressure throughout the area.
- Homogenous and isotropic medium, hence determining a single value of permeability of the region.
- A single fluid of small and constant compressibility
- Applicability of Darcy's law.
- Radial flow in the formation.

Traditional well test analysis tends to determine an overall permeability, which cannot reflect the variation of permeability in the formation. In practical experience there can exist heterogeneous zones or patches in the formation that can have significant effect on the pressure behavior. Pressure well testing along with numerical modeling has provided insight into the pressure effects of different types of heterogeneities and their variations in size, characteristics and distance from the well (Zeng et al 2004).

## **2.7 Pressure transient analysis techniques:**

Since well test analysis provides important dynamic information about reservoirs, several efforts have been made to use transient pressure data to improve reservoir characterization. A variety of transient testing techniques have been developed including pressure buildup, pressure drawdown, injectivity, pressure falloff, and interference testing. Reservoir data calculated from these techniques includes wellbore volume, wellbore damage or stimulation, reservoir pressure, flow capacity (permeability), reserves, fracturing, reservoir discontinuities, fluid discontinuities and swept volume (MacAllister et al, 1987).

When the flow rate is changed and the pressure response is measured in the same well, the test is called a "single well test". Examples of single well test are drawdown test, buildup, injectivity, fall off and step rate tests (Agarwal et al, 1987). When the flow rate is changed in one well and the pressure response is measured in another well, the test is called a "multiple rate



test”(Ezeudembah et al 1983). Examples of multiple rate tests are interference and pulse rate test (Kamal et al, 1983)

Modern techniques not only include analysis of pressure data but in addition pressure derivatives are also interpreted. Multiple-well tests are run to determine the presence or lack of communication between two points in the reservoir. In homogeneous isotropic reservoirs, multiple-well tests are conducted to determine the values of mobility-thickness product  $kh/\mu$  and porosity-compressibility- thickness product,  $\phi ch$ . If one of the wells used in the test intersects a fracture, the orientation of the fracture may be determined.

### **2.7.1 Step rate test:**

A test performed in which injection fluid is injected for a defined period in a series of increasing pump rates. The resulting data are used to identify key parameters like pressure, flow capacity “kh” and wellbore skin (Singh et al,1987). A plot of injection rates and the corresponding stabilized pressure values should be graphically represented as a constant straight line. Plot of this stabilized pressure with log(time) can be used in estimation of permeability.

### **2.7.2 Pressure buildup test:**

This is the most widely used technique used in the industry. This type of testing requires shutting in of a producing well. In this process the well produces at a constant rate for a sufficient period of time to achieve stabilized pressure distribution before it is shut in. After shut in of well, the pressure in the well is left to gradually increase. The pressure is measured immediately before the shut in and is continuously monitored with respect to time during the shut in time. It’s a special case of step rate test with just one cycle of flow period followed by shut-in. Figure 2.5 shows rate versus pressure behavior in an ideal pressure buildup test.

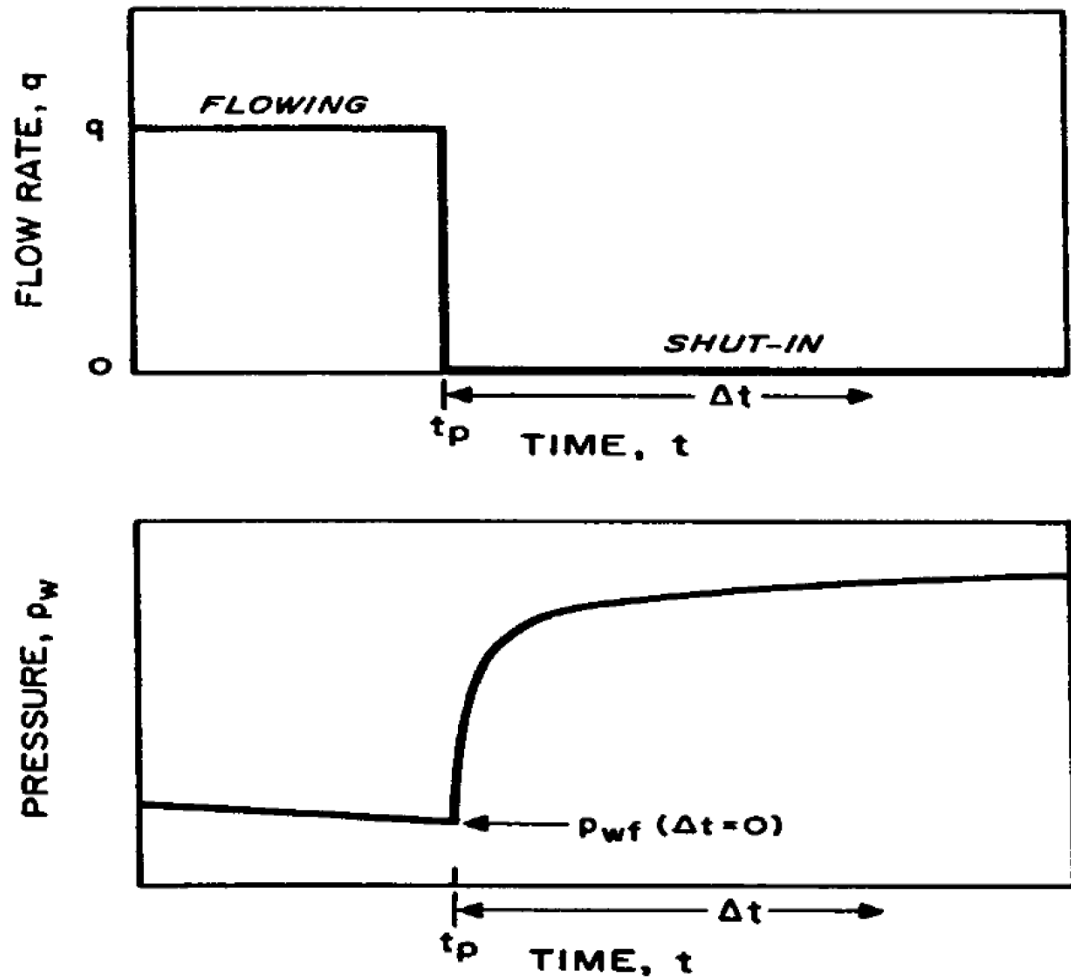


Fig 2.5: Pressure build-up rate schedule and pressure response (Earlougher,1977)

The resulting pressure buildup curve is analyzed to estimate the reservoir parameters and wellbore conditions. Buildup tests are the preferred means to determine well flow capacity, permeability, thickness, skin effect and other information. Soon after a well is shut in, the fluid in the wellbore usually reaches a somewhat quiescent state in which bottom-hole pressure rises smoothly and is easily measured. Some techniques used to analyze build up pressure data are

1. Type curve matching
2. Horner's plot technique
3. Computer reservoir simulation technique

For a pressure buildup test the bottom-hole pressure in the test well is expressed in terms of flow rate and time. At any time after the shut in the pressure equation is given by

$$P_w = P_i - \frac{141.2qB\mu}{kh} \left\{ p_d (t_p + \Delta t)_d - p_d(\Delta t_d) \right\}$$

where  $P_w$  = Measured wellbore pressure

$P_i$  = Initial reservoir pressure

$P_d$  and  $t_d$  are dimensional pressure and time respectively. They are given as

$$t_d = \frac{0.0002637kt}{(\phi\mu c)(r_w^2)}$$

$$P_d = 0.5 \left[ \ln \frac{t_d}{r_d^2} + .80907 \right]$$

### 2.7.2 Injection-Fall off testing:

Injection testing is pressure transient testing during injection into a well. It is similar to drawdown testing for both constant and variable injection rates. Fall off testing is the measurement and analysis of pressure data taken after an injection well is shut-in. Injection rate schedule and corresponding pressure profile is shown in Figure 2.6.

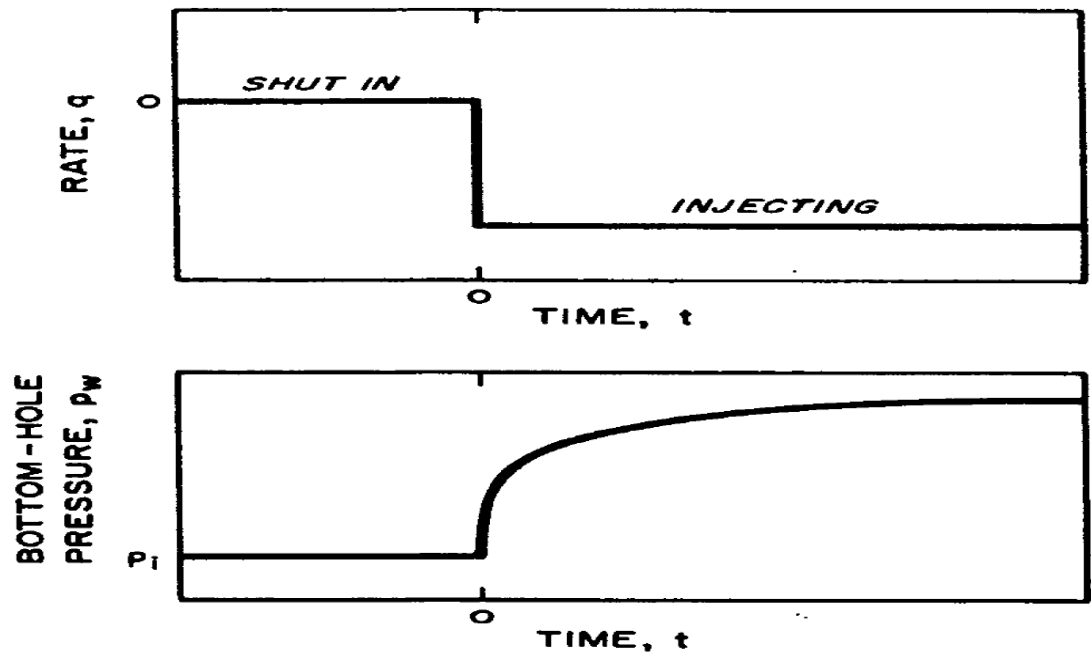


Fig 2.6: Injection test rate schedule and pressure response (Earlougher,1977)

Similar to drawdown testing, plot of bottom-hole pressure vs log(time) can yield in the determination of slope by measuring slope

$$m = \frac{162.6qB\mu}{kh}$$

#### 2.7.4 Superposition in Space and time:

The superposition theorem used to analyze situations that are more complicated than the ideal conditions assumed in classical build up and draw down analysis was first applied by van Everdingen and Hurst (1949). The principle of superposition states that for all linear systems the net response at a given position or time caused by two or more stimuli is the sum of the responses, which would have been caused by each stimulus individually. Adding solutions to a linear differential equation results in a new solution to that differential equation but corresponding to different boundary conditions. Since the diffusivity equation is linear, multiple rate, multi-well problems can be solved using superposition in space and time.

#### 2.7.4.1 Superposition in space:

Principle of superposition in space for reservoir engineering states that the total pressure change (drop or increase) at any well at any time/point in the reservoir is the sum of pressure change at that location at that time caused by flow rate changes in each of the wells in the reservoir. Mathematically it's given by:

$$\Delta P_1(t, r) = \Delta P_1 + \Delta P_2 + \Delta P_3 + \dots$$

$$\Delta P(t, r) = \frac{141.2qB\mu}{kh} \sum_{j=1}^n q_j B_j P_d(t_d, r_d)$$

where  $r_d$  is the dimensionless distance from well  $j$  to the point of interest.

#### 2.7.4.2 Superposition in time:

Superposition in time is required in order to analyze variable rate test. It involves breaking the multi-rate sequence into a set of rate changes. The rate used for each step is the difference between the current rate and the previous rate. Therefore in a well producing at variable rates, the pressure change is dependent only on the last rate (injection/production) that affects the pressure. Pressure drop at a well is given by:

$$\Delta P = \frac{141.2\mu}{kh} \sum_{j=1}^n \{q_j B_j - q_{j-1} B_{j-1}\} [p_d(t - t_{j-1})_d]$$

### 2.7.5 Type Curve Analysis:

A type curve technique is a graphical way of solving the pressure transient equation. It's been widely used in the petroleum industry for the last two decades. Type curves are derived from solutions to the flow equations under specific initial and boundary conditions (Gringarten et al, 1987). The conventional methods of solving pressure transient equations are not adequate for analyzing “early time” data that are obtained before radial flow is established. The biggest advantage of type curve analysis is the recognition of the early time region in the data.

They are usually presented as a log-log plot between dimensionless pressure and dimensionless time. For a given set of data, it can be matched to a single type curve or family of curves by adjusting the shape of the various curves. When the match is made, a good match point is selected, usually an intersection of the major grid lines and formation properties are then calculated from the two set of coordinates. A general type curve with pressure data superimposed on it is shown in Figure 2.7.

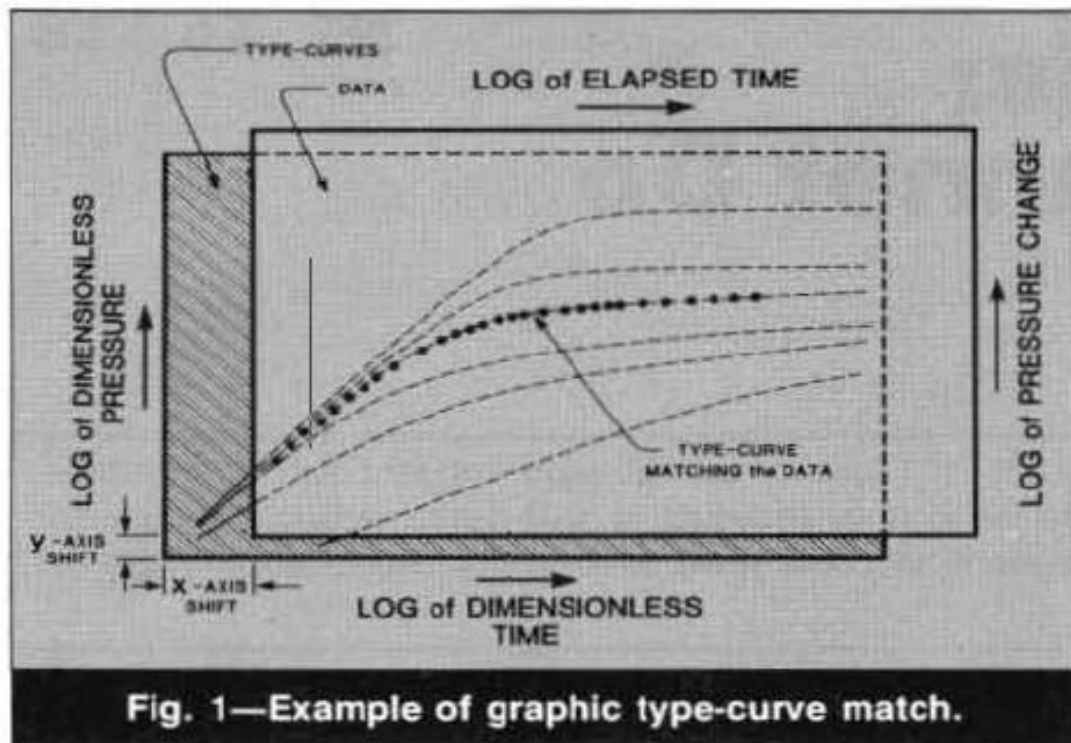


Fig 2.7: Type curve analysis (Gringarten et al, 1987)

## **2.8 Assessment of reservoir heterogeneity through well test analysis:**

Permeability heterogeneity is one of the most important reservoir parameter to be identified in pressure transient analysis. To determine vertical permeability many measures are available like well logs and drilling data. But to determine the horizontal permeability distribution, pressure transient analysis is used.

Traditional well test analysis yields a single value of permeability, which cannot reflect the variation in permeability in the formation. In order to analyze a heterogeneous reservoir with multiple variable permeability sections, many methods have been applied. In most of the studies for the assessment of permeability heterogeneity multiple well multi-rate methods is used. Multiple well tests are more sensitive to reservoir heterogeneity than single well tests.

Effect of location, size and permeability value of heterogeneous permeability sections on the pressure response is explained in Zeng et al (2004). In Babadagli et al (2001), it was concluded that increasing heterogeneity yields higher pressure drop when compared with cases with average permeability values.

There have been not many instances where CO<sub>2</sub> wells have been flow tested to study reservoir parameters. One such study was done by Xu et al (2007) where a field scale study of CO<sub>2</sub> sequestration is done after injecting CO<sub>2</sub> in a depleted gas field. Testing comprised of multiple rate test and extended drawdown test in order to determine well and reservoir characteristics. Parameters like open flow potential, permeability and skin were determined and it was concluded that CO<sub>2</sub> gas exhibit different flow behavior compared to natural gas. Zakrisson and Edman et al (2008) studied well interference when injecting CO<sub>2</sub> in a low permeability reservoir in order to determine the minimum injection rate for commercial projects. Effect of gravity, flow rate and small scale heterogeneity on flow of CO<sub>2</sub> and brine displacement was studied by Chia-Wei Kuo et al (132607). It was concluded that brine displacement efficiency is largely dependent on capillary number and gravity number and therefore flow-rate dependent.

The influence of small scale heterogeneity on average CO<sub>2</sub> saturation is strong in the capillary force dominated regime.

## **2.9 Computer algorithms for pressure transient analysis:**

The problem of reservoir parameter estimation based on well test data has been studied widely. With the advancement in computing capacity to solve non linear regression problems, automated well test analysis has provided a capability for solving complicated reservoir problems. Nowadays most of the techniques used in computer-based well testing rely on least squares based nonlinear regression. In well test analysis this corresponds to minimizing the squared difference between calculated pressure and pressure from measured data.

Significant improvement in the accuracy of pressure transient analysis has been possible using efficient least square algorithms. Two such algorithms are explained in Bonalde et al (1994) and Dastan et al (2009). The former paper estimates reservoir parameters by directly comparing the difference between the actual well tests with the corresponding values obtained from the values calculated from the analytical expression and minimizing it until it reaches the tolerance. In Dastan et al (2009) describes total least square regression analysis which is based on minimization of orthogonal distance of measured data points to the fitted curve, especially for non-linear pressure transient model. He concludes that this method is efficient in estimating the reservoir parameters by minimizing the errors in both pressure and time simultaneously.

Pressure derivative analysis is also used in well testing in order to characterize the reservoir. However it's more affected by the noise produced due to well rate changes and by mathematical procedures involved. Escobar et al (2004) compares results obtained from different algorithms using the pressure derivative data.

One of the drawbacks of type curve analysis is that it can yield non-unique results due to similarity in shape of the curves. To overcome this problem Hongjun et al(1998) proposed a method based on adaptive Genetic algorithm (AGA) to get early time well test interpretation.



The diversity of the population and the convergence capacity of the GA can be maintained by using the adaptively varying probabilities of crossover and mutation depending on the fitness values of the solutions. This method in general is considered superior to non-regression analysis due to its high convergence capacity. Barua et al (1987) also noted that the GM method often has difficulties in convergences when estimating multiple parameters simultaneously. He proposed Newton-Greenstadt (NG) method to overcome this problem. More such algorithms have been implemented by various researchers (Nanba et al 1992, Cinar et al 2006, Mendes et al 1989, Ozkan et al 1994 and Seetharam et al 1989).

The algorithms described in above studies satisfactorily determine unknown reservoir parameters with faster convergence and less number of iterations.

## **2.10 Interpretation of well test:**

By running the reservoir model in a commercial simulator, pressure responses are obtained. During analysis of these responses normally an interpretation model that relates the measured pressure change to the induced rate change and which is consistent with other information about the well and reservoir are identified. This is an inverse approach to interpretation that does not yield a unique solution as a large set of models can be generated which will produce the same pressure response. The problem of non-uniqueness is well recognized in the oil industry and accounts for the increased adoption of stochastic modeling techniques, which aim at providing equiprobable representations of the reservoir to capture the uncertainty associated with the predictions/estimations of the reservoir parameters (Gringarten et al, 2008).

## 2.11 Summary:

Monitoring the CO<sub>2</sub> plume during and after injection phase is an utmost important task for a successful CO<sub>2</sub> sequestration project. The techniques available involve geophysical and geochemical monitoring with numerical simulations of models replicating the field. In conducting the numerical simulations, it is required to assess the reservoir heterogeneity correctly. Permeability distribution is one of the most important factors for performance estimation and field development. The creation and development of numerical models depends on these defined permeability field. Pressure transient analysis has become one of the best methods to estimate reservoir parameters and to detect/predict heterogeneities of the formation. Well test involves the interpretation of bottomhole pressure data to estimate well and reservoir parameters.

Modern methods of interpretation of pressure transient analysis data use not just the measurement of the bottomhole pressure but in addition pressure derivatives. Graphical methods are also applied such as type curve analysis. These methods of analysis are usually developed for ideal conditions such as when no wellbore storage effects are prevalent or when constant wellbore storage coefficients apply (Cinco-Ley et al 1985). Modern techniques also involve matching the actual pressure response with the one obtained from simulation done using an analytical model. The process of creating these reservoir models involves large degree of uncertainty and non uniqueness. Based on the uncertain geological settings, reservoir and fluid properties and formation structure, multiple correct models can be created which will honor the actual pressure response. Thus it becomes important to study what characteristics of this heterogeneity or uncertainty can be resolved using the injection and pressure data.

The last two chapters of this thesis will describe cases where we will infer reservoir properties starting with a single well and then extend to multiple wells. In case of multiple well pressure transient analysis, reservoir parameter groups will be used to constraint spatial models for reservoir thickness, permeability and porosity. The ultimate application of this analysis will

be done in estimating and understanding these multiple attributes that will affect the CO<sub>2</sub> plume migration. The approach also helps in resolving the uncertainty associated with the set of models that best match the field data.

## **CHAPTER 3: ASSESSING THE EFFECT OF RESERVOIR HETEROGENEITY ON CO<sub>2</sub> PLUME MIGRATION**

### **3.1 Chapter Objective:**

Several properties of reservoir, well and fluid affects the migration of CO<sub>2</sub> in the formation. For a successful CO<sub>2</sub> sequestration process developing a detailed understanding of permeability distribution is an important factor. Accurate model depicting the heterogeneous reservoir to carry out reservoir simulations for predicting CO<sub>2</sub> migration depends mainly on correctly estimating reservoir parameters like permeability “ $k$ ”, porosity “ $\Phi$ ”, transmissibility “ $kh$ ” and permeability to porosity ratio “ $k/\Phi$ ”. Previous work has shown that injection data from wells can be utilized for developing models to understand spatial distribution of heterogeneities in the formation. This chapter focuses on understanding the information contained in the injection data (pressure and rate) for different cases of permeability distribution along with injection rate fluctuations. An effort will be made to examine the effect of various kinds of permeability heterogeneity on the injection pressure profile to make a confident estimation of migration of CO<sub>2</sub> plume with time. This approach will be studied using data from In-Salah gas field from Algeria.

### **3.2 In- Salah Gas Field description:**

The In-Salah gas project in Algeria is a one of the biggest industrial scale demonstration of geological sequestration of CO<sub>2</sub>. The main project objective is to produce natural gas in the Saharan desert and supply clean natural gas to the European energy market. The gas that is being produced from the field contains CO<sub>2</sub> in the range of 1-10% (by mole fraction), much higher than the specified limit. Thus, it is absolutely necessary to separate CO<sub>2</sub> from the

produced gas stream in order to bring down its volume fraction to 0.3% to meet the purity standards. In this project instead of expelling/venting the CO<sub>2</sub> into the atmosphere, it was decided to capture, compress, and store the produced CO<sub>2</sub> back into the aquifer leg of the reservoir at three separate locations. The ultimate goal of this project is to monitor continuously the CO<sub>2</sub> migration using latest technologies for permanent capture and storage. Figure 3.1 shows the schematic of gas injection in the Krechba field.

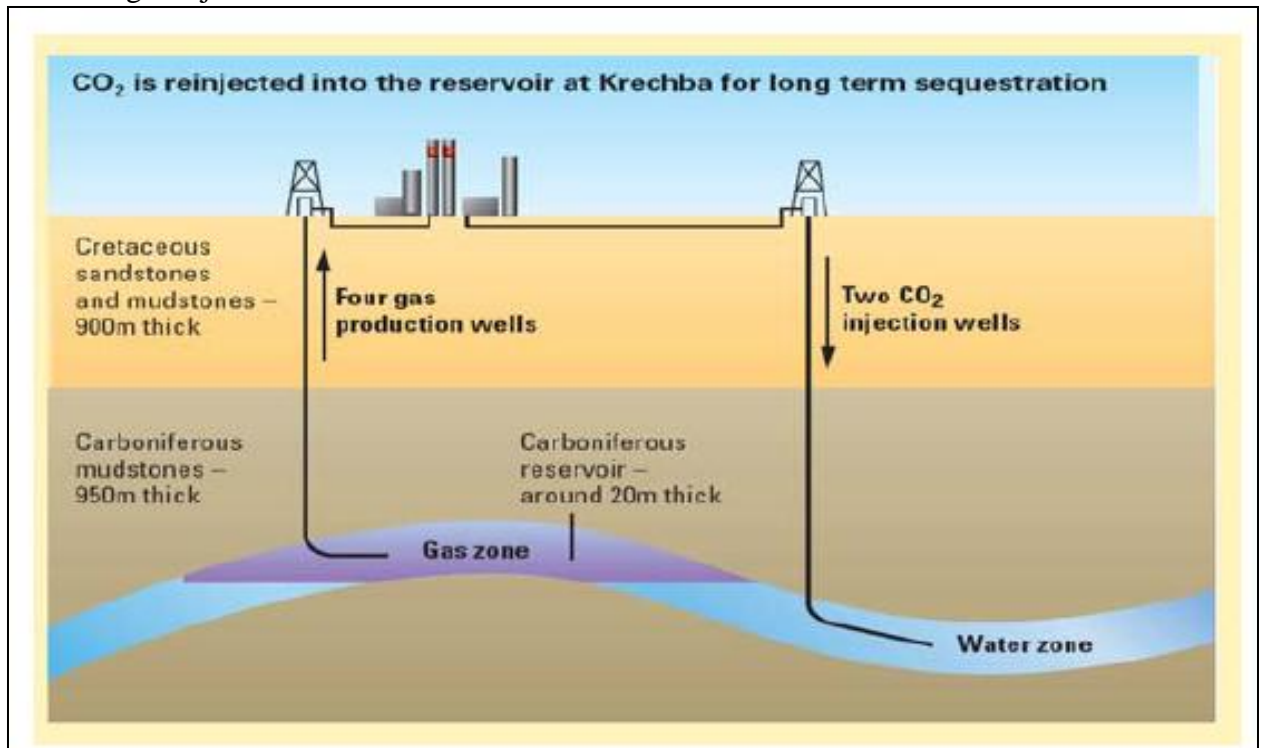


Figure 3.1: Schematic of CO<sub>2</sub> storage at the Krechba field

Krechba is one of eight fields in the In Salah gas project and it is located in the northern part of the development area. In the Krechba field, the aquifer layer C10.2 has been identified as the target zone for CO<sub>2</sub> injection. The captured CO<sub>2</sub> is re-injected back at a depth of 2000m into the Krechba gas field. Figure 3.2 shows the location of the In Salah site.



Figure 3.2: Location of In Salah gas project (Matheson et al, 2010)

Natural gas production occurs from 5 wells while re-injection takes place through 3 horizontal wells into the Krechba field. CO<sub>2</sub> is stripped out from the produced natural gas stream and the separated CO<sub>2</sub> is transported through pipelines from the processing facility to the Krechba storage site. Few abandoned wells are also present in the field and they serve as monitoring wells. The gas field holds an estimated amount of 160 billion cubic meters of gas and is expected to have a successful operation life of 20 more years. More than 3 million tones of CO<sub>2</sub> have been securely stored so far and an estimate to store over 17 million tons over a period of next 20 years is made.

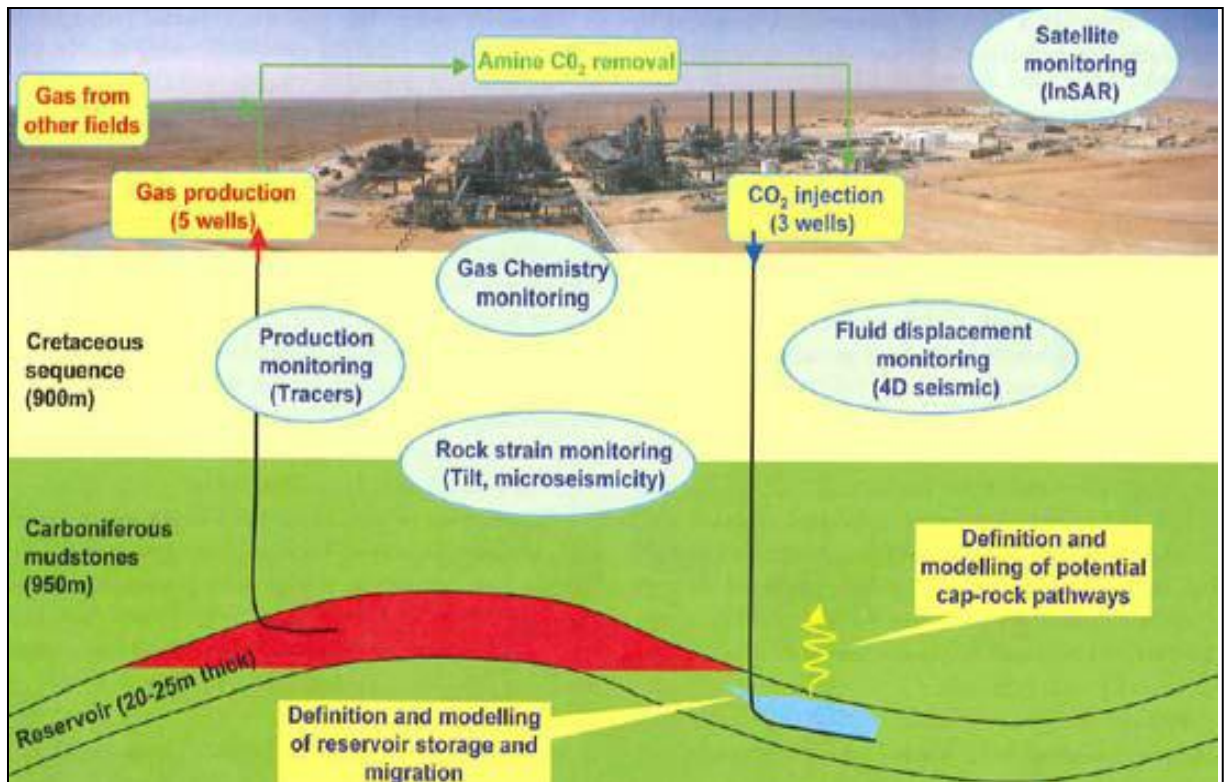


Figure 3.3: CO<sub>2</sub> injection and monitoring in the Krechba field (Ringrose et al 2009)

As is seen in Figure 3.3, CO<sub>2</sub> is re-injected downdip of the reservoir through 3 long horizontal (1500 meters) injectors and monitored actively. Presently there are 3 long horizontal gas injectors at the Krechba field injecting up to 50 mmscf/d of CO<sub>2</sub>. Figure 3.4 shows the location of wells in the Krechba field.



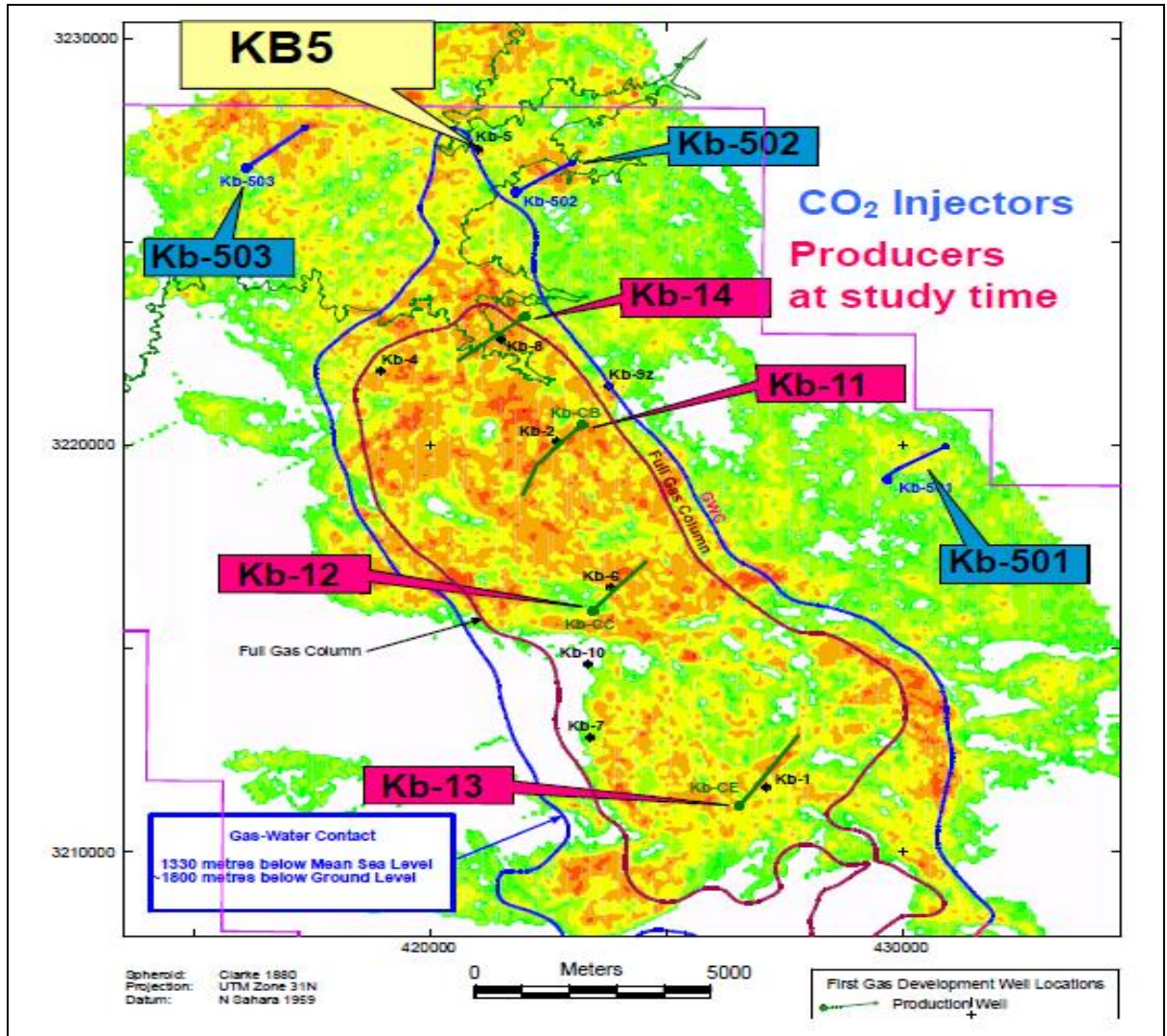


Figure 3.4: Porosity distribution of Krechba field and the location of wells. (Source: Wright 2007)



### **3.3 Krechba Field Geology:**

The Krechba field is an anticlinal structure that extends approximately 130 square kilometer with a low dip. The reservoir is made up of Carboniferous and Devonian sandstones. The Carboniferous reservoir lies at a depth of 1800m below surface and is 5 to 24 meters in thickness. The average reservoir thickness is 20m in the northern and central part of the field. Carboniferous mudstone (mainly clays) lies above these carboniferous sandstone reservoirs with an average thickness of 905m. This acts like an effective trap for the gas. These mudstones are overlain by thick Cretaceous sandstone and mudstone approximately 900m thick. The storage unit involves an anticline formed during a compressive tectonic phase in the late Carboniferous era. During the late carboniferous era a NE-SW compressive stress system deformed this basin into a series of folds. The northern part of the Krechba field remained relatively un-faulted and the 20m thick storage zone is not offset by faults. At present the stress regime in the region is in the NW-SE direction. Understanding this rather complex structural history is significant for appropriately defining the nature of faults and fractures and inferring their impact on CO<sub>2</sub> injection performance.

Initial survey carried out the Krechba field was focused on understanding the gas reservoirs and was not ideally suited for CO<sub>2</sub> sequestration. Further effort was focused on developing a deeper understanding of the faults and cap rock integrity. Figure 3.5 shows the Krechba field stratigraphic structure.

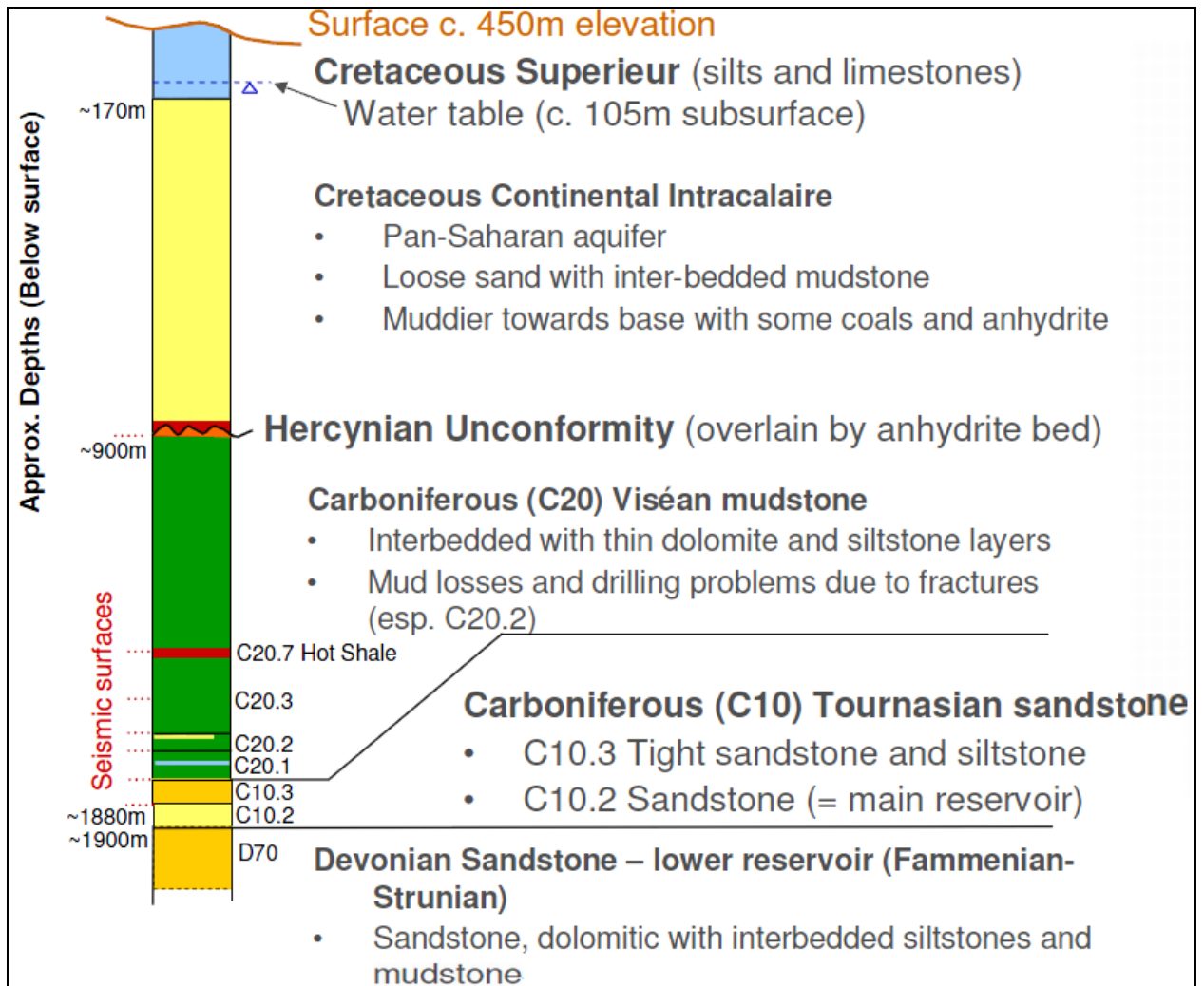


Figure 3.5: Krechba stratigraphic structure ( Source- In Salah JV)

### **3.4 Monitoring Techniques:**

Initial assessment at the In Salah site suggested that well integrity and CO<sub>2</sub> migration along micro-faults and fractures were the key risks associated with the project. Hence active monitoring of CO<sub>2</sub> migration became the utmost priority in the project. Almost all the possible monitoring techniques used in the oil and gas industry were implemented in this project. This includes geochemical, geophysical, production data, 3D and 4D seismic and satellite technologies. These techniques monitor the injection, plume migration, ground and subsurface deformation, surface movement, well integrity, caprock integrity, and pressure development over time. These measurement technologies provide information on how the CO<sub>2</sub> is migrating in the reservoir and provide long term assurance of CO<sub>2</sub> sequestration. A brief summary of some of these monitoring technologies is presented below.

#### **3.4.1. Satellite imaging**

Perhaps the most successful and valuable CO<sub>2</sub> monitoring technique so far at the In Salah field has been satellite imaging. Here the use of satellite based interferometric synthetic aperture radar (InSAR) helps in detecting even the subtle ground deformation changes by comparing phase differences from successive satellite passes. This technique can potentially measure centimeter scale changes in deformation over time spans of days to years.

Satellite imaging done in the Krechba field detects surface uplift in the vicinity of all the three injectors. In-Sar dataset concludes that the observed uplift rate is 5mm/year. Forward and inverse modeling (Rutqvist, et al., 2008) of the subsurface pressure increase due to CO<sub>2</sub> injection confirms that the surface deformation is caused by propagation of the subsurface pressure increase through the overburden rock sequence to the surface. Using the satellite observations, an indirect prediction of the subsurface plume migration was made in the NW-SE fracture direction. Figure 3.6 shows the satellite image of the Krechba field.

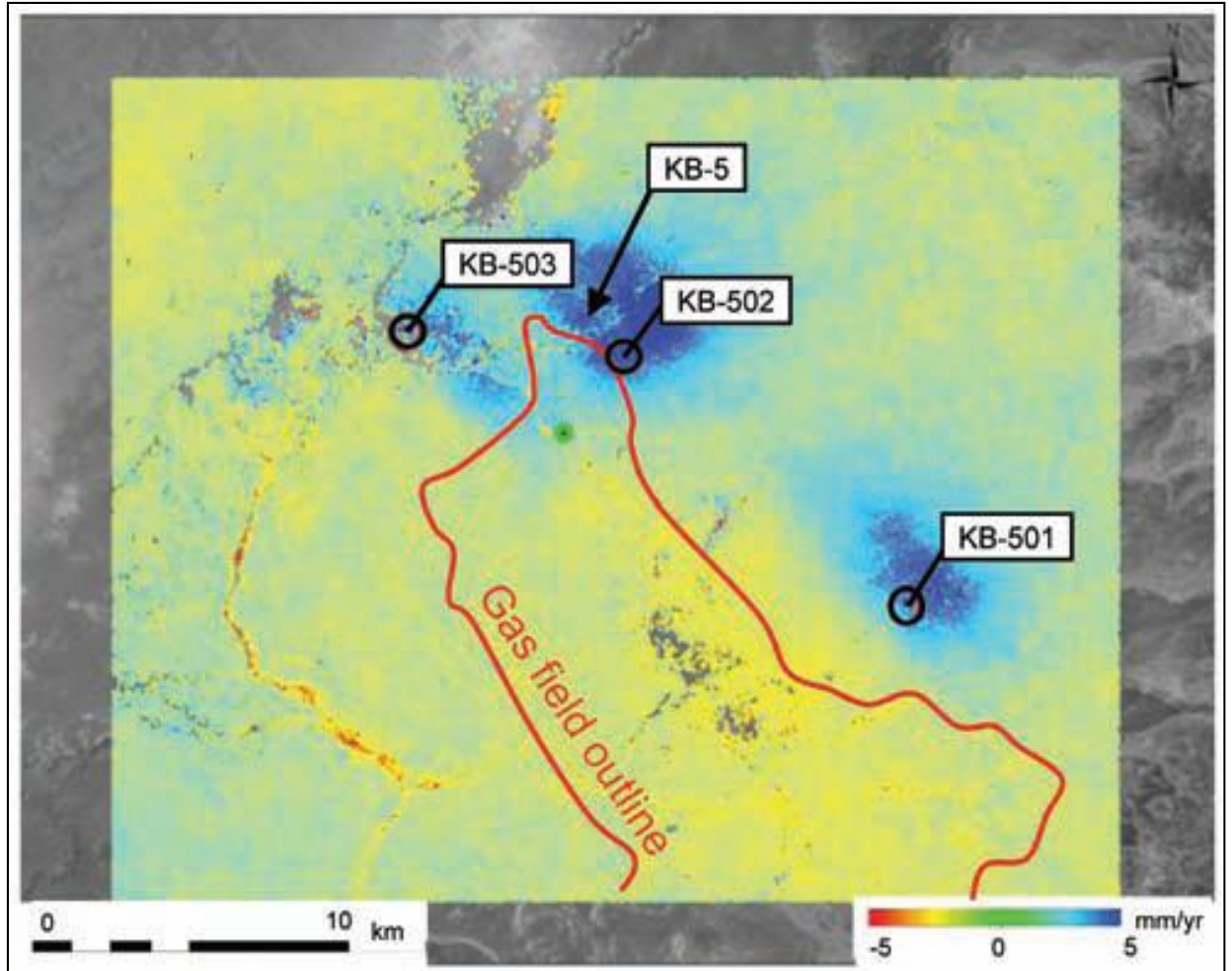


Figure 3.6: Satellite image of the Krechba field (Source- In Salah JV)

### 3.4.2. Well monitoring

Unlike oil and gas wells, in case of CO<sub>2</sub> sequestration the monitoring techniques are implemented to measure directly the migration and flow of CO<sub>2</sub> after injection into the formation. One such technique is the addition of tracers into the injection wells. They are added to the injected CO<sub>2</sub> for a defined period to generate a pulse which travels from the injection well to the monitoring well. For the In Salah gas field, per-fluorocarbon tracers are used that can be detected at very low concentrations. The existence of an open fracture network aligned in the

NW-SE direction was confirmed during tracer analysis. Leak was detected at the abandoned well KB-5 and tracer analysis confirmed that the CO<sub>2</sub> detected came from injector KB-502.

Along with tracer monitoring, lab analysis of fluid from each well and pressure and injection rate analysis was used to detect rise in the pressure indicating backward migration of injected CO<sub>2</sub> back up into the wells. Figure 3.7 shows the location of wells in the In Salah field.

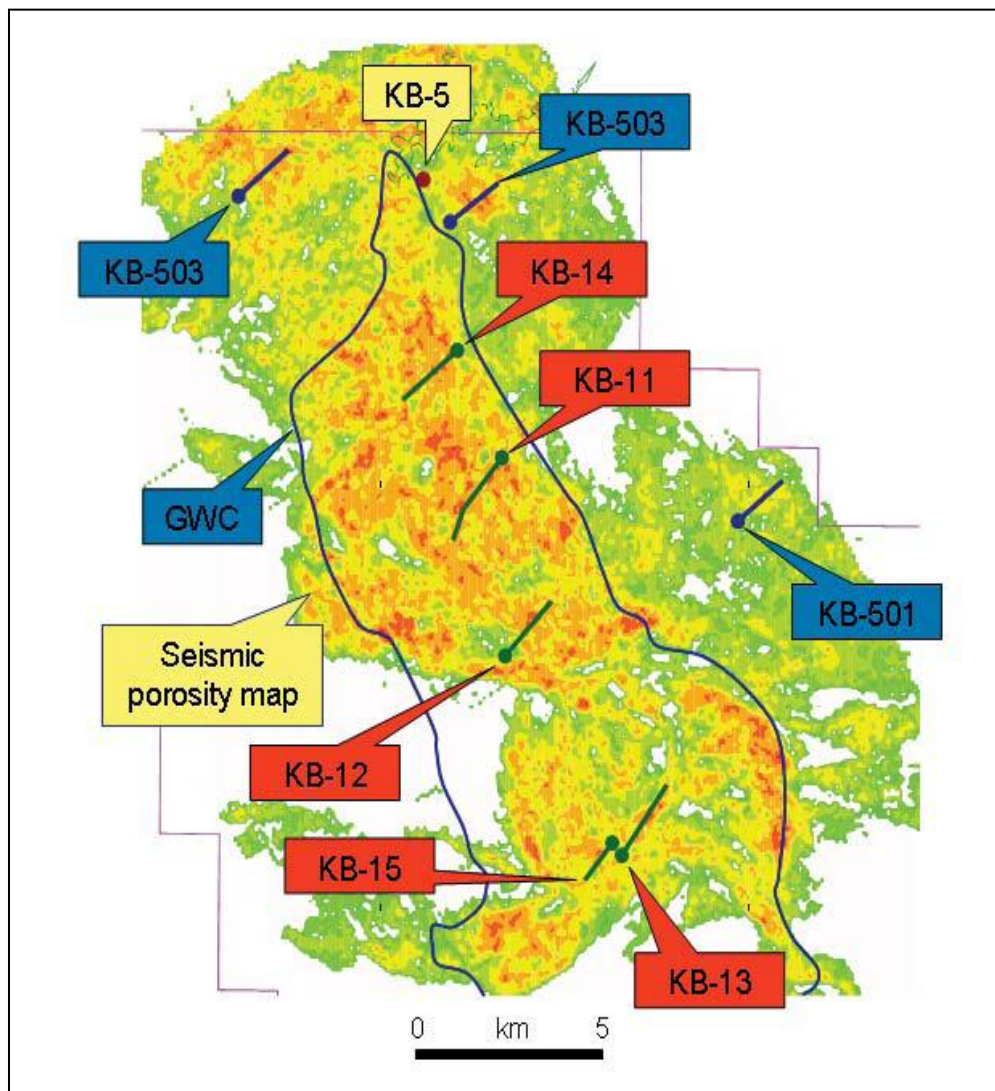


Figure 3.7: Location of Krechba injectors and producers

### **3.4.3. Seismic monitoring**

Controlled source seismic monitoring has many applications like mapping salt domes, faults, anticlines and other geologic traps in petroleum bearing rocks, and geological faults. 2-D seismic analysis done on the Krechba field illustrated significant structural uncertainty on a 2km stretch of the field. 3-D seismic data was acquired and new maps were generated. The survey was done on the northern part of the reservoir in 2009. It looked for differences in signal caused due to density difference between the formation brine and CO<sub>2</sub> in the formation. Using the 3-D seismic data it was concluded that the field is faulted and a total of 10 faults were identified in the northern part of the Krechba field. All these faults were identified as reverse faults with the longest one measuring nearly 9km and the shortest 1km long. The throw offset of the faults varies between 10m to 40m. Coupled with image logs, seismic data were effective in detecting the presence of minor faults and fractures in the Krechba field. A better reservoir model was made from these results in order to predict the CO<sub>2</sub> plume behavior in the deep reservoir.

### **3.4.4. Microseismic monitoring**

The other monitoring method being employed at Krechba field is microseismic monitoring. Microseismic monitoring is a technique that requires drilling holes about 100m deep into the ground and then suspending geophones. Geophones are sensors that can detect small movements in the rock structure due to changes in pressure and temperature that result due to CO<sub>2</sub> injection and movement in the formation.

These techniques when combined together can help predict the fate of injected CO<sub>2</sub> in the subsurface formation. Analysis of well logs, pressure and injection data, tracer analysis, seismic and satellite imagery has been used to indicate the spatial distribution of the injected CO<sub>2</sub>. The detection of CO<sub>2</sub> at the KB-5 wellhead has generated considerable interest among researchers. In order to make these predictions, reservoir models should be developed that accurately represent

reservoir heterogeneity. Careful calibration of reservoir models using injection data is essential. The uncertainty in reservoir heterogeneity with dynamic data at well locations was studied by Bhowmik et al (2009). This paper demonstrates an algorithm that refines an initial set of reservoir models representing the prior uncertainty to create a posterior set of subsurface model that reflect injection performance consistent with the observed data. But in order to verify if the calibration process improves the accuracy, it is necessary to first assess if reservoir heterogeneities do influence the injection well response.

One of the main objectives for the research presented in this thesis is to understand and examine the information contained in the injection data for a range of different reservoir models demonstrating different heterogeneities. This analysis is done using data from the Krechba gas field.

### 3.5 Field Case Study

#### 3.5.1 Model description:

A range of cases involving variations in reservoir heterogeneity and injection rates are implemented using the basic reservoir model for the Krechba reservoir. A forward model is created in CMG-GEM (Generalized Equation of State Model Reservoir Simulator) that will replicate the field information. CMG-GEM is a full equation of state reservoir compositional simulator for modeling recovery using processes where the fluid composition affects recovery. In our case it will be used to capture the interaction of the CO<sub>2</sub>-brine system and flow of CO<sub>2</sub> in deep saline aquifers.

A 3-D synthetic aquifer model is developed in CMG. The aquifer model is made up of 50\*50\*3(400m\*530m\*8m) grid blocks with 3 injection wells injecting at different user-defined rates and 1 producer. In the krechba field natural gas is produced from 5 producers, and CO<sub>2</sub> stripped from the gas is re-injected into the formation. In order to mimic this gas mass balance, the production rate is specified to be four times the total injection through three injectors into the formation, resulting in a voidage replacement of 25%. The injected fluid/solvent is pure CO<sub>2</sub> in the CMG simulations.

The total thickness of model is 20m divided into 3 layers (8m-4m-8m). The reference/base permeability and porosity is heterogeneous. The characteristic feature of this heterogeneous reservoir is the presence of a fracture network aligned in the NW-SE direction. The base case permeability map (without fractures) was created using Sequential indicator simulation (SISIM) (Xu and Journel 1994, Deutsch and Journel 1998). Sequential indicator simulation (SISIM) is a non-parametric simulation technique that is conditioned to available permeability data and reflects the spatial variability implied by the variogram model. The goal of



stochastic simulation is to reproduce geological texture in a set of equiprobable simulated realizations.

Bhowmik et al (2010) shows a method to sequentially generate permeability distribution for this field which is explained diagrammatically below in Figure 3.8.

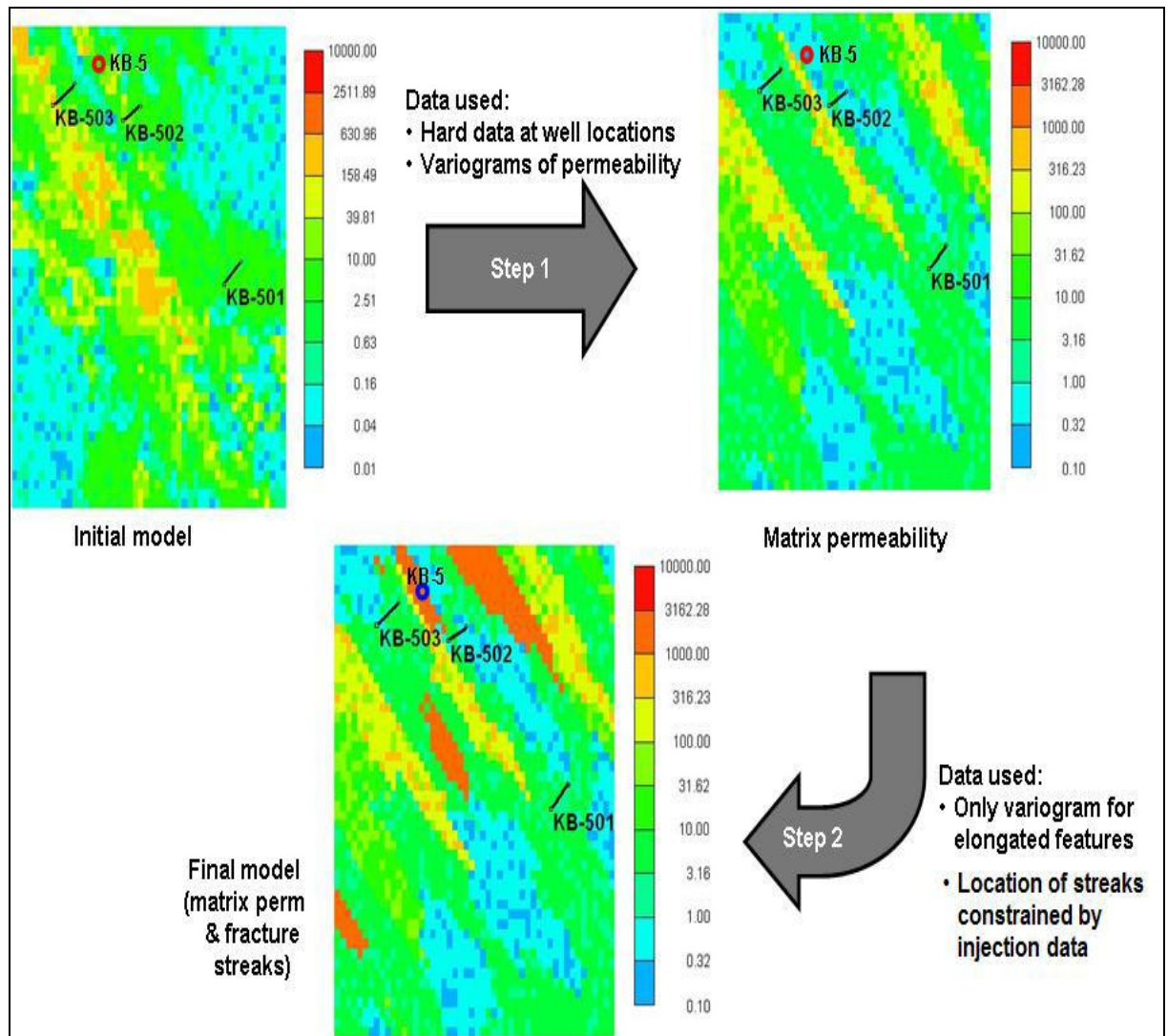


Figure 3.8: Two step process of generating permeability distribution (Source: Bhowmic et al(2010))

The final model depicting the history matched permeability distribution is shown in Figure 3.9.

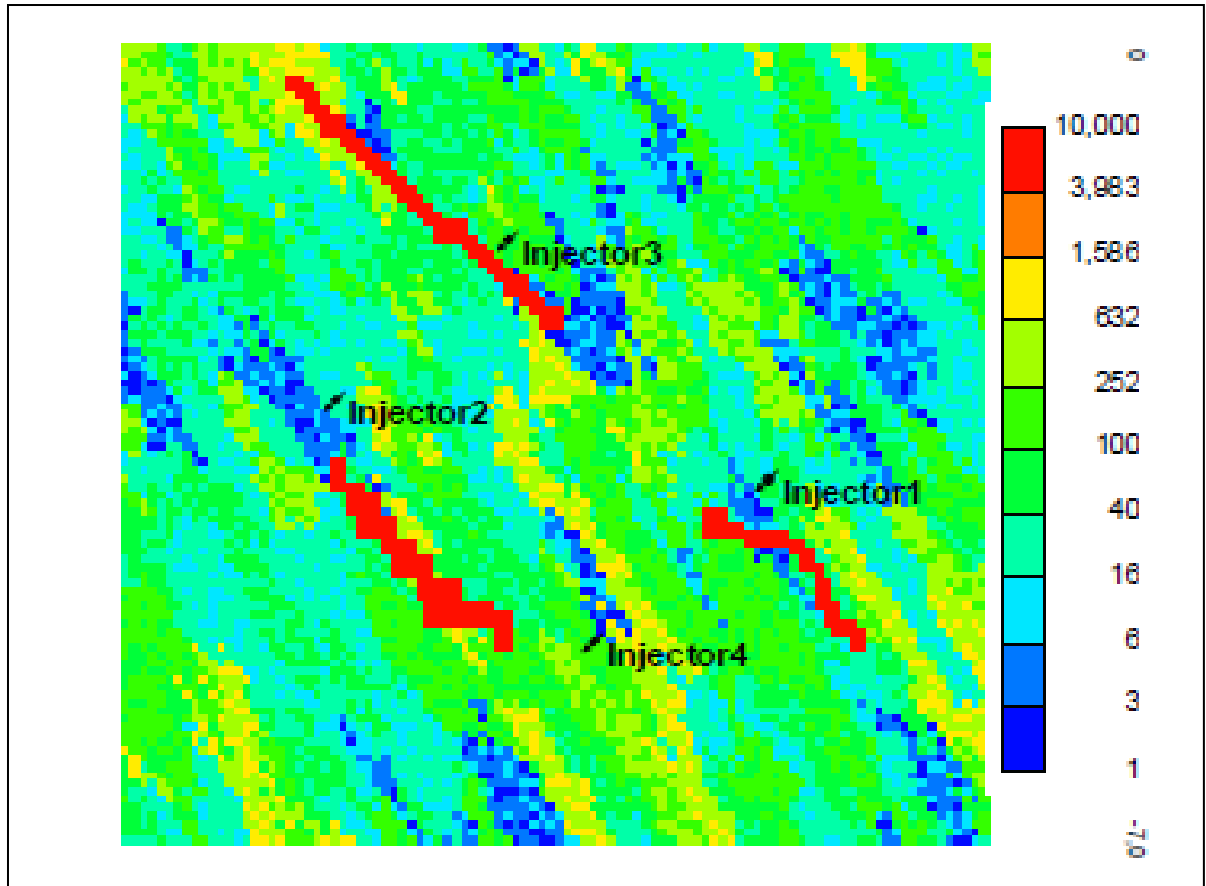


Figure 3.9: Permeability distribution of Krechba field

This characteristic feature will be presented as high permeability streaks in the model traversing in the NW-SE direction. In order to render these streaks as leakage pathways, the permeability values in these streaks were set to be 300% higher than the background permeability. For the In Salah the background permeability ranges from 0.1md to 600md, with the high permeability streaks having the values of permeability as high as 9000md. While history matching by perturbing the location and extent of these permeability streaks has been the subject of previous papers by Bhowmick et al. (2011) and Mantilla et al. (2010), these high permeability streaks will be added manually in the CMG model in the current study. This is because our intent is to study the impact of such permeability heterogeneity on flow responses and for

accomplishing the position of the streak will be varied manually in this study. The average permeability of the formation is 10md.

The porosity distribution in the reservoir is also not constant throughout. A qualitative map of porosity distribution in the Krechba field is shown below in Figure 3.10. Initial model of size 50\*50 for porosity distribution was created from well logs and surface contour maps. The qualitative map (Figure 3.10) was scanned and porosity values were assigned to the grid based on the color scale to each block. Few points were then randomly sampled out of this grid and used to create indicator variograms for the different categories (high: 0.25, medium: 0.15 and low: 0.05) of porosity. The indicator variograms were then used together with the data at the well locations in SISIM to generate a model for porosity distribution. (Bhowmik et al, 2010). The formation has porosity in the range between 6-28% with mean porosity of 15%.

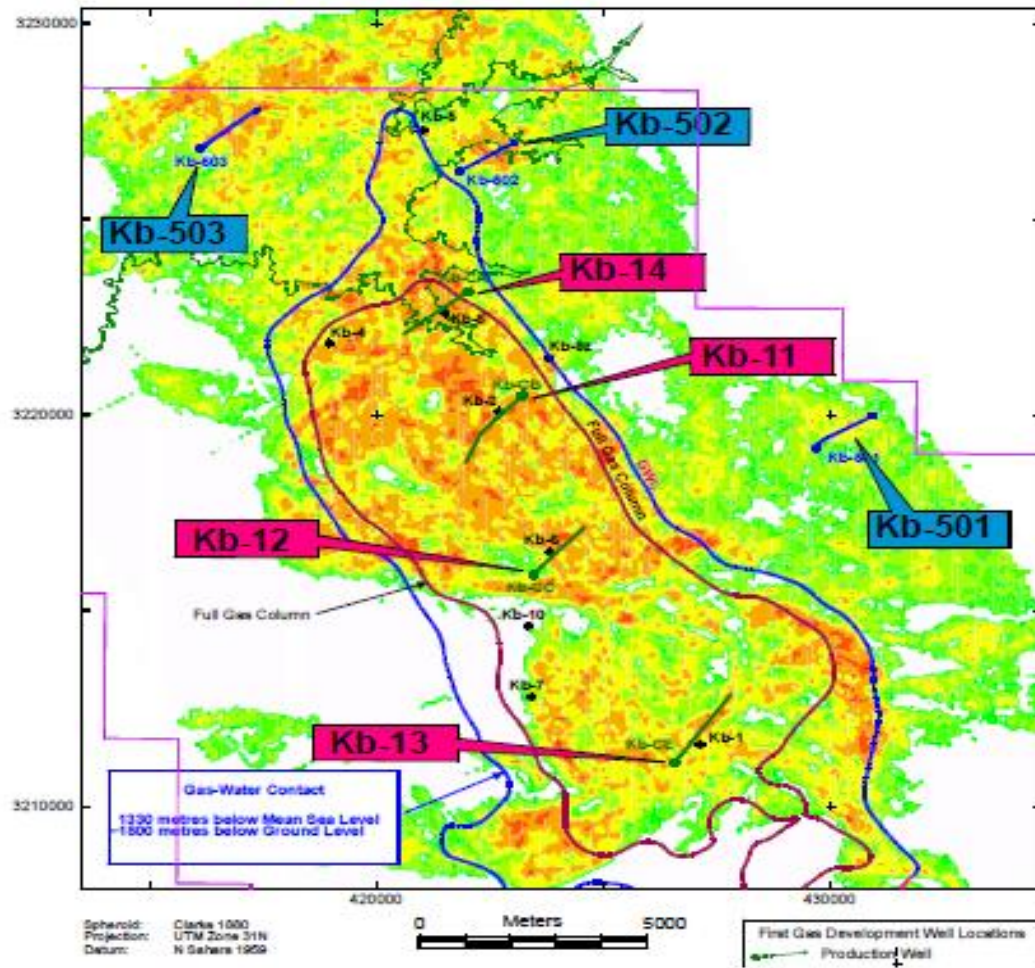


Figure 3.10: Porosity distribution map of In Salah field.

For our analysis we will consider only the northern part of the Krechba field. The porosity map for the aquifer model in CMG-GEM is shown in Figure 3.11.

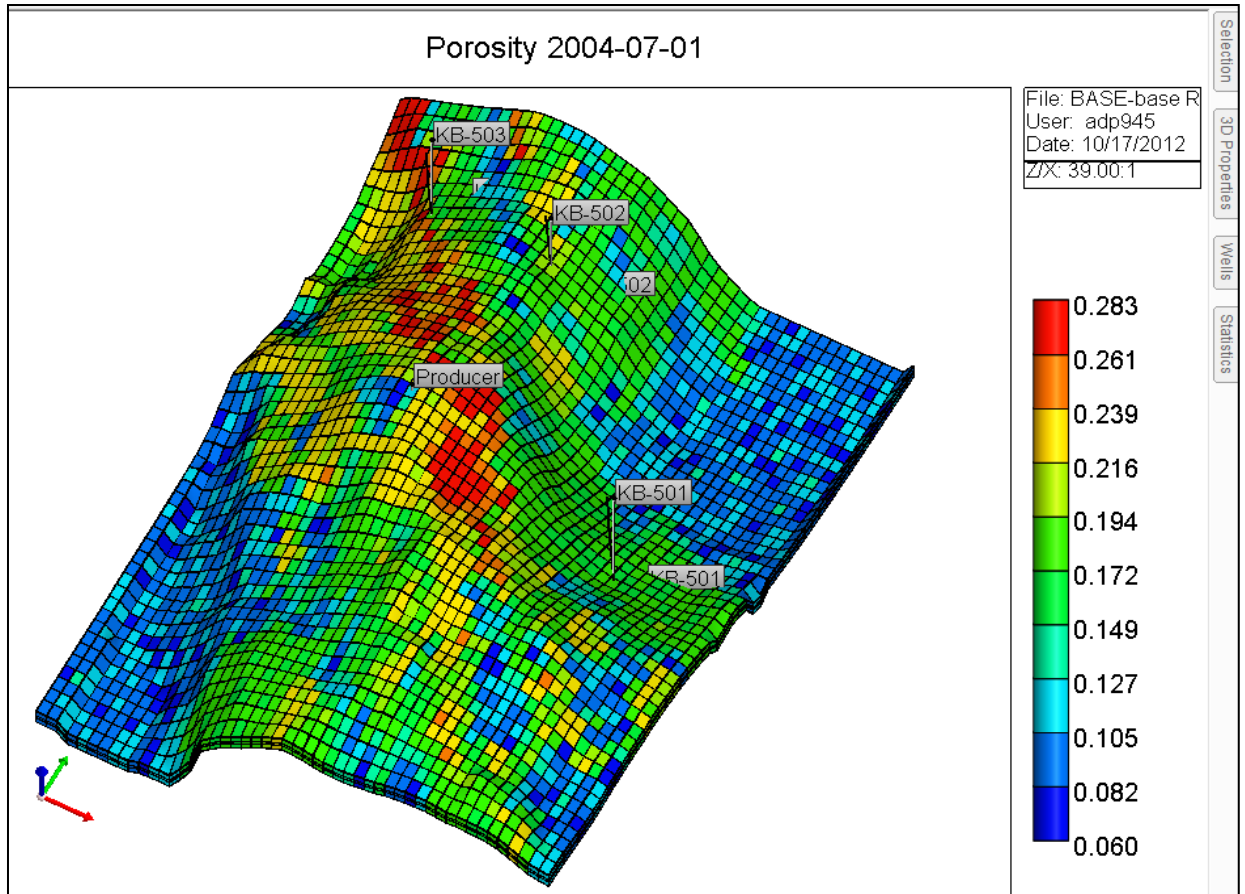


Figure 3.11: CMG-GEM model showing porosity distribution

The reservoir reference pressure is specified to be 17484.5 Kpa at a reference depth of 1300m. The simulation model is initialized using this reference reservoir pressure. Water oil contact lies at 2000m and Gas-Oil contact is present at 1300m. In total 3 components are defined in the formation:  $H_2O$ ,  $CH_4$  and  $CO_2$ . The oil zone composition consists of 100% water while 100%  $CH_4$  is present in the gas cap zone with no trapped saturations. The reservoir is considered to be isothermal with constant temperature of 76C. Also very high volume multipliers of 1000 are used for the boundary blocks in order to mimic an infinite acting reservoir and reduce the influence of reservoir boundaries on the well pressure and rate profiles. Shown below is the grid top view of the model in Figure 3.12.

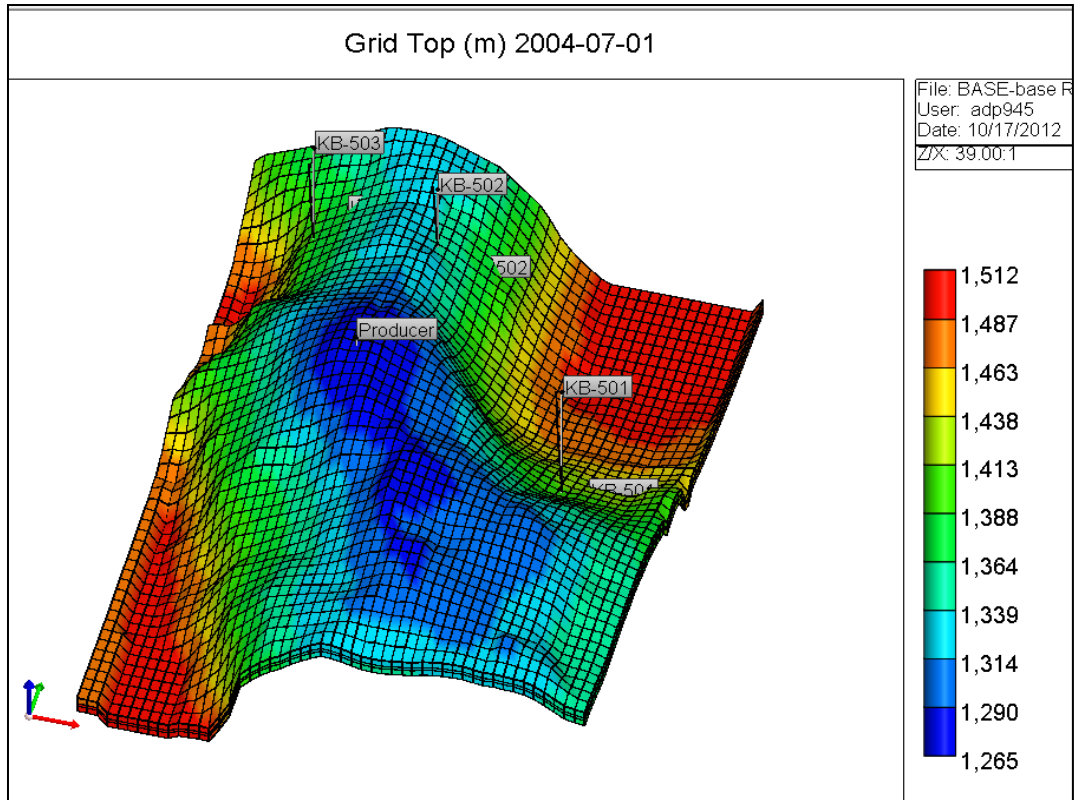


Figure 3.12: CMG-GEM model showing grid top

In the northern part of the Krechba field there are 3 injectors and 1 producer. These wells are irregularly spaced and are drilled in the down flank regions of the reservoir. The injectors are named KB-501, KB-502 and KB-503. Injection was initiated in 2004 in two wells KB-501 and KB-503 and a third well in 2005. Injection was stopped first in KB-502 in 2007 while KB-501 & KB-503 kept injecting till early 2009. In mid June 2007 it was observed that CO<sub>2</sub> was leaking from an abandoned well KB-5 located in-between KB-502 & KB-503. The expected migration path of the CO<sub>2</sub> plume was up dip in a direction away from KB-5. Deviation of the plume from this expected path indicates/suggests the presence of high permeability streak present in the direction of KB-5. This will be tested by performing a range of sensitivity cases representing different heterogeneous nature of permeability. Combined injection rate schedule is shown below in Figure 3.13.



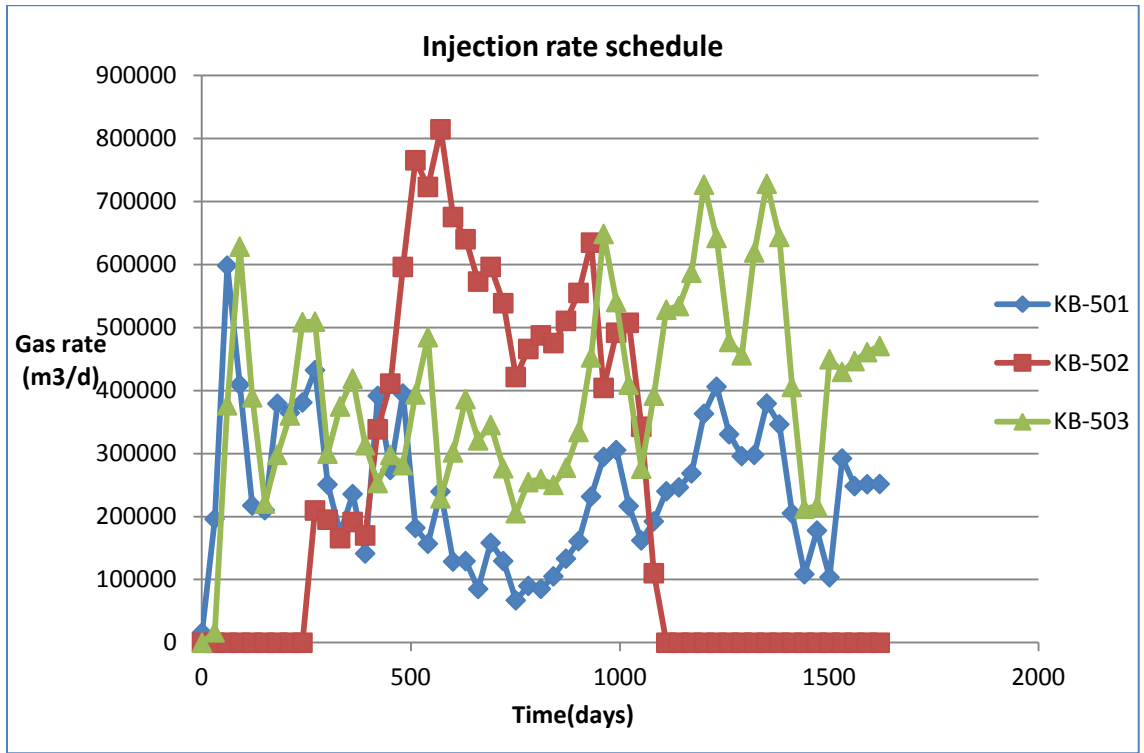


Figure 3.13: Combined injection rate schedule

KB-501 & KB-503 inject for a period of 55 months while KB-502 injects CO<sub>2</sub> for 28 months. The injection rates at these wells are fluctuating and are subjected to a maximum bottom hole injection pressure constraint of 1000000 Kpa. Modeling of the bottom hole pressure for KB-501 for a wide range of well head pressures and injection rates suggests that injection pressures may be above the 24 MPa injection pressure threshold established to limit upward fracturing into the C20 (Oldenburg et al, 2011). The injection pressure is monitored continuously at each well and reported on a daily basis. In CO<sub>2</sub> simulations, the movement of CO<sub>2</sub> plume during the injection phase is driven by viscous forces dominated by the heterogeneous permeability field. CO<sub>2</sub> will preferentially flow in the direction of high permeability zones. Subsequently when the injection is stopped, other forces such as capillarity, buoyancy may play a role. The main objective of this chapter is to investigate if the location/presence of the high permeability pathways indeed has an imprint on the injection pressure data so that inverse

modeling could have alerted the operators to possible deviation in the plume migration path prior to the leakage observed in the abandoned well KB-5.

In the model shown in Figure 3.9, the high permeability streak passes in-between the two injectors KB-502 and KB-503 and the producer. Hence we should observe its direct effect more on the bottom hole profile (BHP) of these two injection wells. We would expect the presence of high permeability streak should reduce the injection pressure significantly as compare to cases where we have a low permeability barrier or a streak of lower permeability value. Also the effect should be most on the wells close to the streak. Along with injection pressure and injection rate profile, gas saturation extent will also be analyzed to visualize the deviation in the plume migration path.

### **3.5.2 Sensitivity Cases**

#### **3.5.2.1 Permeability Sensitivity**

There are four different types of permeability variation considered here.

##### **1. Base Permeability Field with base injection rate:**

Base permeability is shown in Figure 3.14. This permeability map represents the permeability distribution for the northern part of the Krechba field. Several streaks of high permeability exist in the NW-SE direction with an average permeability value of 350md. The background permeability in this field is less than 10md. There are multiple high permeability streaks present in all the three layers but the analysis was done only for one particular streak passing in-between injectors KB-501, KB-502, KB-503 and the Producer.



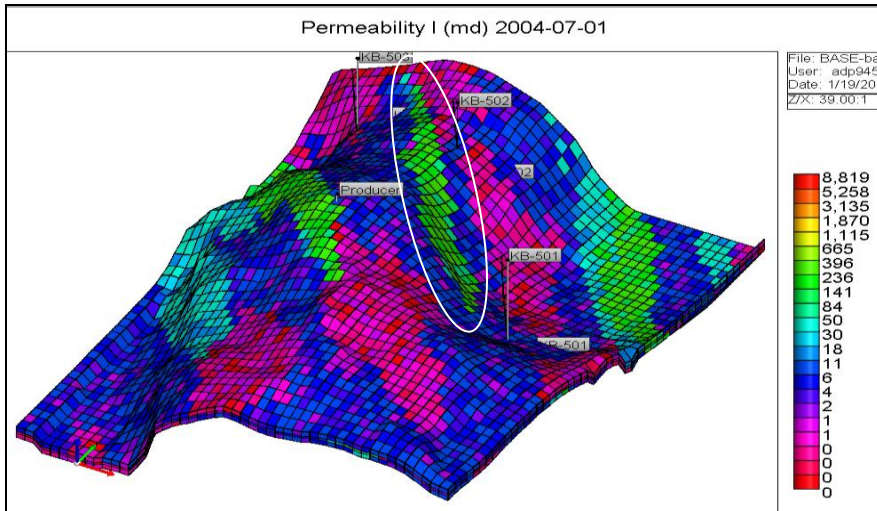


Figure 3.14: Map showing permeability distribution of the base case

#### Reference Injection rate:

The injection rate schedules at the three injectors for the base case is shown in Figure 3.13 corresponding to which the pressure profile during the injection period is shown in Figure 3.15.

Pressure profile for the base case at all the injectors is shown in Figure 3.15, 3.16 & 3.17.

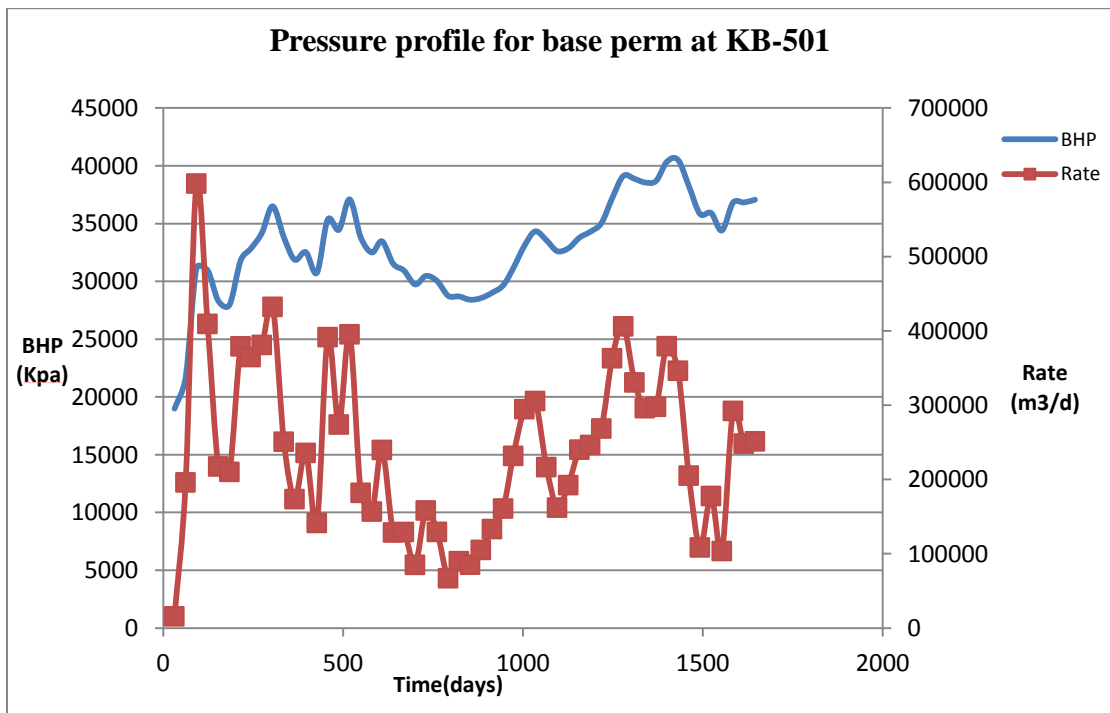


Figure 3.15 : Pressure profile for base injection rate at KB-501

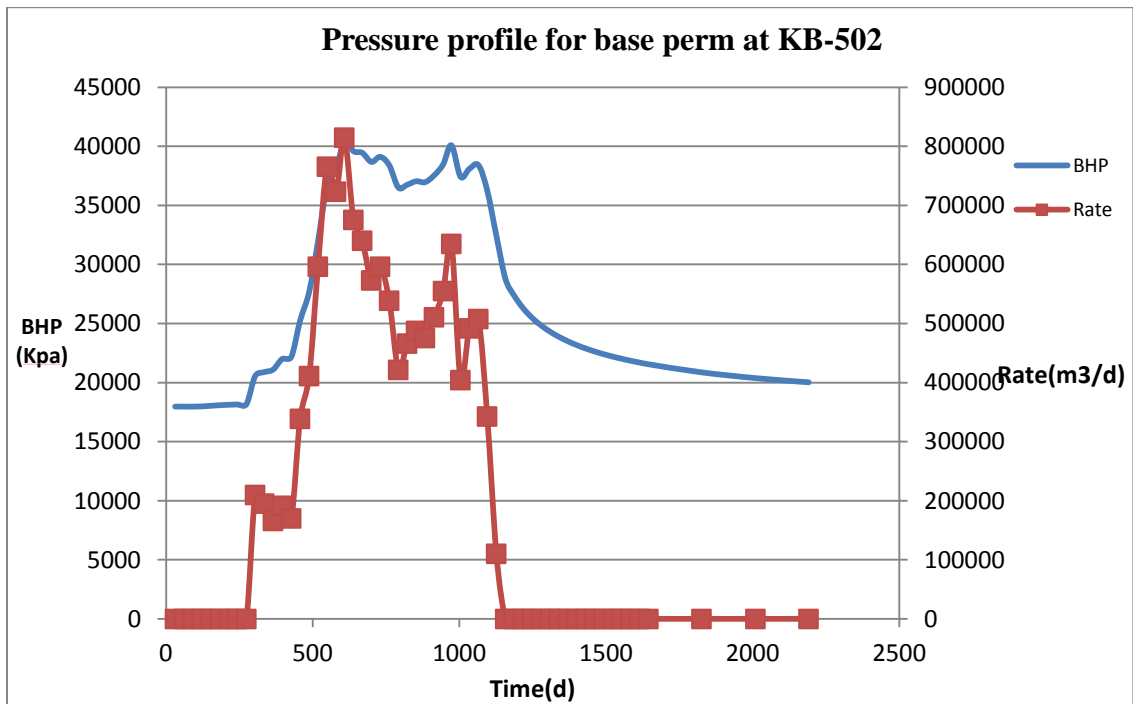


Figure 3.16 : Pressure profile for base injection rate at KB-502

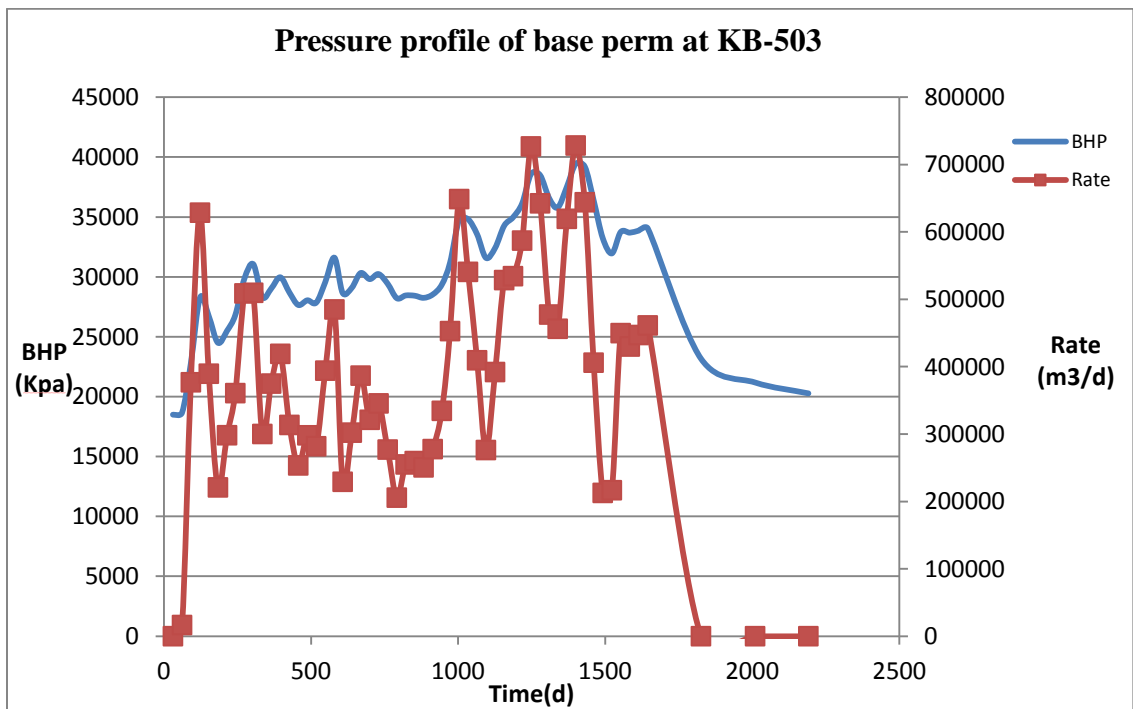


Figure 3.17 : Pressure profile for base injection rate at KB-503

## 2. High Permeability case

In order to check how the permeability of the streak affects the performance of a well, the base permeability streak was modified and changed to a high permeability streak with values of permeability ranging from a value of 30000-70000md. The mean value of permeability in the streak is 50000\_md.

The background permeability for all the other grid blocks was kept exactly the same as the base case. This is shown in Figure 3.18.

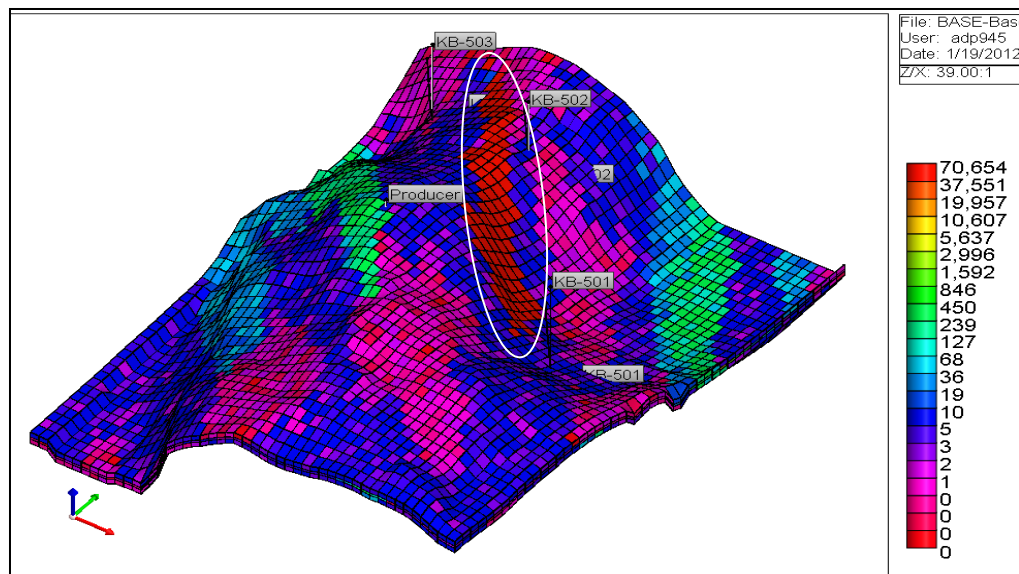


Figure 3.18: Map showing permeability distribution corresponding to the high permeability case

## 3. Low Permeability barrier

For the case representing a presence of a flow barrier near the injector, the base streak was changed to a low permeability streak. The value of permeability in the streak spanning between the injectors varies between 0-2md. Again background permeability distribution was kept constant. Map of low permeability distribution is shown in Figure 3.19.

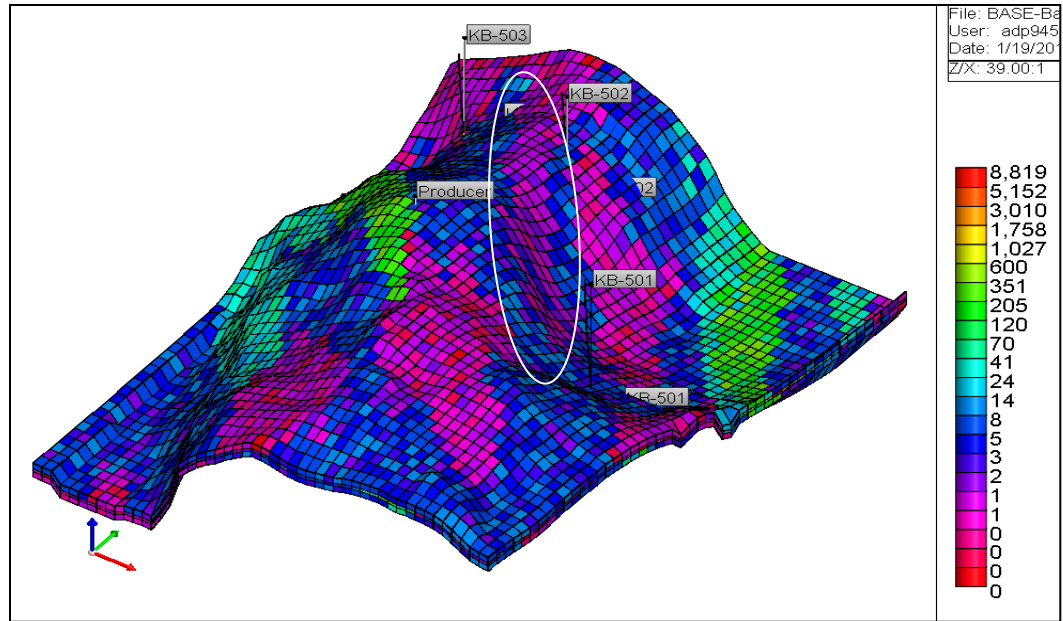


Figure 3.19: Map showing permeability distribution of the low permeability case

#### 4. No streak present

We will also consider a case where there is no characteristic streak present between the injectors and whole model is considered to be heterogeneous with a low average value. Permeability distribution is shown in Figure 3.20.

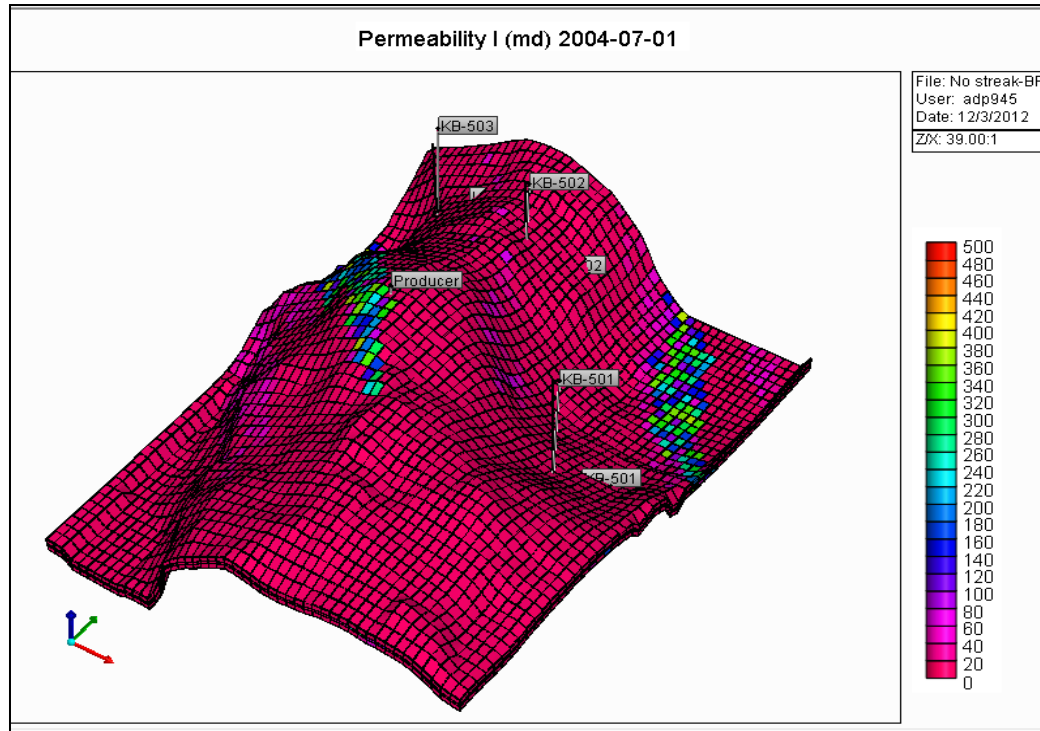


Figure 3.20 : Map showing permeability distribution for no streak case

### 3.5.3 Injection rate Sensitivity

The impact of reservoir heterogeneity on the well responses is likely sensitive to the magnitude of the injection rate fluctuations. When the fluctuations are small, the pressure perturbations triggered by permeability contrasts in the reservoir are likely to be dampened as opposed to when the injection rate fluctuations are substantial. For this reason, sensitivity cases corresponding to different injection rate profiles were performed.

#### 1. Base Injection rate

The injection rate schedules at the three injectors for the reference case are shown in Figure 3.13.

## 2. Double injection rate

The injection rates at each well are doubled over the same period of injection as in the base case and the resultant impact on BHP is studied. The double injection rate schedule is shown in figure 3.21.

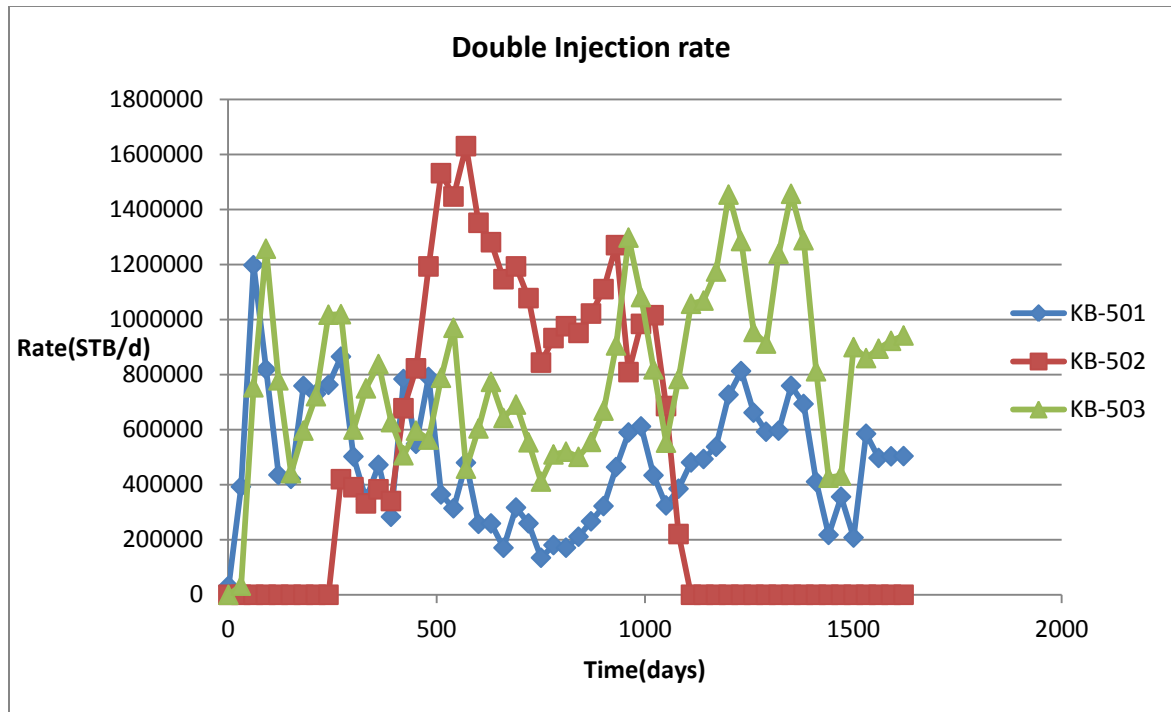


Figure 3.21: Injection rate schedule for double injection case

## 3. Random Injection rate

The same mean injection rate as the base case was assumed but the rate at which the fluctuations occurred was increased. The resultant rate profile is noisier as shown in Figure 3.22.

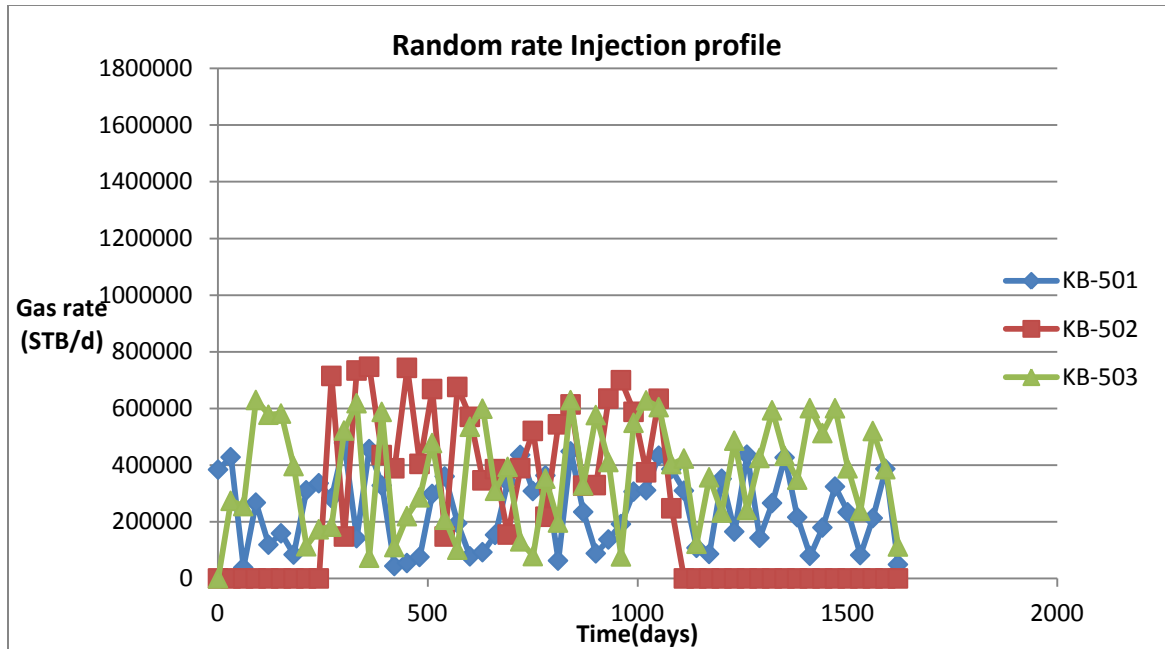


Figure 3.22: Injection rate schedule for random injection case

### 3.6 Result and analysis:

A wide range of sensitivity cases were run and pressure profiles were plotted along with injection rate to study the combined effect of heterogeneity and injection rate on well.

Keeping the same injection rate schedule, changes in permeability was made and results were plotted in Figure 3.23.

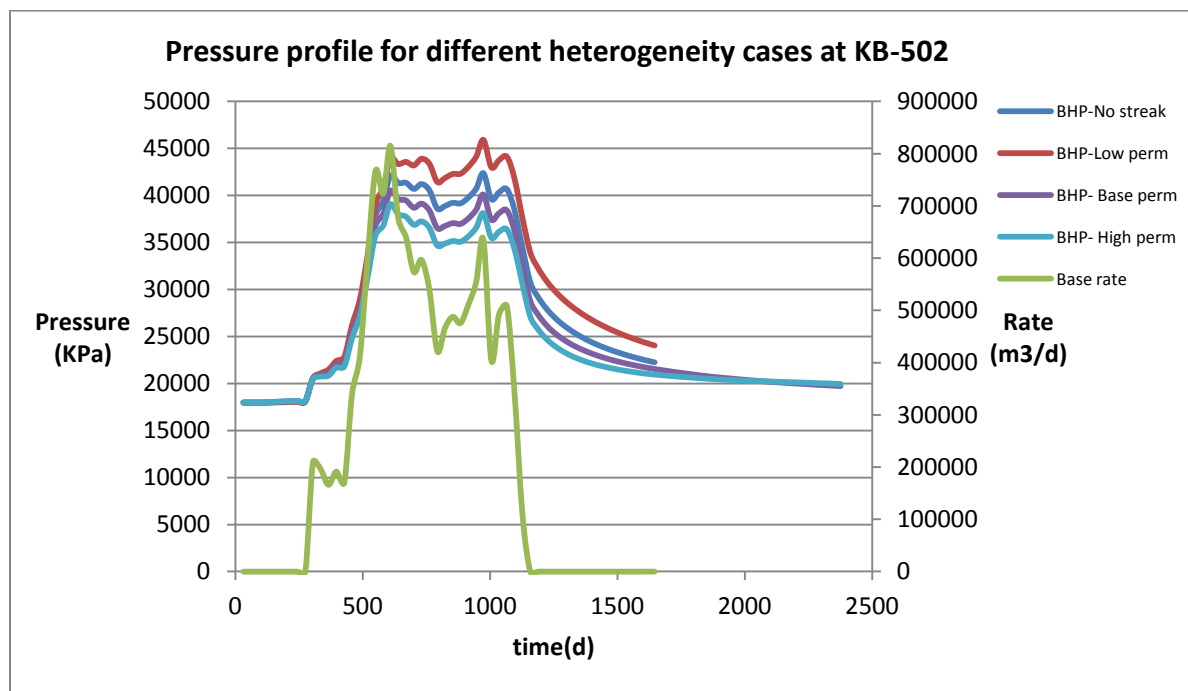
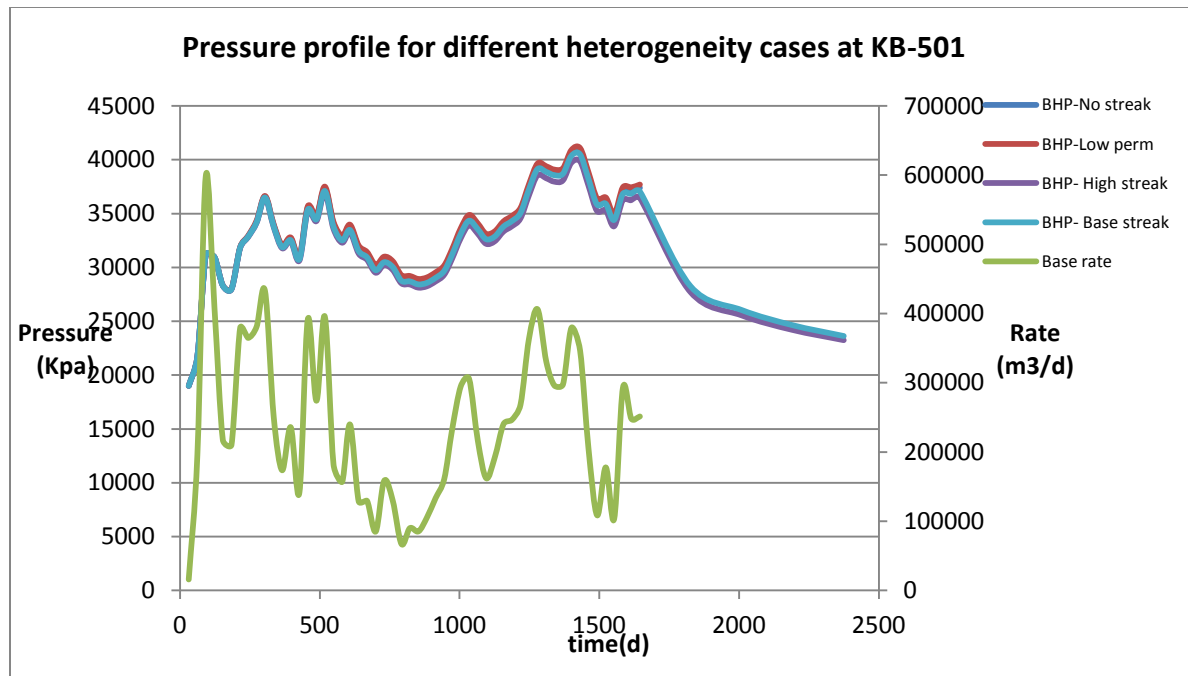


Figure 3.23: Pressure profiles for different permeability variations



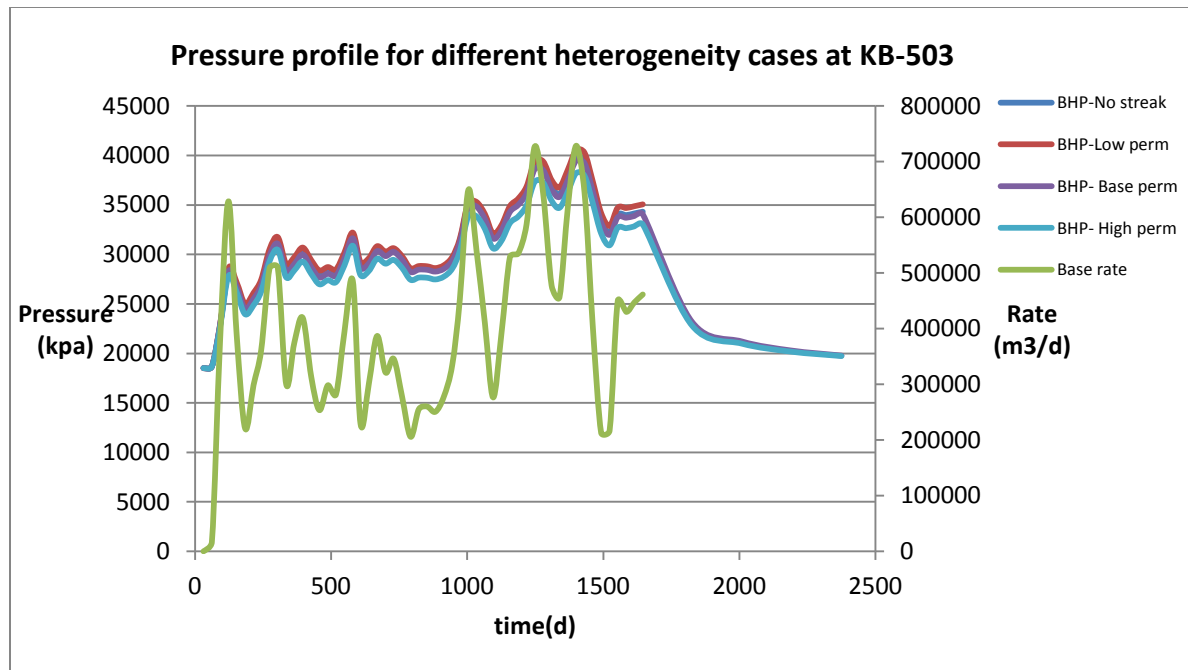


Figure 3.23: Pressure profiles for different permeability variations

Comparison of injection pressure between the reference case and different permeability cases shows that there is an imprint of the permeability distribution on well. Also inferred that most significant affect is on injector KB-502, which is located close to the streak as compare to the other injector. Since injector KB-501 is present relatively far from the streak the injection pressure profile is almost similar for all the three permeability variation and we observe no considerable changes in the pressure values.

One thing which is observed in all the three wells is that the presence of a high permeability streak reduced the injection pressure while presence of a low permeability barrier at the same location increases the injection pressure.

The effect of presence of permeability is also seen on the gas saturation profile. Figure 3.24 shows the saturation profile for different permeability heterogeneity. Clearly the high permeability streak is affecting the CO<sub>2</sub> migration. It is acting like a pathway to drive CO<sub>2</sub>. In case of a low permeability barrier, more dispersion is observed around the injector as there is no preferential path for CO<sub>2</sub> to migrate.

### Base Permeability case

### High Permeability case

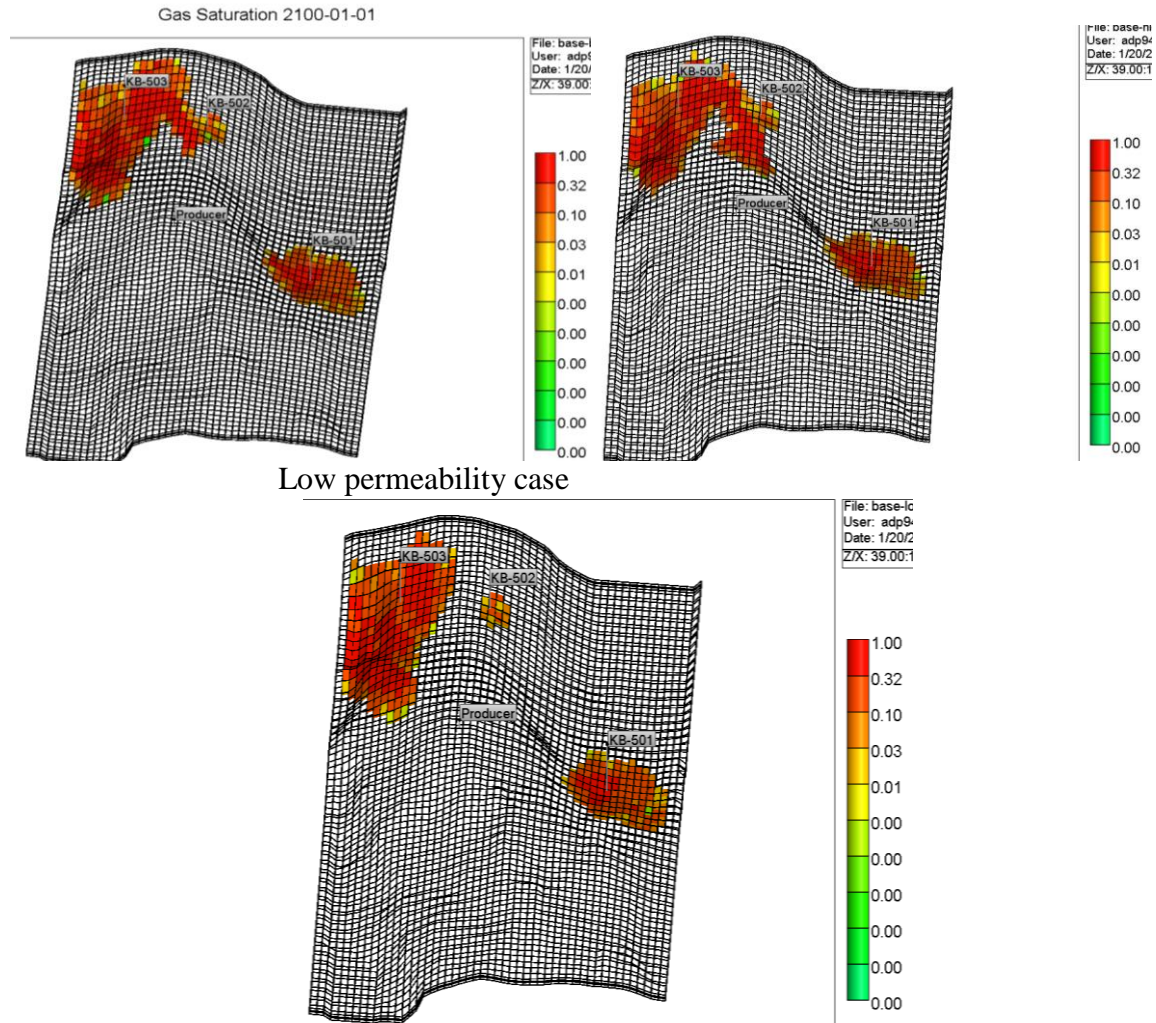


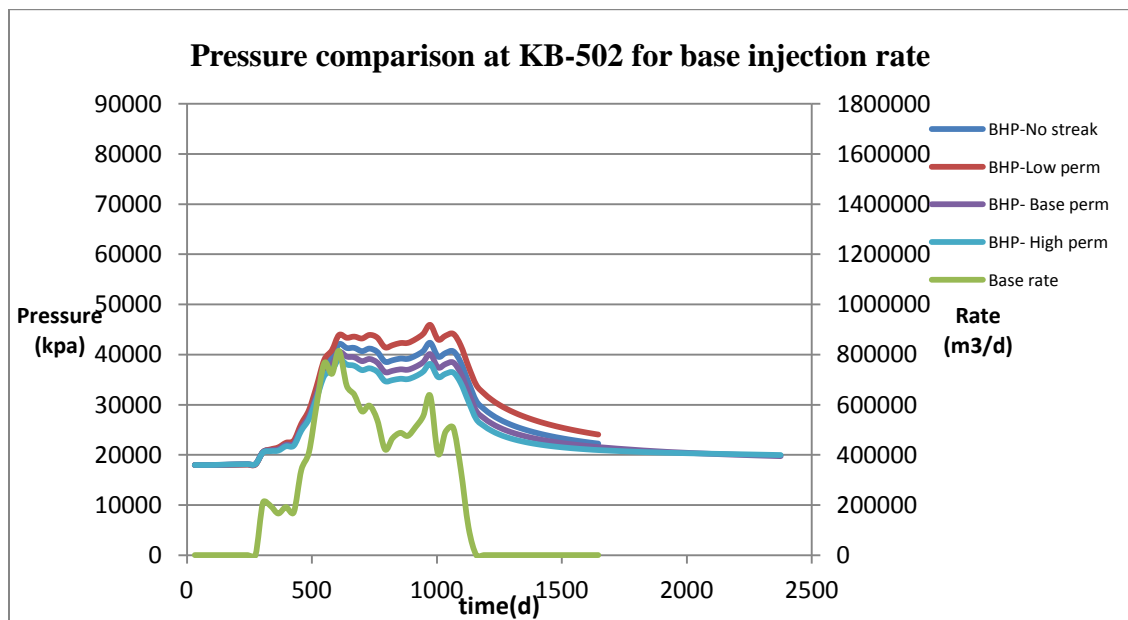
Figure 3.24: Gas saturation profile for 3 different permeability cases

The next step was to integrate the permeability pathways with injection rate variations. Since the affect of permeability is most significant on KB-502, sensitivity analysis of injection rate was studied exclusively for this well. Figure 3.25 shows the injection pressure profiles with 3 different permeability distribution and variations in injection rate. With base and double injection rate variation the injection pressure profile trend is similar, only the pressure values are doubled.

In random injection rate case, the low permeability field behaves in a slightly different fashion as compare to the base and high permeability case.

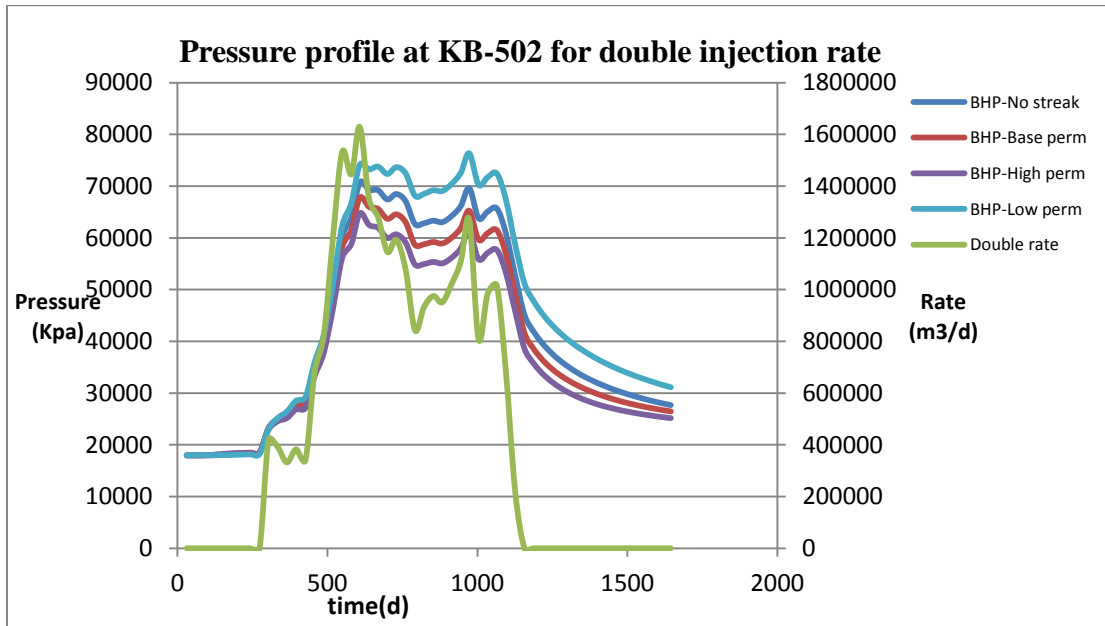
Quantitatively the similarity in the pressure curves at KB-502 can also be studied using a mathematical tool called Discrete Frechet distance (DFD) (Eiter and Manilla, 1994). DFD is a measure of similarity between polynomial curves that takes into account the location and ordering of the points along the curves. Higher the value of DFD, lesser is the similarity between the curves.

Figure 3.25 compares the pressure profiles at KB-502 for different permeability heterogeneity and injection rates.



Quantitatively they can be compared as

Curves	DFD Value
No streak and base perm streak	2102.1
No streak and high perm streak	3830.8
No streak and low perm barrier	3559.3



Curves	DFD Value
No streak and base perm streak	4306
No streak and high perm streak	6889
No streak and low perm barrier	5970

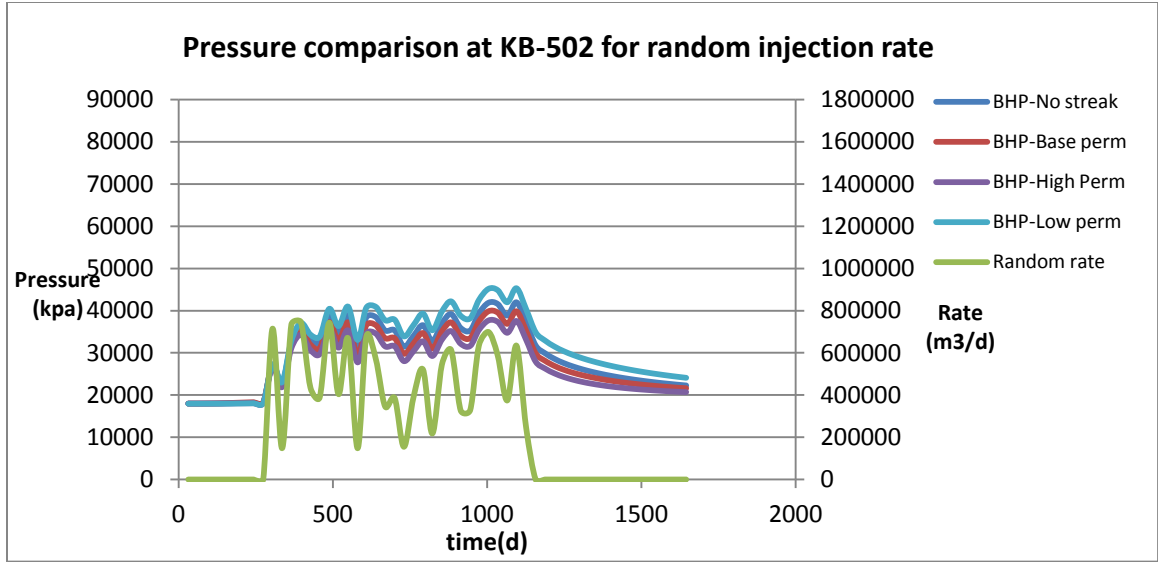


Figure 3.25: Pressure profile with 3 different permeability and injection variations

Curves	DFD Value
No streak and base perm streak	2115.6
No streak and high perm streak	4283.9
No streak and low perm barrier	3350.4

From the analysis of the pressure curves and DFD values corresponding to random injection rate it can be concluded that the effect of reservoir heterogeneity specially high and low permeability streak can be seen largely when there are rate fluctuations in the well. When the injection rate was doubled, the pressure curve as well as the DFD values correspondingly got doubled, but when more fluctuations were introduced in the rate, high permeability and low permeability feature impact injection pressure significantly with corresponding large value of DFD.

### 3.7 Conclusion:

Characterization reservoir heterogeneity is important for detailed understanding and optimization of production/injection of oil and gas. Reservoir can contain open channels or impermeable lithological units/barriers, heterogeneous porosity and permeability distribution that affect the injection well performance in different manner. There affect is significant on the fluid flow paths and migration.

The following are the conclusion based on a comparison of injection pressure between the base case with the high permeability case and the low permeability case.

- There is an effect of different permeability feature on the well injection response.
- The presence of a high permeability streak reduces the injection pressure while the presence of a low permeability barrier increases the bottom hole pressure significantly.
- The imprint of reservoir heterogeneity is clearly seen in wells present closer to the streaks as compare to wells that are relatively far.
- The identification of high permeability features established by history matching data for the In Salah filed wasn't incidental.
- Rate fluctuations (planned or otherwise) can provide considerable information about permeability distribution in the reservoir.

## **CHAPTER 4: ASSESSMENT OF RESERVOIR PARAMETERS USING INJECTION DATA**

### **4.1 Chapter Objective:**

The objective of the work described in this chapter is to analyze the BHP response at a well in order to infer reservoir parameters in the vicinity of a well. In order to accomplish this, we will use analytical well test equations and an optimization algorithm for estimation of reservoir parameters. We handle flow rate fluctuations using the principle of linear superposition and the case of multiple injectors using spatial superposition. In all these cases we consider single phase flow of CO<sub>2</sub> in an aquifer with constant pressure boundaries conditions. For this chapter we will study only homogenous reservoir with constant porosity, permeability and thickness in all the directions. Cases involving a single well as well as multiple wells will be considered. For multi-well injectivity analysis, superposition in space and time is used. In all these cases, estimation of reservoir parameters will be made with the use of an optimization technique known as the Dekker-Brent algorithm. The algorithm yields an optimal value of the desired reservoir parameters corresponding to a minimum value of the objective function within the tolerance specified. Objective function for the analysis is the square of the difference between on the pressure response obtained from the simulated model and the one obtained using well test equations. Standard injection well testing equations will be applied to define the objective function. It was pointed out in chapter 3 that there is an effect of injection rate fluctuations on the pressure response obtained at the well, which will be used in this chapter in order to estimate the value of some reservoir parameters and attributes keeping other reservoir and fluid parameters fixed. It was also shown in the previous chapter that permeability variations yield different pressure responses. Consequently, an effort will be made to relate the well test derived effective permeability values to the average permeability of the gas (CO<sub>2</sub>) swept region in the formation at the end of the injection period assuming different types of averaging.

## 4.2 Motivation and Method

For the assessment of permeability variations in the field using pressure transient analysis, two approaches can be applied. One approach is to guess a spatial distribution of permeability and solve for the pressure at the well corresponding to the spatial distribution. The permeability field is iteratively perturbed until a match to observed pressure response is obtained. According to Babadagli et al (2001), the permeability distribution can be generated using stochastic, simulated annealing and fractal geometry. Once we have quantified the permeability distribution, it can be correlated or matched to the pressure response.

The second approach is when we analyze the pressure transient test in a reservoir in order to derive values for reservoir attributes or parameter groups. Performing such analysis to a wide range of synthetic cases, we can gain an understanding of the influence of different types of reservoir heterogeneity on well pressure response.

In this chapter, the second approach described above is implemented and discussed. The synthetic pressure responses were obtained by running a forward model simulation using CMG-GEM and an optimization algorithm called the Dekker-Brent algorithm is used to yield optimal values of reservoir parameters pressure transient equations and concepts are used to compute the pressure response corresponding to different reservoir heterogeneities. Non-linear regression techniques along with constrained optimization methods have extensively been used in well test analysis. These procedures converge fast and enhance the parameter determination process. The procedure starts by holding the values of the unknown parameter in physically reasonable intervals. This interval is chosen on the basis of some prior knowledge based on geological, core and log analysis. Iterative numerical comparisons between the observed response and the calculated response obtained from the simulated model system with various updates of the parameter values are made. The iteration will end when a numerically acceptable tolerance is achieved. We obtained convergence for initial guesses four order of magnitude from the final estimate. The purpose of this chapter is to make a general comparison between cases exhibiting



different types of permeability distribution along with studying the effect of injection rate fluctuations.

We start the analysis by investigating a single well injecting at constant rate into a reservoir. In the subsequent section of this chapter we also apply the above algorithm for cases having multiple wells injecting both at constant rate as well as at fluctuating/multiple rates. In all the cases discussed in this chapter, CO<sub>2</sub> injection has been fixed for a continuous period of two years followed by 90 years of plume monitoring. The value of the best final estimate of the reservoir parameter obtained from the algorithm will be compared with the actual value to check the validity of the algorithm.

Following are the cases considered in this chapter:

- Homogenous reservoir with single well and constant injection rate
- Homogenous reservoir with single well and two-rate injection rate
- Homogenous reservoir with single well and multi varying injection rate
- Homogenous reservoir with multiple wells with constant injection rate at both the wells.
- Homogenous reservoir with multiple wells with variable injection rate at both the wells.

The reservoir parameters that we have tried to estimate in this chapter are average permeability ( $k$ ), average porosity ( $\Phi$ ), transmissibility ( $kh$ ), permeability to porosity ratio ( $k/\Phi$ ).

### 4.3 Dekker Brent Algorithm:

In this research, the estimation of reservoir parameters like  $k$ ,  $kh$ ,  $\Phi$  and  $k/\Phi$  constrained to geological and dynamic injection response is done using Dekker-Brent iterative optimization algorithm. In numerical analysis terms, it's a root finding algorithm that combines root bracketing, bisection and inverse quadratic interpolation. Brent(1973) explains that this algorithm will converge as long as the values of the function are computable within a given range containing a root. The algorithm yields an optimal value of the reservoir parameters corresponding to a minimum value of the objective function within the tolerance specified. The minimization of the objective function is possible for various combinations of the reservoir parameters. In such cases we will have multiple reservoir models representing the pressure response and hence non unique solution. In order to improve the robustness of the minimization algorithm, the estimation of a reservoir parameter will be carried out in two steps:

- First an estimate of an unknown reservoir parameter/attribute (Permeability “ $k$ ” and transmissibility “ $kh$ ”) will be made by specifying values of the other reservoir parameter (Porosity “ $\Phi$ ” and Permeability to porosity ratio “ $k/\Phi$ ”) and using the minimization technique.
- Once we have the estimated value of the unknown parameter, the known parameters will be then estimated using the estimated value and will be cross checked against the actual values for these parameters.

The Dekker-Brent algorithm has the advantage of being a non-gradient based approach that only requires the calculation of the objective function corresponding to different guesses of reservoir parameters as elaborated below.

#### 4.3.1 Iteration method:

First a three initial guesses for the reservoir parameter are selected and corresponding to these guesses, the objective function is calculated. Denoting these three guesses, objective function pairs as  $[x_1, f(x_1)]$ ,  $[x_2, f(x_2)]$  and  $[x_3, f(x_3)]$ . They are chosen such that  $x_1 < x_2 < x_3$  and  $f(x_1) > f(x_2)$  and  $f(x_2) < f(x_3)$  (i.e. in the form of a parabola). Brent's method uses a Lagrange interpolating polynomial of degree 2 which is given by:

$$x = \frac{[y - f(x_1)][y - f(x_2)] * x_3}{[f(x_3) - f(x_1)][f(x_3) - f(x_2)]} + \frac{[y - f(x_2)][y - f(x_3)] * x_1}{[f(x_1) - f(x_2)][f(x_1) - f(x_3)]} + \frac{[y - f(x_3)][y - f(x_1)] * x_2}{[f(x_2) - f(x_3)][f(x_2) - f(x_1)]}$$

Here “x” is the reservoir parameter in interest to be estimated. The estimated value of “x” with the minimized objective function is calculated by fitting an inverse parabola through these  $[x_1, x_2, x_3]$  points. The process start with an initial set of guess for  $[x_1, x_2$  and  $x_3]$  corresponding to which objective functions  $f(x_1)$ ,  $f(x_2)$  and  $f(x_3)$  is estimated. Then the real objective function corresponding to  $f(x)$  is calculated based on the above formula and set of three next points are selected  $[x_1, x_2, x]$  or  $[x_1, x, x_2]$  based on which condition in the algorithm is satisfied. In all cases the middle point of the new triplet is the abscissa whose ordinate is the best minimum achieved so far. In each iteration, these set of three points is updated with one corresponding to minimum calculated objective function and two adjacent points. The process of bracketing is continued until the distance between the outer points of the triplet is tolerably small and global minimum is reached.

The interpolation formula is also shown diagrammatically in Figure 4.1. The initial triplet of points is  $[a, b, c]$ . Hence we will start the minimization process by assuming that the function has a minimum in the interval  $(a, c)$ . New point,  $x$ , will be either between  $a$  and  $b$  or between  $b$  and  $c$ . Then we evaluate  $f(x)$  and based on the condition new bracketing triplets of points is

(a,b,x) or (b,x,c). In all cases the middle point of the new triplet is the abscissa whose ordinate is the best minimum achieved so far.

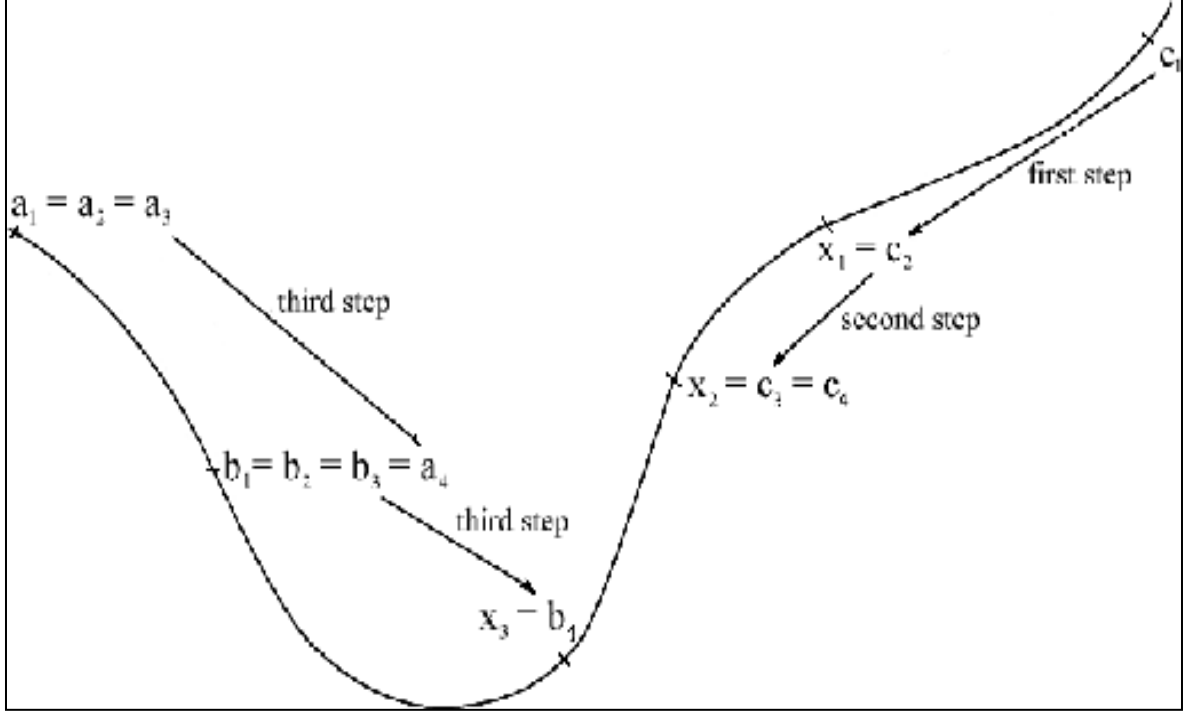


Figure 4.1: Process of successive bracketing of a minimum

The above figure illustrates the process of convergence of an objective function for a single parameter problem using the Dekker-Brent algorithm.

#### 4.4 Objective Function:

In this optimization algorithm, the objective function to be minimized is a measurement of square of the difference between the simulated injection response and the response from well test equation. The exponential integral solution of the line source flow model for pressure “P” and at location “r” and time “t” for a single well case can be written as

$$P_{wf} = P_i - \frac{162.6qB\mu}{kh} \left[ \log\left(\frac{kt}{\phi\mu cr_w^2}\right) - 3.23 \right]$$

The objective function will be developed using this equation. A wide range of different variables such as: single and multiple injection rates, permeability heterogeneity, number of wells has been considered when applying the algorithm. The square difference between the simulated pressure response and the response obtained using the well test equations are minimized in order to match the simulated pressure response during the injection period. The proposed objective function for “N” variables over a time step of  $\Delta t$  is given by

$$Obj\ func = \sum_{i=1}^n \sum_{j=1}^t (Press_{sim(i,t)} - Press_{welltest(i,t)})^2$$

Here  $Press_{sim(i,t)}$  represent pressure response from the simulation run of injection variable “i” at time “t” and  $Press_{welltest(i,t)}$  represents pressure response obtained from well test equation at the same time. The sum of the square of the difference between them is minimized.

$Press_{welltest}$  is calculated using the above well test equation.

$$Press_{welltest} = P_i - \frac{162.6qB\mu}{kh} [\log(\frac{kt}{\phi\mu cr_w^2}) - 3.23]$$

#### 4.4.1 The principle of Superposition:

For cases having multiple wells with varying injection rates, different set of well test equations are used and correspondingly the objective function is also modified. Well test equations are derived from diffusivity equation and because diffusivity equation is linear, multiple rate and multiple well problem can be considered by applying principle of superposition. Superposition in space stated that the total pressure drop at a well is the sum of the pressure change at that location by flow rate changes in all the well present in the reservoir.

Well test equation for superposition in space is given below

$$\Delta P_1(t, r) = \Delta P_1 + \Delta P_2 + \Delta P_3 + \dots$$

Where 
$$\Delta P(t, r) = \frac{141.2qB\mu}{kh} \sum_{j=1}^n q_j B_j P_d(t_d, r_d)$$

To illustrate an application of principle of superposition to varying flow rate following formula is used

$$\Delta P = \frac{141.2\mu}{kh} \sum_{j=1}^n \{q_j B_j - q_{j-1} B_{j-1}\} [p_d(t - t_{j-1})_d] + s$$

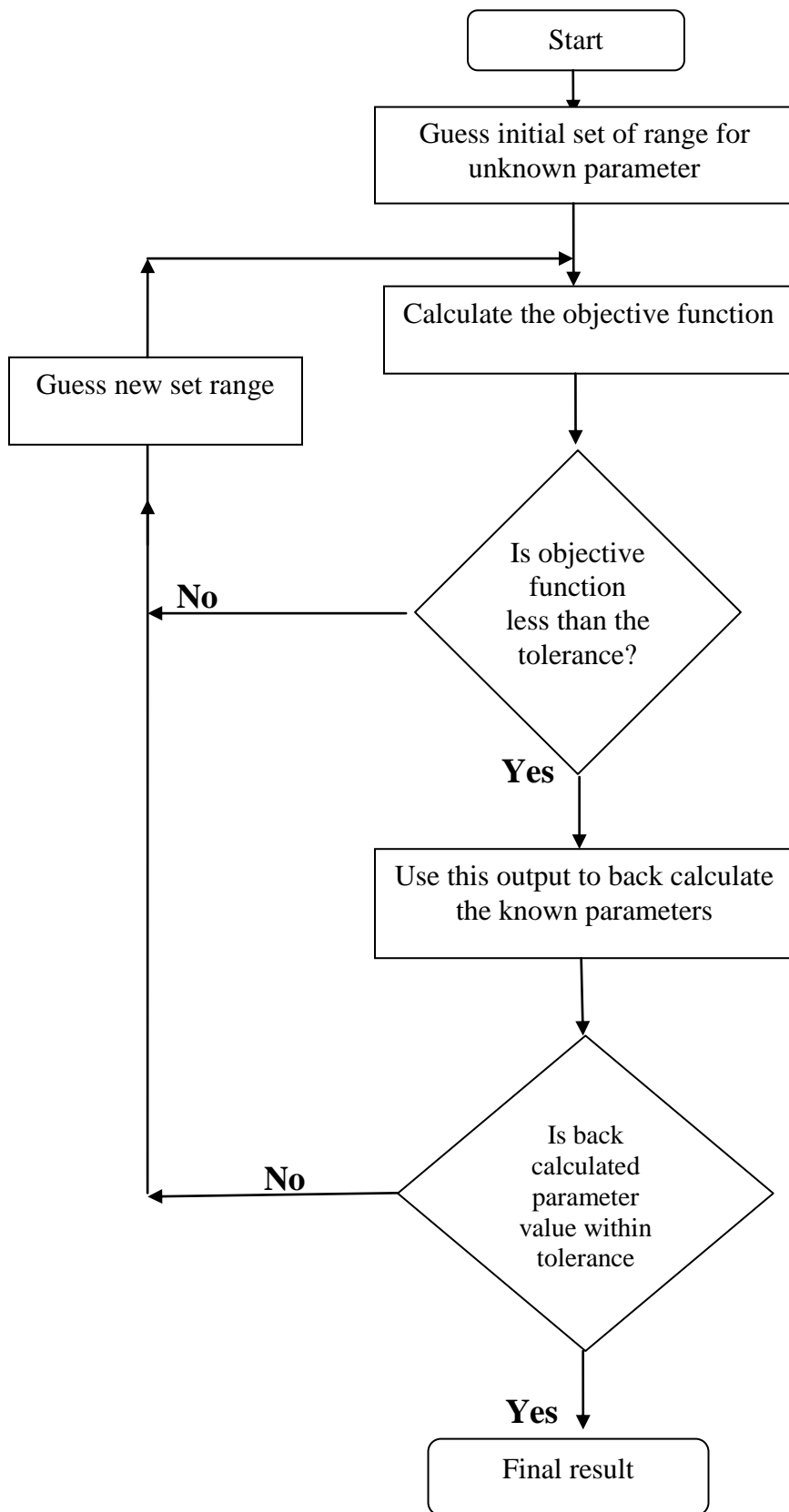
For these the objective function essentially remains the same, but the term incorporating the well test equation changes.

$$Obj\ func = \sum_{i=1}^n \sum_{j=1}^t (\Delta P_{sim(i,t)} - \Delta P_{welltest(i,t)})^2$$

where  $\Delta P_{sim(i,t)} = P_{wf} - P_i$

and  $\Delta P_{welltest(i,t)} = \sum_{i=1}^n \Delta P_i$

The process of minimization is summarized in a flowchart below in Figure 4.1.1



#### 4.5 Model of homogenous reservoir:

For describing the homogenous reservoir, a 3-D analytical model was developed in CMG-GEM. The numerical model is made up of 100\*100\*3 grid system with grid size of 50m\*50m\*8m. A homogenous isotropic reservoir with single and multiple wells are considered. The reference permeability field for all the cases discussed in this chapter will be totally homogenous and isotropic. These initial cases were set up to validate the solution method. Porosity distribution is also constant with a value of 0.2 in all cases. The reservoir is considered to be isothermal with constant temperature of 76°C. Number of wells will be varied from 1 to 3. The analysis will consider both constant rate injection as well as multi-rate injection schedule. The depth of top of the formation is 1290m with total thickness of 24m. The reference reservoir pressure is specified to be 17484.5Kpa at a reference depth of 1300m. In total 2 components are defined in the formation: CO<sub>2</sub> and H<sub>2</sub>O. Water-gas contact lies at 1350m, making the whole formation to be 80% saturated with CO<sub>2</sub> and 20% with water. Peng-Robinson EOS model is used to model the aqueous phase for flash calculation measurement. Pedersen's correlation (Pedersen and Fredenslund 1987) parameters were tuned to obtain the viscosities of CO<sub>2</sub> and brine. In addition high volume modifiers of 1000 are used on the boundary blocks to reduce the effect of boundary on the well performance. The injection strategy includes two years of injection of pure and supercritical CO<sub>2</sub> followed by 90 years of monitoring. The reservoir parameters considered for history matching purpose include permeability (k), porosity ( $\Phi$ ), and transmissibility (kh). All these properties are equally weighted in the objective function of the optimization algorithm. Figure 4.2 shows the grid top view of the model.



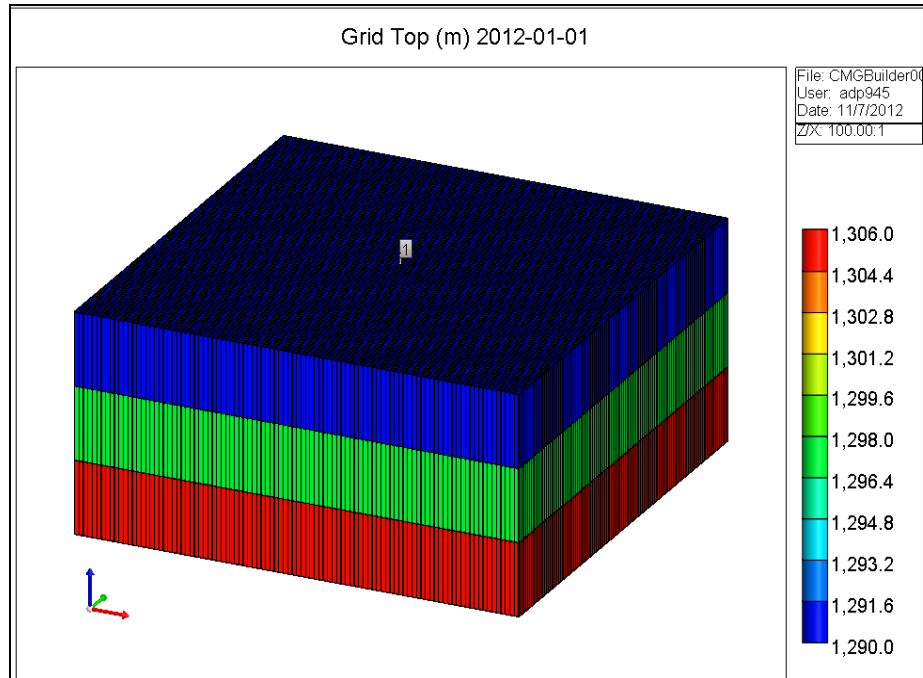


Figure 4.2: Shows grid top view of the simulator model with single injection well

Porosity and permeability distribution is shown in Figure 4.3 and 4.4.

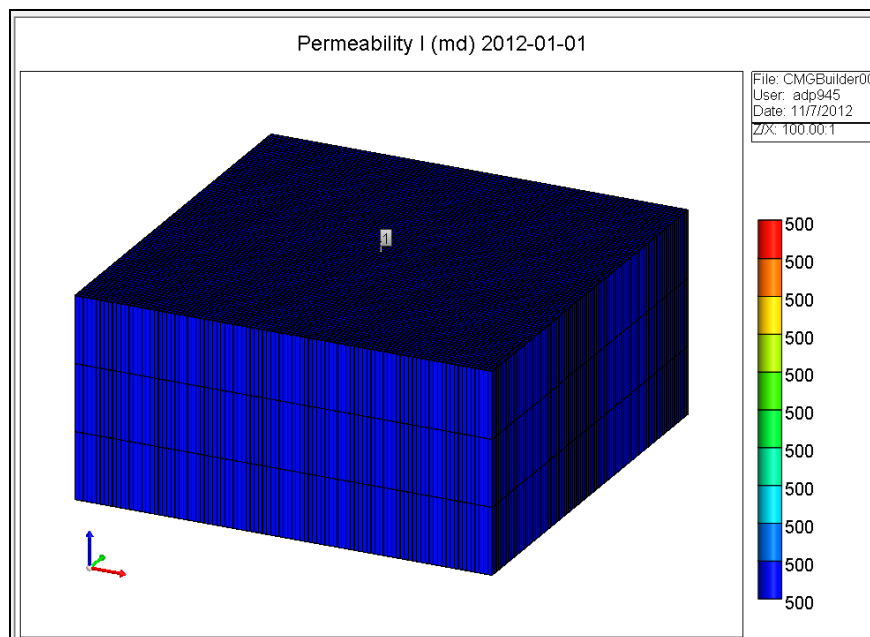


Figure 4.3: Represents homogenous permeability distribution in the field

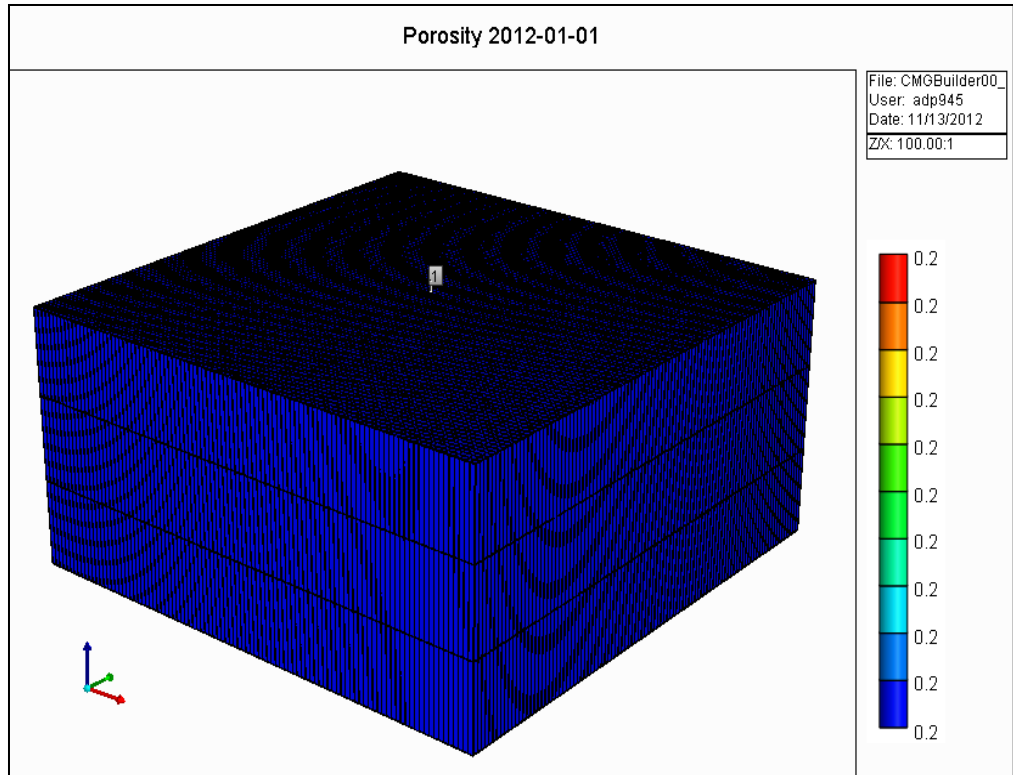


Figure 4.4: Represents homogenous porosity distribution in the field

The model properties are summarized in Table 1.

Simulation model description	Value
Simulator Model	CMG-GEM
Model dimensions	3D
Number of grids (Cartesian)	100*100*3 = 30000
Grid size, m <sup>3</sup>	50*50*8
Number of layers	3
Thickness of each layer (m)	8
Porosity ( $\Phi$ )	0.2
Permeability (md) $K_x = K_y = K_z$	500
Reservoir Temperature, °C	76
Number of injection wells	Single well tests- 1

	Multiple well tests – 2 or 3
Reservoir top depth, m	1290
Water-Gas Contact (WGC),m	1350
Reference depth, m	1300
Reference pressure @ 1300m, Kpa	17484.5
EOS Model	Peng-Robinson
Wellbore radius, $r_w$ , m	0.25 m
Injection fluid	CO <sub>2</sub>
Producer	None

Table 4.1: Summary of reservoir properties specified in CMG-GEM

## 4.6 Results and validation of code:

### 4.6.1 Single Well Tests:

#### 4.6.1.1 Case I: Homogenous isotropic single well reservoir with constant injection:

For this case the grid blocks in all the three layers are assigned a constant value of 500md and a constant porosity of 0.2. There is a single well in the reservoir with constant gas injection rate for 2 years. The well is then shut off and CO<sub>2</sub> migration is monitored over the following 90 years. Well pressure response and 3-D map of the extent of CO<sub>2</sub> migration are obtained. The pressure response obtained by simulation of this reservoir model will be used as an input into the Dekker-Brent algorithm in order to ascertain reservoir properties such as  $k$ ,  $\phi$ ,  $kh$ ,  $k/\phi$  using an inverse approach. Injection profile for this case is shown in Figure 4.5.

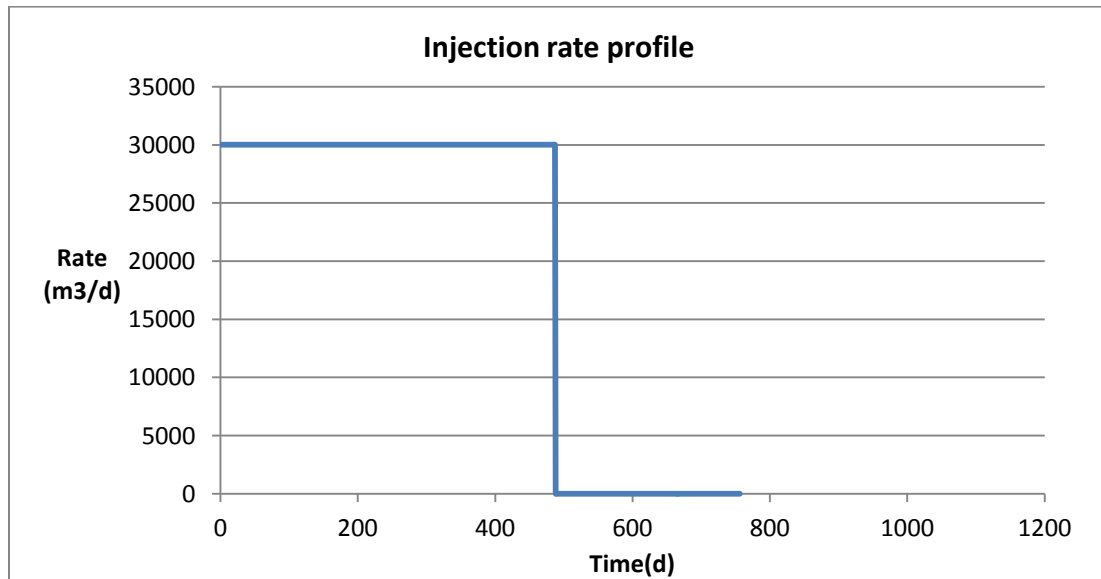


Figure 4.5: Injection rate profile for constant rate injection for a single well case

By running the algorithm we try to predict  $k$ ,  $kh$ ,  $\phi$ ,  $k/\phi$  constrained to knowledge of other parameters such as fluid compressibility, viscosity beforehand.

The following table compares the actual values to the outputs from the algorithm.

### 1. Estimation of average permeability

In order to find out the average permeability of the field, cases with different initial guesses for reservoir parameter were considered to check the robustness of the code. The actual value of porosity in the field is 0.2 and this value was doubled or halved and the corresponding average permeability that resulted in the best match was computed.

Case #	Unknown Parameter	Input value		Number of iterations	Actual value (md)	Code output (md)
	Average Permeability	Porosity $\Phi$	Total thickness H(ft)			
1	k	0.2	78.74	19	500	487
2	k	0.4	78.74	21	500	503
3	k	0.1	78.74	19	500	518

We conclude from the three different cases of different guesses of porosity that the average permeability of the reservoir is 502.66 md, which is similar to the actual value of 500md. Now with this permeability value, average porosity will be estimated using the same algorithm in order to check the validation of the code.

### 2. Estimation of average porosity using above average permeability

Unknown parameter	Average permeability (md)	Total thickness (ft)	Actual value	Code output
Porosity ( $\Phi$ )	502.66	78.74	0.2	0.22

The estimate of average porosity is also close to the input and correct. Hence we conclude that the code converges to the correct value when estimating the homogeneous permeability.

### 3. Estimation of transmissibility (kh)

For the estimation of the transmissibility (kh), the porosity  $\Phi$  is required to be known. In many reservoirs, both permeability and porosity as well as the reservoir thickness are unknown and in that case both the grouping – kh as well as  $k/\Phi$  are required to be estimated from the observed well test response. With an initial guess of  $k/\Phi$  the grouping “kh” can be calculated. The bulk volume of the reservoir “ $\Phi h$ ” is assumed known. Then the updated “ $k/\Phi$ ” is calculated by dividing “ $kh/\Phi h$ ”. If we get the updated value close to the starting value for “ $k/\Phi$ ” then the process is stopped, otherwise the updated value of “kh” is calculated using the updated “ $k/\Phi$ ” value. This process is summarized in the form of a flowchart in Figure 4.6.

Flowchart describing parameter group estimation:

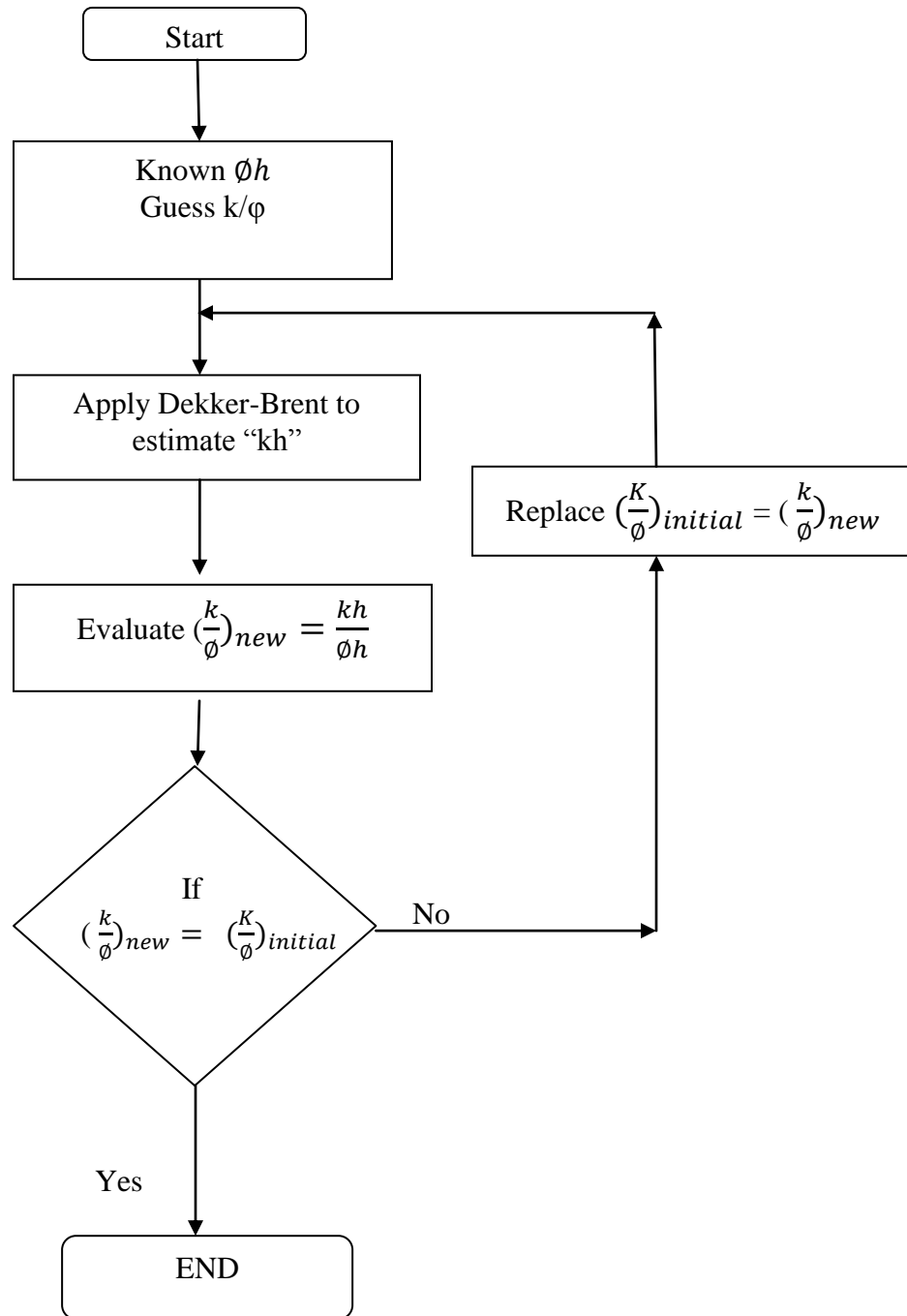


Figure 4.6: Generic workflow for estimating reservoir parameter group

For all the cases described in this chapter  $\Phi h$  has been assigned a value of 15.748 ft. Correct value for in all cases is  $kh = 39370$  md-ft and  $k/\Phi$  is 2500 md.

		Iteration Cycle 1		Iteration Cycle 2		Iteration Cycle 3	
Case #	Initial guess $k/\Phi$ (md)	Code estimate $kh$ (md-ft)	$Kh/\Phi h$ $=k/\Phi$ (md)	Code estimate $kh$ (md-ft)	$k/\Phi$ (md)	$Kh$ (md-ft)	$k/\Phi$ (md)
1	2500	39599	2514.54	39602	2514	39601	2514
2	5000	40796	2590.55	39661	2518	39603	2514
3	1250	38401	2438.46	39565	2512	39608	2516

Final reservoir estimates for Case I obtained from the algorithm are tabled below.

Parameter	Value estimated from algorithm	Actual value
Average Permeability (k), md	502	500
Average Porosity	0.22	0.2
Transmissibility (kh), md-ft	39600	39370

#### 4.6.1.2 Case II: Homogenous isotropic single well reservoir with two rate injection:

In practice, it is difficult to maintain a constant rate for a long period of time. Before investigating the effect of continuous rate fluctuations, we extend the single rate well test analysis in the previous section to a two-rate well test. For this case, the reservoir is homogenous with single well injecting at a two-rate schedule. The two-rate injection profile is shown in Figure 4.7.



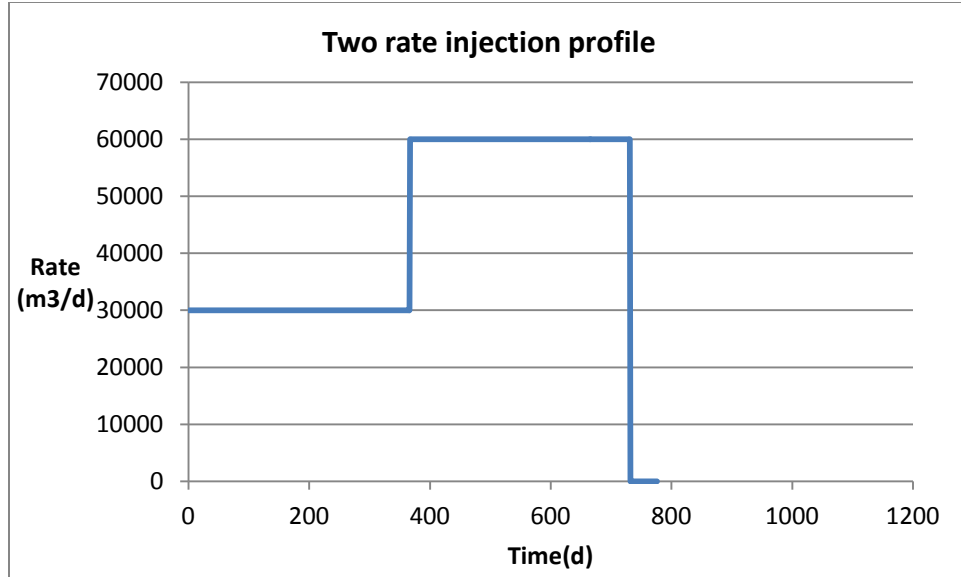


Figure 4.7: Two rate injection profile for single well field

Total duration of the injection period is 2 years followed by 90 years of monitoring. We try to predict reservoir parameters using the optimization algorithm described above.

The following table compares the actual values to the code outputs.

#### 1. Estimation of average permeability

Here again the same procedure is applied to evaluate values of the reservoir parameters. Unlike in the previous case where, parameter groupings were perturbed, in this case the objective was to estimate a single parameter: Permeability (k), assuming that the other parameters: Porosity ( $\Phi$ ) and thickness (h) are known.

Case #	Unknown Parameter	Input Value		Number of iterations	Actual value (md)	Code output (md)
	Average Permeability	Porosity $\Phi$	Total thickness H(ft)			
1	k	0.2	78.74	23	500	517

2	k	0.4	78.74	25	500	500
3	k	0.1	78.74	25	500	533

We conclude that given the uncertainty in our guess for porosity, the expected (average) value of permeability of the reservoir is 516 md, which is close to the actual value of 500md. Now with this permeability value, the average porosity will be estimated to check the correctness of the code.

## 2. Estimation of average porosity using above average permeability

Unknown parameter	Average permeability (md)	Total thickness (ft)	Actual value	Code output
Porosity ( $\Phi$ )	516	78.74	0.2	0.23

Judging by the results presented above, we conclude that the code converges to the correct value for two-rate injection profile.

## 3. Estimation of transmissibility (kh) :

Next we implemented the algorithm for estimating parameter groupings using the proposed optimization technique. We summarize the results in the following table.

Estimation of parameter groups using the optimization procedure is summarized below.

		Iteration Cycle 1		Iteration Cycle 2		Iteration Cycle 3	
Case #	k/ $\Phi$ (md)	kh (md-ft)	k/ $\Phi$ (md)	kh (md-ft)	k/ $\Phi$ (md)	kh (md-ft)	k/ $\Phi$ (md)
1	2500	40653	2581.4	40709	2585.02	40713	2585.2
2	5000	41885	2660	40764	2588	40714	2585.3
3	1250	39421	2503.23	40654	2581	40709	2585.02

Final reservoir estimates for Case II are listed below.

Parameter	Value estimated from algorithm	Actual value
Average Permeability (k), md	516	500
Average Porosity	0.23	0.2
Transmissibility (kh), md-ft	40710	39370

It must be emphasized that by application of the above algorithm, estimates for multiple uncertain attributes are obtained simultaneously. In actual reservoir modeling scenarios, it is likely that multiple attributes that impact the well response are unknown and uncertain. The procedure outlined above allows estimation of these multiple attributes while preserving the implicit dependencies between them.

#### **4.6.1.3 Case III: Homogenous isotropic single well reservoir with multi-rate injection:**

In this case a homogenous reservoir with single well injecting at fluctuating rate is considered. The fluctuations are planned to occur in every six months continuously for 2 years. Figure 4.8 shows the multiple rate injection profile.

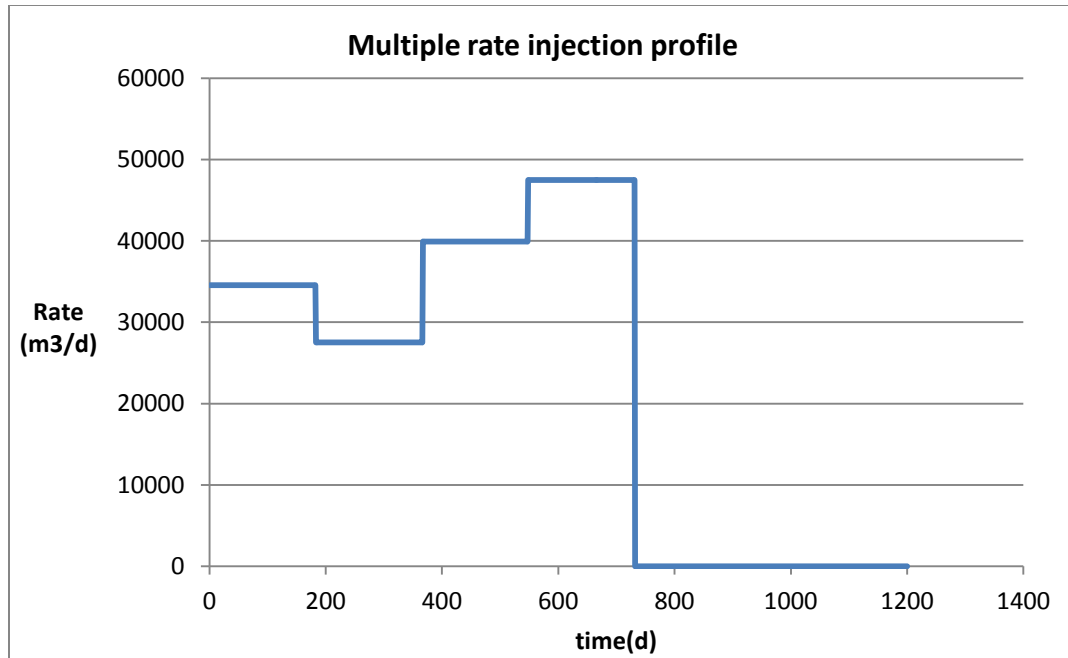


Figure 4.8: Multiple rate injection profile for a single well in a homogeneous reservoir.

#### 1. Estimation of average permeability

Case #	Unknown Parameter	Initial guess		Number of iterations	Actual value (md)	Code output (md)
	Average Permeability	Porosity $\Phi$	Total thickness H(ft)			
1	k	0.2	78.74	19	500	433.65
2	k	0.4	78.74	21	500	410
3	k	0.1	78.74	19	500	456

We observe here that the estimation is little underestimated and we get an average permeability value to be equal to 425 md. Tolerance limit is kept the same for this case, but final estimation comes out be underestimated due to the assumption of logarithmic approximation while solving the well test equation. This permeability value will be used to estimate the porosity value.

## 2. Estimation of average porosity using above average permeability

Unknown parameter	Average permeability (md)	Total thickness (ft)	Actual value	Code output
Porosity ( $\Phi$ )	425	78.74	0.2	0.2585

The porosity estimate is a little overestimated for Case III. This is because of the underestimated value of average permeability used within the optimization procedure.

## 3. Estimation of transmissibility (kh)

		Iteration Cycle 1		Iteration Cycle 2		Iteration Cycle 3	
Case #	k/ $\Phi$ (md)	kh (md-ft)	k/ $\Phi$ (md)	kh (md-ft)	k/ $\Phi$ (md)	kh (md-ft)	k/ $\Phi$ (md)
1	2500	34493	2190	34169	2170	34147	2168.3
2	5000	36191	2300	34290	2177	34155	2168.8
3	1250	32796	2082.5	34047	2162	34138	2168

Final reservoir estimates for Case III evaluated from algorithm are shown below.

Parameter	Value estimated from algorithm	Actual value
Average Permeability (k), md	425	500
Average Porosity	0.2585	0.2
Transmissibility (kh), md-ft	34150	39370

From the above results we conclude that the overall accuracy of the predictions is somewhat lower than for the single rate or two-rate cases. This could be because of numerical

errors incurred by making the logarithmic approximations to the infinite acting well test solution and that is subsequently used within the linear superposition.

#### **4.6.2 Multiple well tests:**

In this research, reservoir properties are determined by indirect measurements of two variables, well injection rate and well pressure. In actual reservoirs, multiple-well tests (interference and pulse tests) are used to establish communication between wells and determine the inter-well reservoir properties. Multiple-well tests are run to determine the presence or lack of communication between any two locations in the reservoir. In homogeneous isotropic reservoirs, multiple-well tests are conducted to determine the values of mobility-thickness product  $kh$  and porosity-compressibility- thickness product,  $\phi ch$ . For the homogeneous isotropic systems analyzed in this chapter, realistic and reasonably identical values of  $kh$  and  $\phi ch$  can be calculated from several tests in the same area. In addition, the value of  $kh$  calculated from interference tests should agree reasonably with those calculated from single-well tests. Hence we can compare results from this section with results from Case I, II and III.

##### **4.6.2.1 Case IV: Homogenous isotropic multiple well reservoir with constant rate injection:**

A scenario involving three wells injecting  $\text{CO}_2$  at constant rate into a homogeneous reservoir is considered first. The injection rate at all the three wells was maintained at 30000 m<sup>3</sup>/d and was kept constant for 2 continuous years. Pressure responses from these wells were obtained and used in the algorithm to estimate the reservoir parameters for regions around each well. Aerial view showing grid top and three wells is shown in Figure 4.9. The injection rate profile for all the wells is shown in Figure 4.10. The linear superposition principle will be used to compute the effect of fluctuations in the rate at a particular well on the bottom hole pressure at the same well as well the influence of rate fluctuations in other wells on the BHP of the well. The objective

function in this case takes into consideration, the square difference between the actual BHP at a well and the corresponding result obtained by linear superposition.

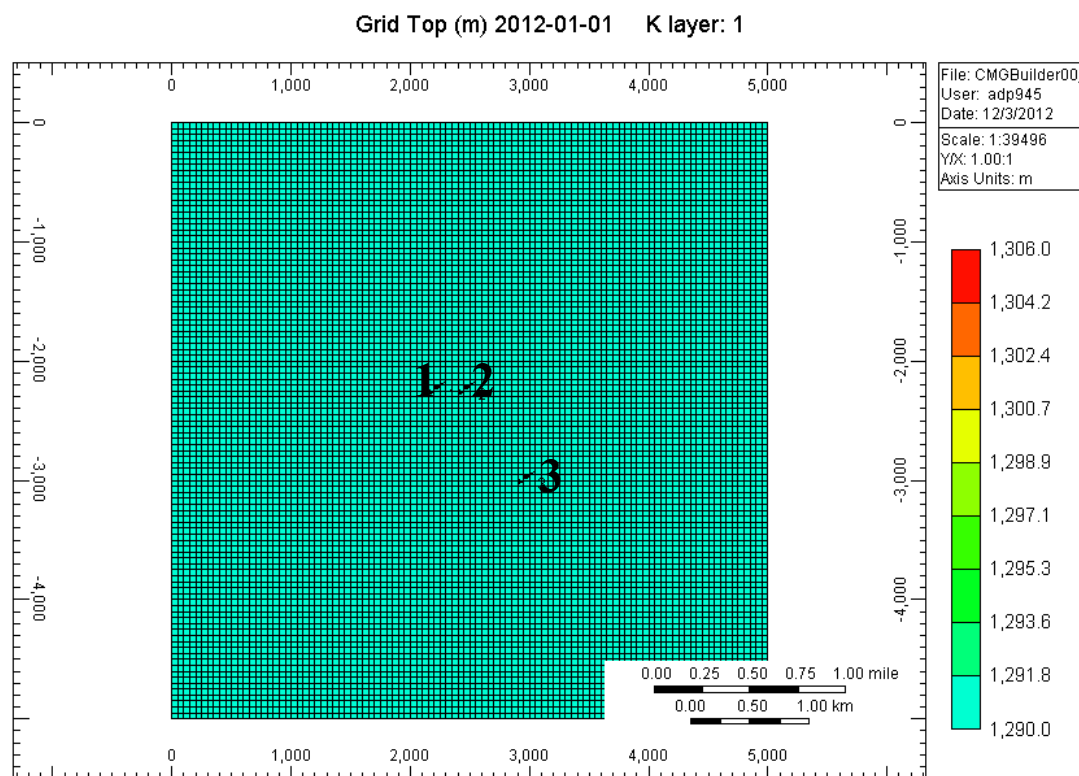
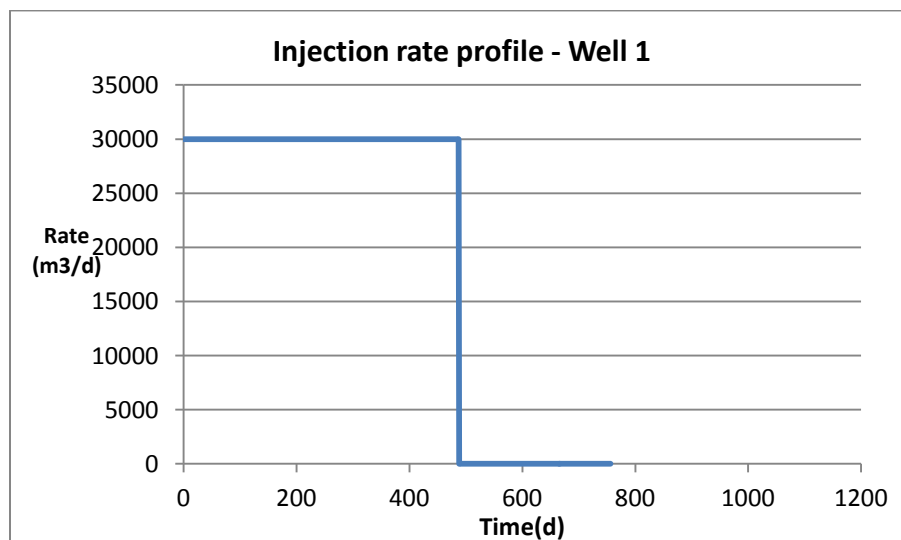


Figure 4.9: Aerial view of grid top model for multiple well field



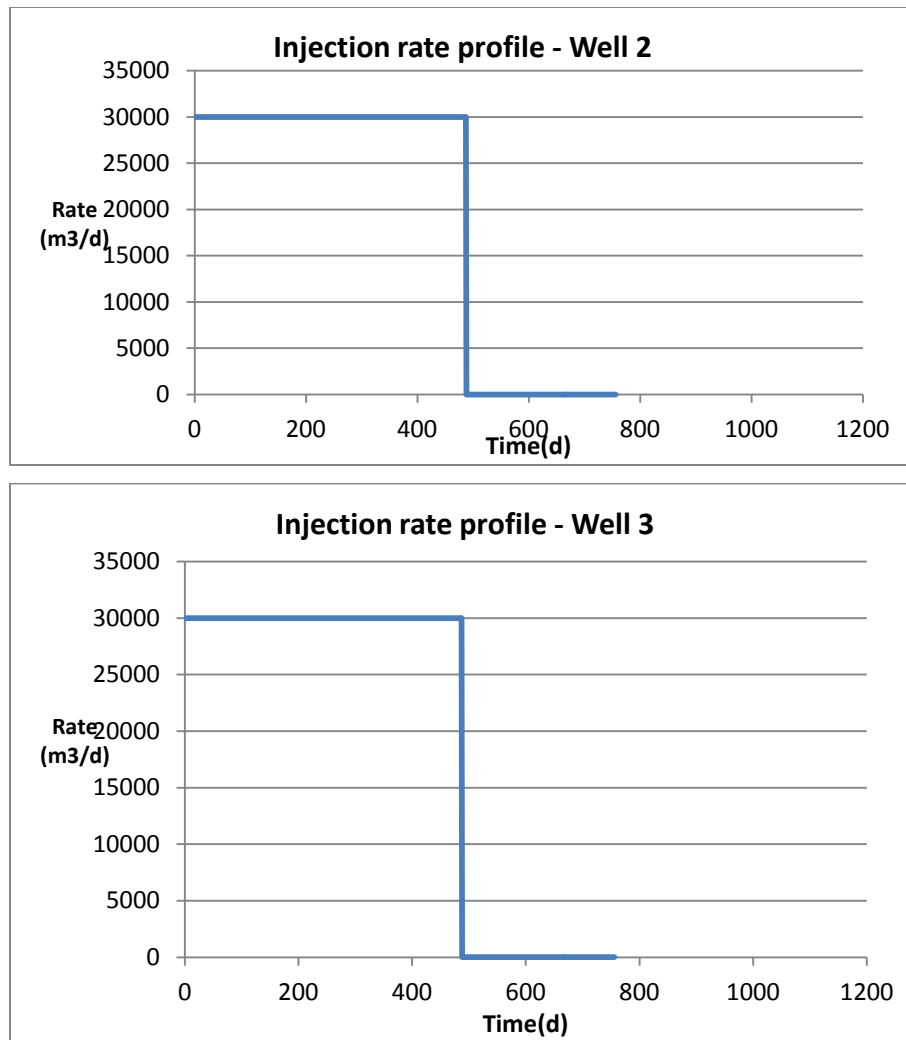


Figure 4.10: Constant and similar injection rate profile at three wells

1. Estimation of average permeability around the wells

Case #	Unknown Parameter	Initial guess		Iterations	Actual value (md)	Code output (md)		
		Porosity $\Phi$	Total thickness H(ft)			@ well 1	@well 2	@well 3
1	k	0.2	78.74	21	500	557	555	500
2	k	0.4	78.74	22	500	521	518	465
3	k	0.1	78.74	21	500	595	593	540



Average permeability (k), md		550	550	500
------------------------------	--	-----	-----	-----

## 2. Estimation of average porosity using above average permeability

Well	Unknown parameter	Average permeability (md)	Total thickness (ft)	Actual value	Code output
@ well 1	Porosity ( $\Phi$ )	550	78.74	0.2	0.2317
@ well 2	Porosity ( $\Phi$ )	550	78.74	0.2	0.221
@ well 3	Porosity ( $\Phi$ )	500	78.74	0.2	0.2119

From the values obtained for this case, we can infer that the homogenous properties for the reference case are reasonably well estimated using the optimization procedure. The combination of the Dekker-Brent optimization procedure and the linear superposition principle yields correct answers.

## 3. Estimation of transmissibility (kh)

@ Well 1

		Iteration Cycle 1		Iteration Cycle 2		Iteration Cycle 3	
Case #	k/ $\Phi$ (md)	kh (md-ft)	k/ $\Phi$ (md)	kh (md-ft)	k/ $\Phi$ (md)	kh (md-ft)	k/ $\Phi$ (md)
1	2500	35719	2268	35380	2246	35346	2244
2	5000	38260	2429	35617	2261	35369	2245
3	1250	33422	2122	35151	2232	35325	2243

@ Well 2

		Iteration Cycle 1		Iteration Cycle 2		Iteration Cycle 3	
Case #	k/ $\Phi$ (md)	kh (md-ft)	k/ $\Phi$ (md)	kh (md-ft)	k/ $\Phi$ (md)	kh (md-ft)	k/ $\Phi$ (md)
1	2500	35311	2242	34936	2218	34899	2216
2	5000	37823	2401	35170	2233	34921	2217
3	1250	33039	2097	34708	2203	34875	2214

@ Well 3

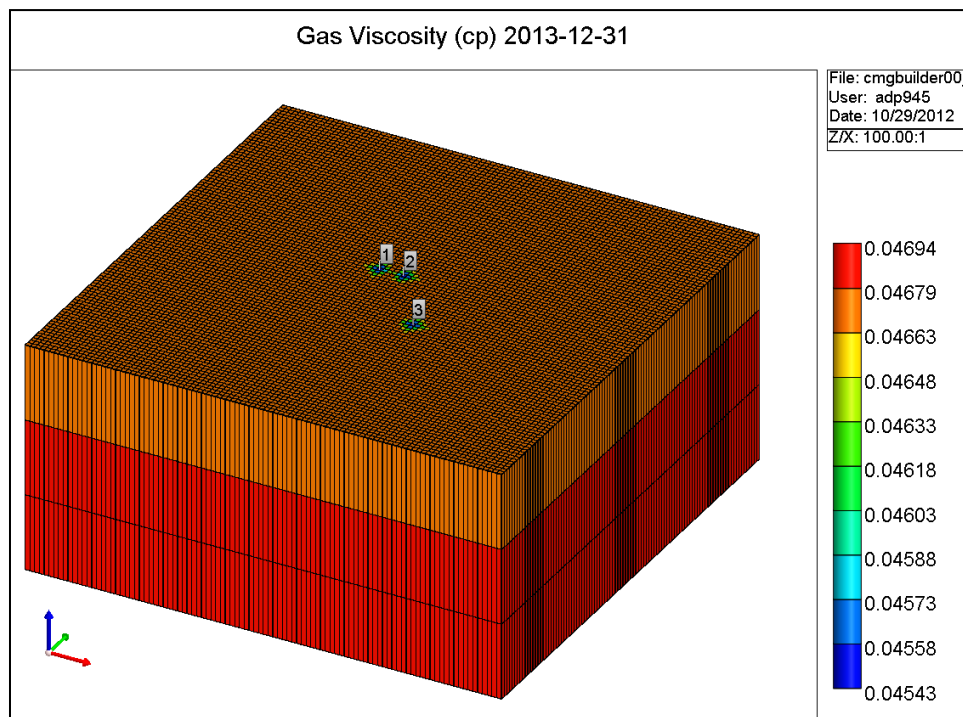
		Iteration Cycle 1		Iteration Cycle 2		Iteration Cycle 3	
Case #	k/ $\Phi$ (md)	kh (md-ft)	k/ $\Phi$ (md)	kh (md-ft)	k/ $\Phi$ (md)	kh (md-ft)	k/ $\Phi$ (md)
1	2500	39454	2505	39462	2505	39462	2505
2	5000	42263	2683	39729	2500	39489	2507
3	1250	36918	2344	39206	2489	39438	2504

Transmissibility estimation at three wells shows that at well 1 and 2, the value is little underestimated while at well 3, the result is very close to the actual answer. Since well 1 and 2 are very close to each other, interference between them affects the estimation. Interference effect is much lesser on well 3 as it's far from both the wells. The same reason can be applied to higher estimation of individual parameters at well 1 and 2 shown above.

Final estimations are shown below.

Parameter	Value estimated from algorithm	Actual value
Average Permeability (k), md	533	500
Average Porosity	0.22	0.2

The gas swept region is shown in Figure 4.11. The extent of migration is same in all the wells which is due to the fact that the reservoir and injection conditions is same everywhere.



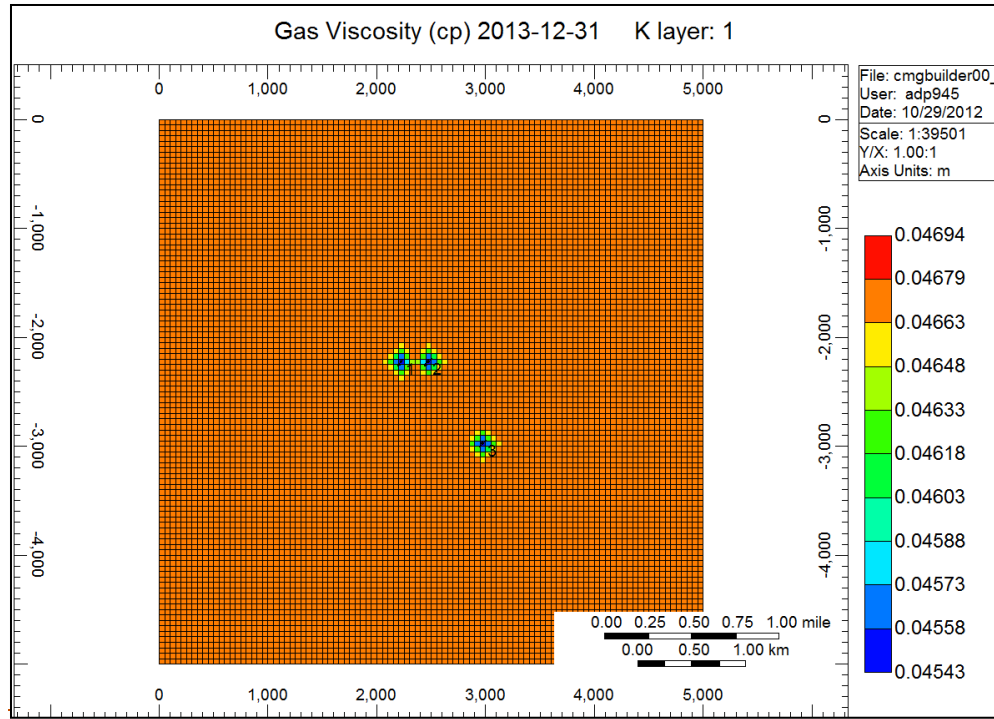


Figure 4.11: Shows gas viscosity map of the field at the end of the injection period

#### 4.6.2.2 Case V: Homogenous isotropic multiple well reservoir with multiple rate injection:

The model developed for this case has three injection wells injecting at different fluctuating rate. The aerial model for this field is shown in Figure 4.9. Well injection profile is shown in Figure 4.12. All three wells are injecting CO<sub>2</sub> for two years, with well 2 injecting cumulatively the most CO<sub>2</sub> at the end of injection period.

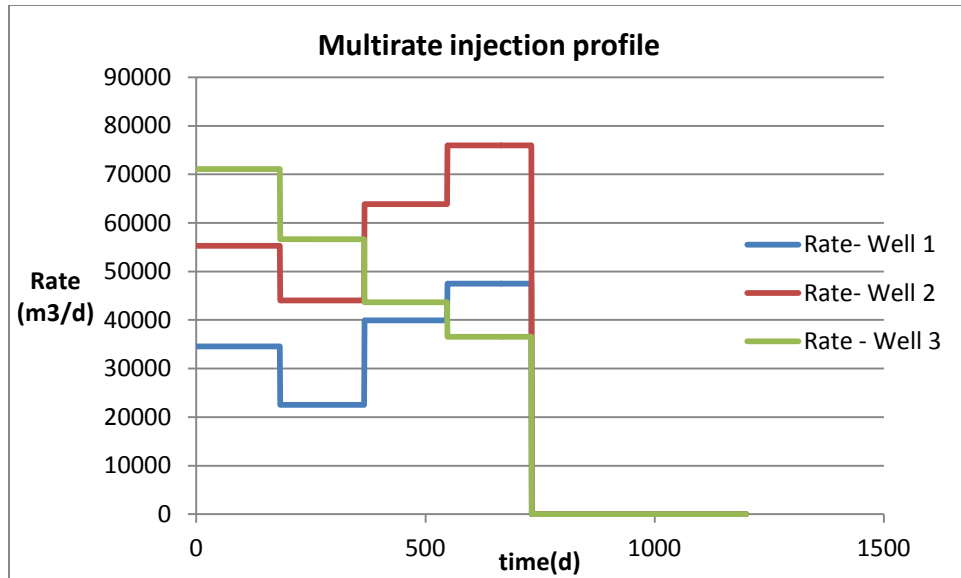


Figure 4.12: Multiple rate injection profile at wells 1, 2 and 3

#### 1. Estimation of average permeability

Case #	Unknown Parameter	Initial guess		iterations	Actual value (md)	Code output (md)		
		Porosity $\Phi$	Total thickness H(ft)			@well 1	@ well 2	@ well 3
1	k	0.2	78.74	23	500	507	489	508.46
2	k	0.4	78.74	25	500	502	519	490
3	k	0.1	78.74	15	500	525	482	523
Average permeability (k), md						511	497	507

We conclude from the three different cases of different guesses of porosity that the average permeability of the around well 1 is 511 md , well 2 is 497 md and around well 3 is 507

md, which is close to the actual value of 500md. Now with this permeability value, we estimate the average porosity.

## 2. Estimation of average porosity using above average permeability

Well	Unknown parameter	Average permeability (md)	Total thickness (ft)	Actual value	Code output
@ well 1	Porosity ( $\Phi$ )	511	78.74	0.2	0.233
@ well 2	Porosity ( $\Phi$ )	497	78.74	0.2	0.2055
@ well 3	Porosity ( $\Phi$ )	507	78.74	0.2	0.2033

The estimate of average porosity around all the three wells is close to the actual value.

## 3. Estimation of transmissibility (kh)

Since it's a homogenous reservoir estimate of “kh” and “k/ $\Phi$ ” should be similar for all the wells. In the cases described in this chapter  $\Phi h$  has been assigned a value of 15.748 ft. Correct value for kh is 39370 md-ft and k/ $\Phi$  is 2500 md.

@ Well 1

		Iteration Cycle 1		Iteration Cycle 2		Iteration Cycle 3		Iteration Cycle 4	
Case #	k/ $\Phi$ (md)	kh (md-ft)	k/ $\Phi$ (md)	kh (md-ft)	k/ $\Phi$ (md)	kh (md-ft)	k/ $\Phi$ (md)	Kh (md-ft)	k/ $\Phi$
1	2500	36082	2291	35118	2230	34820	2211	34726	2205
2	5000	43730	2776	37237	2364	35464	2251	35000	2212
3	1250	39509	2508	36805	2290	35782	2272	35693	2266

@ Well 2

		Iteration Cycle 1		Iteration Cycle 2		Iteration Cycle 3		Iteration Cycle 4	
Case #	k/ $\Phi$ (md)	kh (md- ft)	k/ $\Phi$ (md)	kh (md- ft)	k/ $\Phi$ (md)	kh (md- ft)	k/ $\Phi$ (md)	kh (md- ft)	k/ $\Phi$ (md)
1	2500	38671	2455	38543	2447	38520	2446	38518	2445
2	5000	43546	2765	39380	2500	38671	2455	38515	2445
3	1250	33797	2146	37597	2387	38346	2434	38483	2443

@ Well 3

		Iteration Cycle 1		Iteration Cycle 2		Iteration Cycle 3		Iteration Cycle 4	
Case #	k/ $\Phi$ (md)	kh (md- ft)	k/ $\Phi$ (md)	kh (md- ft)	k/ $\Phi$ (md)	kh (md- ft)	k/ $\Phi$ (md)	kh (md- ft)	k/ $\Phi$ (md)
1	2500	37484	2380	37210	2362.8	37167	2360	37162	2360
2	5000	41350	2625	37756	2397	37249	2365	37174	2360
3	1250	33618	2134	36601	2324	37077	2354	37148	2359

The transmissibility estimation at well 2 and 3 is close to the actual value while at well 1, the estimation is slightly underestimated. Interference between the wells, numerical error, assumptions made while calculations are the reason for slight underestimation.

Final values for this case are listed below.

Parameter	Value estimated from algorithm	Actual value
Average Permeability (k), md	@ Well 1 = 511	500
	@ Well 2 = 497	
	@ Well 3 = 507	
Average Porosity	@ Well 1 = 0.233	0.2
	@ Well 2 = 0.2055	
	@ Well 3 = 0.2033	
Transmissibility (kh), md-ft	@ Well 1 = 35000	39370
	@ Well 2 = 38500	
	@ Well 3 = 37150	

#### 4.7 Conclusion:

The Dekker-Brent algorithm for determining an optimum set of estimates of reservoir parameters that yield a response close to the reference pressure. Once again it is emphasized that the novel procedure described in this chapter yields simultaneous estimation of multiple reservoir parameters that impact the observed response. Application of this approach to reservoirs having injection of CO<sub>2</sub>, yield satisfactory results. The use of injection data coupled with pressure transient analysis for cases of single well as well as multiple wells in order to estimate reservoir parameters have been conducted and the following observations are made.

- We can interpret well pressure history using pressure transient analysis principles, making constrained stochastic simulation of parameter fields possible.
- The Dekker-Brent approach provides a stable optimization algorithm and is fast in achieving convergence.
- The algorithm utilized in this work satisfactorily determines the unknown reservoir parameters in the case when the reservoir properties are homogeneous.



The next task will be to apply the above approach for heterogeneous reservoirs containing multiple wells and having fluctuating injection profile. It is postulated that heterogeneity will affect multiple-well tests more significantly. The next chapter will consider a wide range of cases having different types of heterogeneity along with multiple wells to predict average reservoir properties. Here also problem with uncertainty in multiple reservoirs attributes will be considered and a procedure for joint estimation of multiple attributes will be developed accordingly.

## **CHAPTER 5: UNCERTAINTY ANALYSIS OF RESERVOIR HETEROGENEITY USING INJECTION DATA**

### **5.1 Chapter Objective:**

In Chapter 4, sensitivity cases were performed only for homogenous fields having constant values of porosity and permeability everywhere. In order to estimate the effect and influence of reservoir heterogeneities on different variables describing the injection performance, similar approach will be applied for cases representing different kinds of permeability heterogeneity. The estimate of reservoir parameters will be made constrained to knowledge of other reservoir and fluid properties. The main objective of this chapter is to validate the optimization algorithm used in Chapter 4 for heterogeneous fields in order to estimate average values of reservoir parameters corresponding to single-phase flow of CO<sub>2</sub> in an aquifer. The focus of this chapter is also on dealing with the uncertainty in multiple reservoir attributes and their effect on the final estimation of reservoir parameters.

### **5.2 Introduction:**

Reservoir characterization is one of the most important aspects of reservoir engineering because a better description of reservoir heterogeneities is necessary in order to make accurate predictions of reservoir performance. Understanding and mapping reservoir heterogeneities, includes porosity, permeability and thickness of reservoir is critical to successfully operating a carbon sequestration project. Reservoir heterogeneity implies that geological and petrophysical properties of reservoir rock change spatially in the reservoir. The heterogeneities existing in the reservoir exhibit a wide range of length scales that controls the overall performance of

subsurface flow of CO<sub>2</sub> after injection. Reservoir simulation requires detailed data on the heterogeneity of the reservoir properties that control the injection of CO<sub>2</sub> in the reservoir. Better reservoir description reduces the risk associated with the successful storage of CO<sub>2</sub>. For most of cases, laboratory measurements and well test interpretations provide valuable data to characterize the reservoir. From well test analysis we obtain an averaged permeability for the volume of the reservoir that has been investigated during the test.

This chapter reviews means of assessing this heterogeneity by using injection data using well test analysis principles and an optimization algorithm.

### **5.3 Method:**

Reservoir simulation requires specification of reservoir heterogeneity both in the vertical direction as well as in the lateral extent. Vertical variability is readily available from well logs analysis and seismic data. However to obtain lateral variations in reservoir properties, stochastic simulation techniques using models for spatial correlation have to be implemented and results have to be analyzed.

Pressure transient analysis is an excellent source of information that has been used in reservoir characterization for a fairly long time now. Pressure transient analysis is especially appropriate in CO<sub>2</sub> injection setting because pressure measurements are routinely made and easily available at any time in the project. The well test data can be used to calculate various reservoir and well parameters. Pressure response during the injection period of CO<sub>2</sub> was reviewed and analyzed. One of the most important parameter obtained from the analysis will be the value of average permeability. An attempt will be made to relate this average permeability to the average permeability of the gas swept zone in the vicinity of the injector.

The effective radial permeability calculated by well test analysis is based on analytical solution to the diffusivity equation. The solution for an infinite acting, transient flow period is given by

$$P_{wf} = P_i - \frac{162.6qB\mu}{kh} [\log t - \log(\frac{k}{\phi\mu cr^2}) - 3.2275]$$

This solution is based on the assumption that the reservoir is homogenous. However because no reservoir is homogeneous, for practical purposes the permeability determined from the well test analysis will represent some average permeability within a radius of investigation or drainage radius. As time increases, more of the reservoirs is influenced by the well injection and the radius of investigation keeps on increasing. The classical Van Poolen et al (1964) equation defining the radius of investigation is given by

$$r = A \sqrt{\frac{k_{wt} t}{\phi\mu c}}$$

For all the cases analyzed in this chapter, the radius of investigation will be assumed to be the extent of the region around the injector over which the gas saturation shows an increase from the initial saturation.

The value of the reservoir permeability obtained from the optimization algorithm will be compared with the value of average permeability calculated from the gas extent. The well test permeability will be compared to the arithmetic and geometric averages of permeability values within the gas-invaded region.

### **Principle of linear superposition:**

The superposition in time function has been used as a tool to analyze transient pressure data measured under the influence of a variable flow rate. The superposition operation is designed to convert variable rate data into the equivalent constant rate behavior. It involves

breaking up a multi-rate sequence into a set of single rates. The rate used for each step is the difference between the current rate and the previous rate.

Superposition in space takes into account the pressure response at a well due to its injection rate as well due to the presence of other well present in the same field. Simply stated, the anticipated pressure response from a well in a complex reservoir can be modeled by combining pressure responses from other well present.

Principle of superposition is explained in detail in Chapter 2 and 3.

#### **5.4 Model Validation using optimization algorithm**

This chapter will include the same minimization algorithm used in the Chapter 4. The objective function developed will reflect the difference between the observed injection pressure and the calculated value of pressure using well test equations. The objective function is given by

$$Obj\ func = \sum_{i=1}^n \sum_{j=1}^t (Press_{sim(i,t)} - Press_{welltest(i,t)})^2$$

The Dekker-Brent algorithm will be used to minimize the objective function in order to arrive at the best-matched estimate of reservoir parameters.

#### **5.5 Reservoir simulation model**

In this study, a 3-D numerical simulation model was constructed in CMG-GEM that consists of 100\*100\*3 orthogonal Cartesian grid blocks with block dimensions of 50m\*50m\*8m. The overall thickness of the reservoir is 24m which is constant everywhere. The reservoir is considered to be isothermal with constant temperature of 76°C. The depth to top of

the formation is 1290m. Reference reservoir pressure is specified to be 17484.5Kpa at a reference depth of 1300m. Water gas contact (WGC) lies at a depth of 1350m.

Simulation model with single and multiple injection wells (2) are considered for study. The analysis will also consider both constant rate injection as well as multiple rate injection. The injection well is perforated in all the three layers of the reservoir. For a single well test, injection well is placed at the centre of the grid-block at the center of the reservoir. A composition of 100% CO<sub>2</sub> was considered as the injection fluid. The injection of CO<sub>2</sub> is scheduled for two continuous years followed 90 years of monitoring.

It is assumed that all other reservoir properties are constant and only the distribution of permeability is varied. The degree of heterogeneity will be varied in all the cases. Porosity distribution is considered homogenous initially with constant value of 0.2 everywhere. The reservoir structure and well location is shown in Figure 5.1.

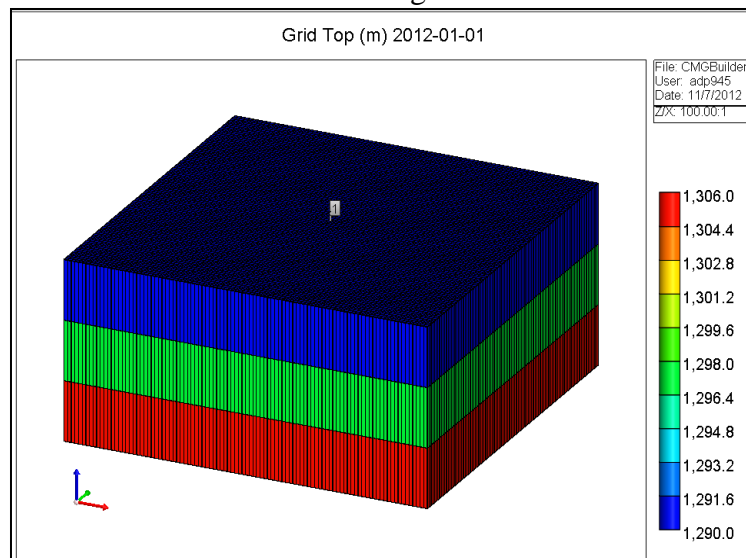


Figure 5.1: Shows CMG-GEM grid top view of the simulation model

### 5.5.1 Permeability Sensitivity cases:

For analyzing the effect of permeability heterogeneity on the pressure transient analysis, three different types of permeability heterogeneity cases will be considered in this chapter. They are described and shown below.

### 5.5.1.1 Case A: Heterogeneous permeability region around the injection well

In this case, the background permeability of the simulation model will be kept constant, but the permeability of the grid blocks at the centre of the reservoir will be modified. The size of the region around the injector where the permeability is modified is 10\*10\*3 grid blocks in extent. For the single well case, the injection well is placed right at the centre of this square heterogeneous block. Map showing the permeability distribution for this case is shown in Figure 5.2.

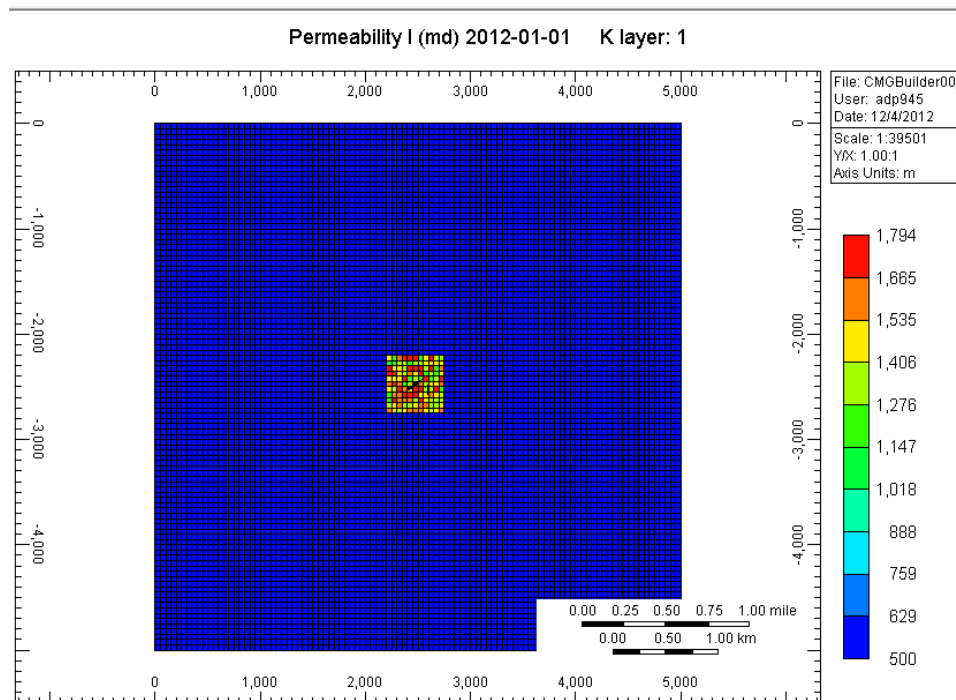


Figure 5.2: Permeability distribution of a single well in a heterogeneous block

Range of permeability in this block varies between 1200-1800md with average permeability being 1500md. The values at all other grids will be kept constant to 500md. CO<sub>2</sub> is planned for injection for 2 years; pressure response due to this injection will be obtained.

### 5.5.1.2 Case B: Presence of high permeability streaks with constant background permeability

In this case, long streaks of high permeability will be introduced manually in the reservoir. Heterogeneous permeability streaks extending in the NW-SE direction will be

considered in this case while the background permeability will be kept constant. The permeability values in the streaks will range from 500-1000md, while permeability in the other blocks will be kept constant at 500md. These characteristic high permeability streaks will be present in all the three layers.

Map of permeability distribution for this case is shown in Figure 5.3.

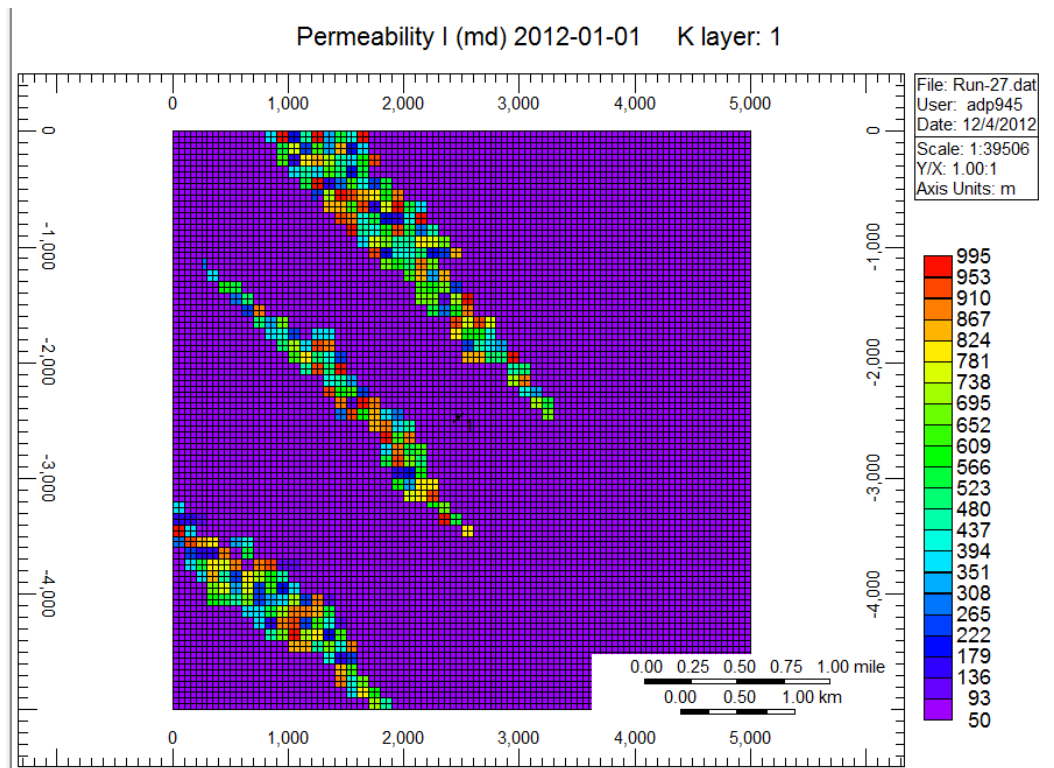


Figure 5.3: Permeability distribution for case with high perm streaks embedded within a constant background

### 5.5.1.3 Case C: Presence of high permeability streaks with varying background permeability

Similar to Case B, in this case also similar high permeability streaks will be considered with modifications done in the other grid blocks value also. The assumption that the permeability values of the background grids are constant is not realistic. Real reservoirs have reservoir heterogeneity at meter scale that can affect the flow behavior significantly. To incorporate this in



the reservoir model, heterogeneity will be introduced in all the grids. For this case, background grids will have randomly generated permeability ranging between 50-100md with the high permeability streaks having range varying from 500-1000md. The permeability distribution map is shown in Figure 5.4.

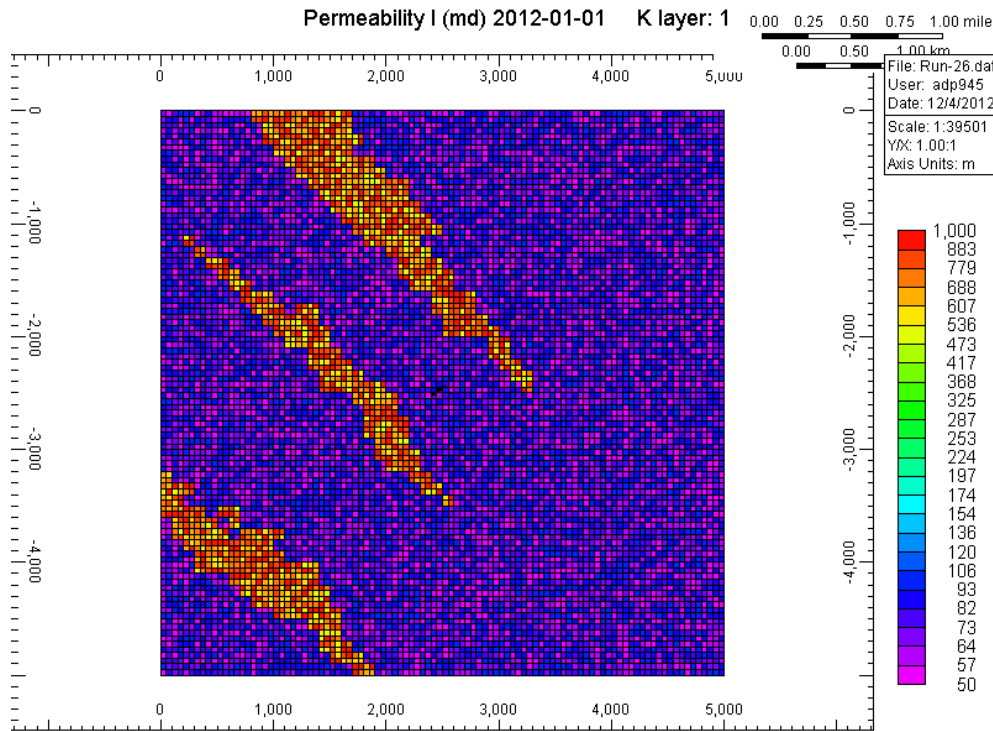


Figure 5.4: Map of permeability distribution for the case with high permeability streaks embedded within a heterogeneous background

### 5.5.2 Injection Rate Sensitivity:

For all single-well cases considered in this chapter, CO<sub>2</sub> is injected at a fluctuating rate for two years. The rate change is scheduled to occur after every 6 months. The injection profile is shown in Figure 5.5.

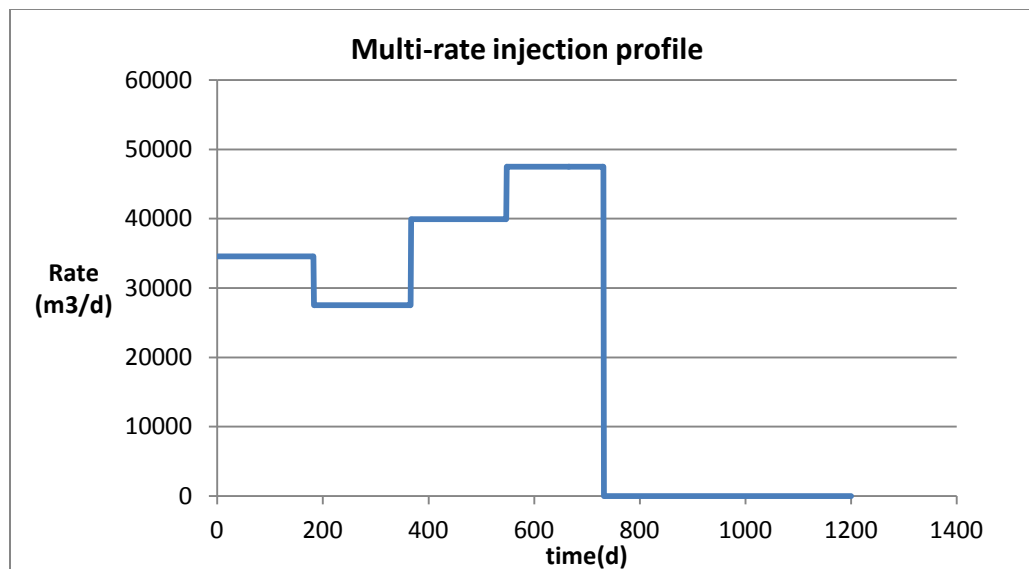


Figure 5.5: injection profile for single well injection test

For multiple well fields, two-wells are considered both injecting at pre-defined fluctuating rates. The injection profile for this type is shown in Figure 5.6. Cumulatively well-2 injects more CO<sub>2</sub> than well-1 at the end of injection period. For both the wells the rate change occurs every 6 months.

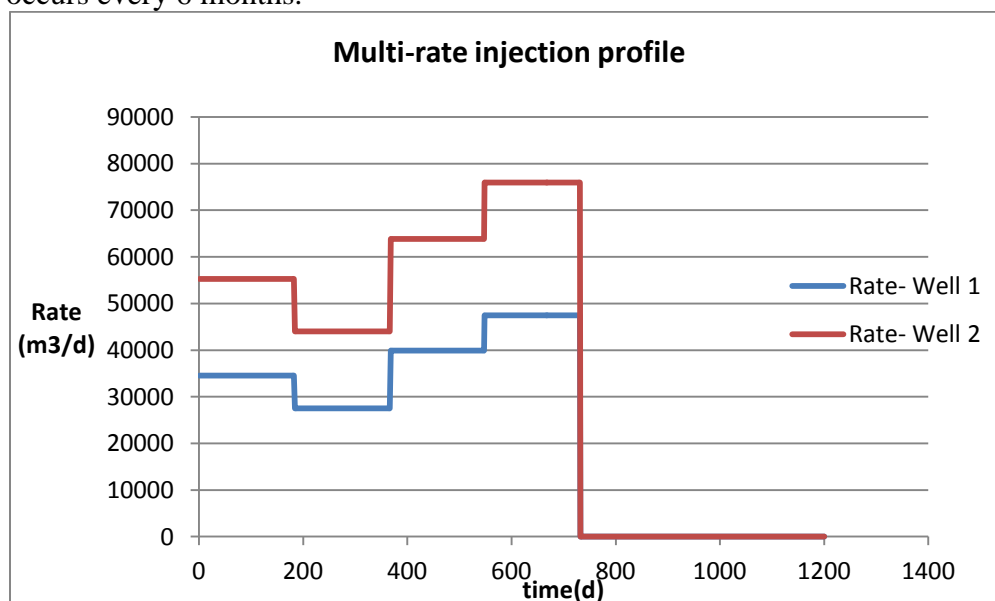


Figure 5.6: Injection profile for multiple rate well test.

## **5.6 Results and discussion:**

### **5.6.1 Single well cases:**

#### **5.6.1.1 Case I: Single well with heterogeneous block at the centre and multiple rate injection**

The injection well is present at the centre of the reservoir (heterogeneous block) injecting CO<sub>2</sub> for two years with rate change occurring every 6 months. At the end of two years, the well is shut in and CO<sub>2</sub> migration is monitored. Pressure responses is obtained and input into the optimization algorithm to predict reservoir parameters. The value estimated will then be compared to the actual values for the gas migrated region to validate the approach. Permeability distribution map for this case is shown in Figure 5.2. The pressure distribution in the reservoir at the end of injection is shown in Figure 5.7. As expected, the pressure perturbation travels fast and to a large extent of the reservoir. In order to isolate a smaller region around the well, where a significant accumulation of gas occurs, the gas viscosity map is also considered (Figure 5.8). The viscosity is a function of pressure and the regions where the viscosity exhibits an abrupt increase correspond to locations where a large volume of gas has migrated to. The extent of the region over which the gas viscosity shows appreciable change is considered for calculating permeability averages.

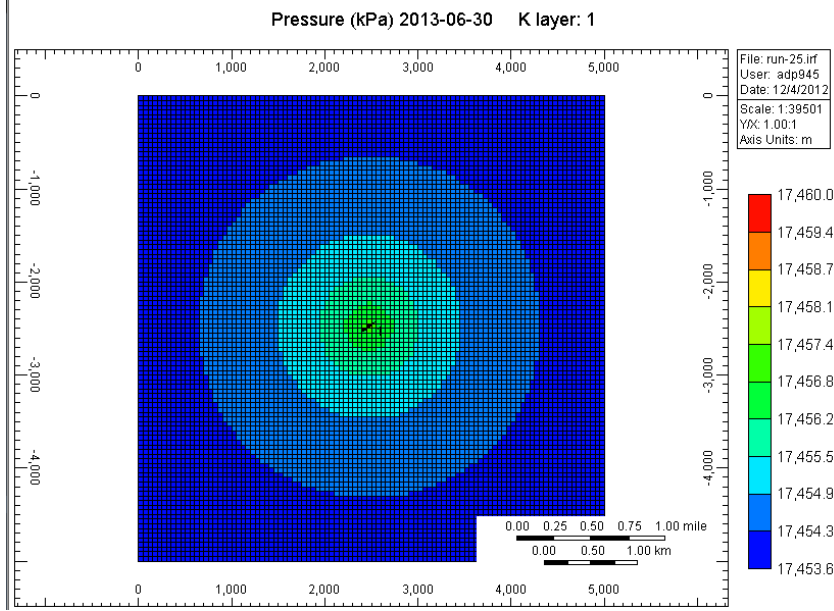


Figure 5.7: Permeability distribution map of the heterogeneous block

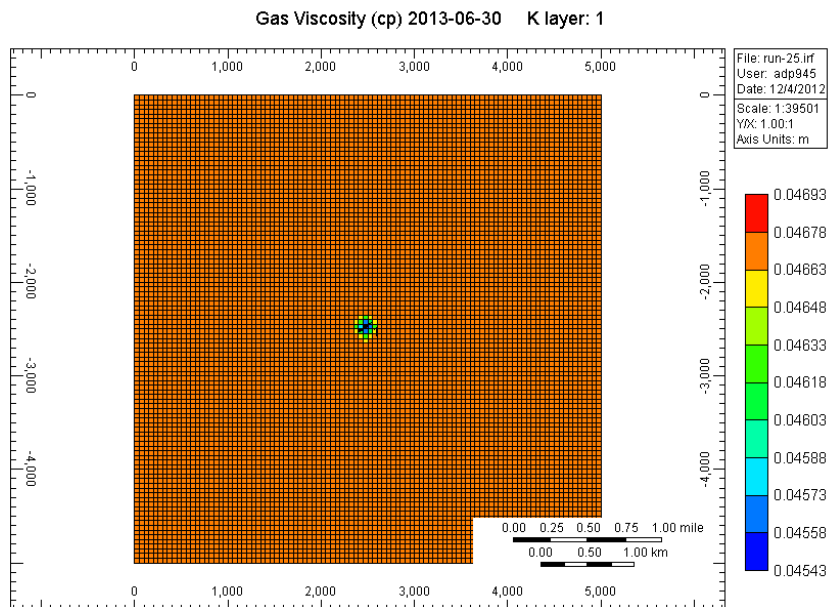


Figure 5.8: Gas viscosity map at the end of injection period

From the gas saturation map it can be concluded that gas migration at the end of two years is still within the extent of the heterogenous block. The arithmetic average permeability of the gas saturated region is around 1500 md which is used as the actual value to compare with the algorithm output.

### 1. Estimation of average permeability

In order to find out the average permeability of the field, cases with different initial guesses for reservoir parameter were considered to check the correctness of the code.

Case #	Unknown Parameter	Initial guess		Actual value (md)	Code output (md)
	Average Permeability	Porosity $\Phi$	Total thickness H(ft)		
1	k	0.2	78.74	1500	1456
2	k	0.4	78.74	1500	1394
3	k	0.1	78.74	1500	1512

We conclude from the three different cases of different guesses of porosity that the average permeability of the reservoir is 1454 md, which is close to the actual value of 1500md. This average value can be interpreted as the predicted value of permeability given that the porosity of the reservoir may be uncertain. Now with this permeability value, average porosity will be estimated using the same algorithm in order to check the validation of the code.

### 2. Estimation of average porosity using above average permeability

Unknown parameter	Average permeability (md)	Total thickness (ft)	Actual value	Code output
Porosity ( $\Phi$ )	1454	78.74	0.2	0.2

The calculated value of porosity is close to the average porosity considering that the porosity value is uncertain. Furthermore, this value is close to the reference value of 0.2

confirming that the optimization code does converge to fairly accurate answers despite the heterogeneity in the vicinity of the injection well.

### 3. Estimation of transmissibility (kh)

Suppose in reality, the pore volume of the reservoir ( $\Phi h$ ) is known and we have to estimate both the transmissivity  $kh$  as well as the ratio  $k/\Phi$ , then we modify the optimization procedure to perform estimation of these multiple parameter groups. Assuming an initial value for  $k/\Phi$ , we calculate “ $kh$ ”. Using this value of the transmissivity, we update  $k/\Phi$  by dividing  $kh/\Phi h$ . If the updated value of  $k/\Phi$  is different from the initial guess, then the process is continued until a constant value of both “ $kh$ ” and  $k/\Phi$  is achieved.

For all the cases described in this chapter  $\Phi h$  has been assigned a value of 15.748 ft. The value of  $kh$  for the reference model is 118110 md-ft and  $k/\Phi$  is 7500 md.

		Iteration Cycle 1		Iteration Cycle 2		Iteration Cycle 3	
Case #	Initial guess $k/\Phi$ (md)	$kh$ (md-ft)	$Kh/\Phi h$ $=k/\Phi$ (md)	$kh$ (md-ft)	$k/\Phi$ (md)	$Kh$ (md-ft)	$k/\Phi$ (md)
1	7500	104600	6642	104070	6602	104050	6607
2	15000	107650	6835	104200	6616	104040	6607
3	3750	101550	6448	103900	6600	104040	6607

The converged values of  $kh$  and  $k/\Phi$  are close but not exactly equal to the reference values. This is because the problem of joint parameter estimation is quite stiff. The results are nevertheless close and immune to the initial guess for the parameter groups.

### 5.6.1.2 Case II: Single well with high permeability streak and constant background

A single well field injecting at multi-rate for two years is considered in this case. Well is located at the centre of the reservoir. 3-D permeability distribution map of this field is shown in Figure 5.3. At the end of the injection period the gas swept region is shown in Figure 5.9. The gas plume hasn't reached the nearest high permeability streak but is migrating towards it. The background grids have constant permeability value of 50md in this case; hence the average value of the gas swept region be 50md as the gas plume has not reached the streak.

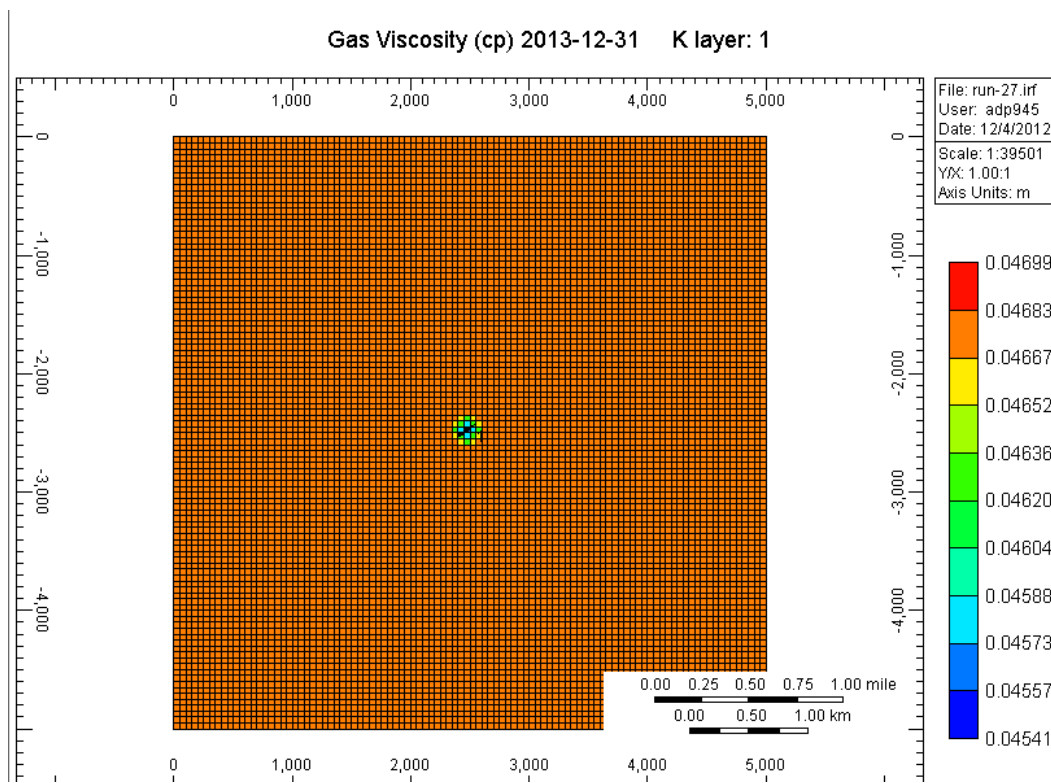


Figure 5.9: Gas viscosity map for single well with high perm streak and constant background

#### 1. Estimation of permeability

In order to find out the average permeability of the field, cases with different initial guesses for reservoir parameter were considered to check the robustness of the code.

Case #	Unknown Parameter	Initial guess		Actual value (md)	Code output (md)
	Average Permeability	Porosity $\Phi$	Total thickness H(ft)		
1	K	0.2	78.74	50	51
2	K	0.4	78.74	50	49
3	K	0.1	78.74	50	54

The estimated permeability considering uncertainty in porosity is 51.6 md and that is close to the actual value. Now with this average permeability value, average porosity for the reservoir will be estimated using the same algorithm.

## 2. Estimation of average porosity using above average permeability

Unknown parameter	Average permeability (md)	Total thickness (ft)	Actual value	Code output
Porosity ( $\Phi$ )	51	78.74	0.2	0.23

Porosity estimate obtained is also close to the actual value implying that the implemented optimization procedure is robust.

## 3. Estimation of transmissibility (kh)

$\Phi h$  has been assigned a value of 15.748 ft. Within the gas invaded region, the reference model indicates  $kh = 3937$  md-ft and  $k/\Phi$  is 250 md. The iterative procedure described earlier was implemented and the results are summarized below.



		Iteration Cycle 1		Iteration Cycle 2		Iteration Cycle 3	
Case #	Initial guess $k/\Phi$ (md)	kh (md-ft)	$Kh/\Phi h$ $=k/\Phi$ (md)	kh (md-ft)	$k/\Phi$ (md)	Kh (md-ft)	$k/\Phi$ (md)
1	250	4181.3	265.5	4193.5	266.3	4194.3	266.3
2	125	4039.4	256.5	4186.6	265.8	4193.8	266.3
3	500	4323	274.5	4200.3	266.7	4194.5	266.35

Again the results obtained by the procedure are close to the reference values.

#### 5.6.1.3 Case III: Single well with high permeability streak and varying background

To analyze a more realistic scenario, a single well injecting at multiple rates into a heterogeneous field is considered. In this case all the grid blocks in the reservoir have different permeability value is considered. The permeability distribution map is shown in Figure 5.4. Since the background permeability varies between 50-100md and the same injection rate as in Case II is employed, similar gas extent as for that case is observed at the end of the injection period. The gas saturation map is shown in Figure 5.10. Arithmetic average of permeability for all the gas swept grid blocks in this case is 77md.

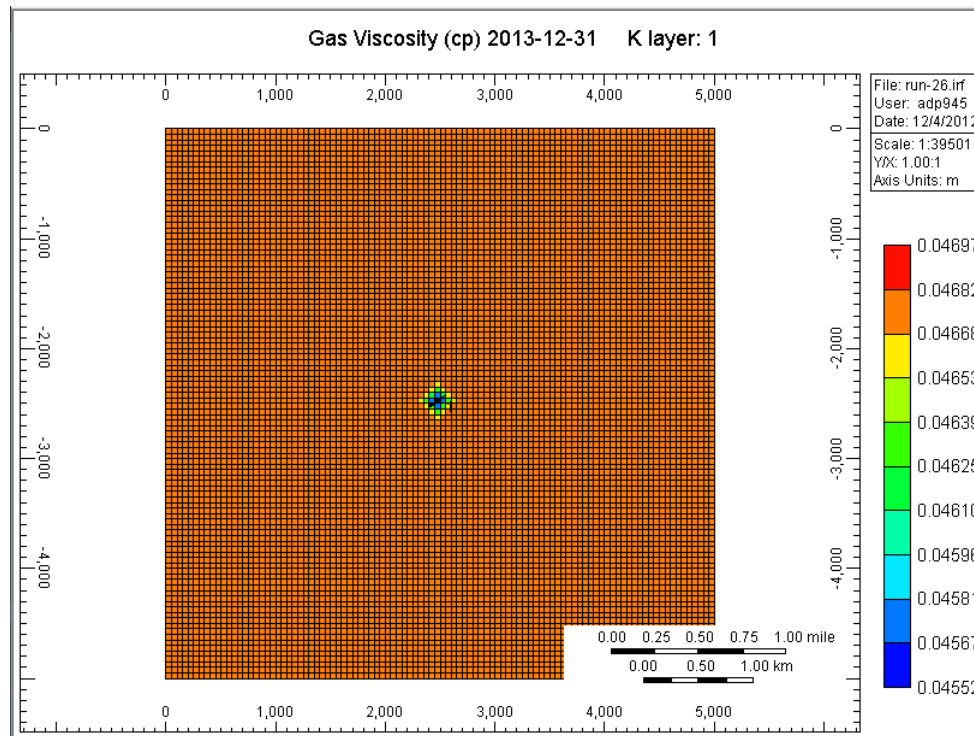


Figure 5.10: Gas viscosity map for single well with high perm streak and varying background

### 1. Estimation of permeability:

Case #	Unknown Parameter	Initial guess		Actual value (md)	Code output (md)
	Average Permeability	Porosity $\Phi$	Total thickness H(ft)		
1	k	0.2	78.74	77	70.43
2	k	0.4	78.74	77	61.75
3	k	0.1	78.74	77	68.10

Average permeability from the algorithm considering the uncertainty in porosity is 67md, which is close to the actual value of 77md.

## 2. Estimation of average porosity using above average permeability

Unknown parameter	Average permeability (md)	Total thickness (ft)	Actual value	Code output
Porosity ( $\Phi$ )	67	78.74	0.2	0.19

The estimate of average porosity is also close to the reference value.

## 3. Estimation of transmissibility (kh)

The reference values for this case are  $kh = 6063$  md-ft and  $k/\Phi$  is 385 md.

		Iteration Cycle 1		Iteration Cycle 2		Iteration Cycle 3	
Case #	Initial guess $k/\Phi$ (md)	Code estimate kh (md-ft)	$Kh/\Phi h$ $=k/\Phi$ (md)	2 <sup>nd</sup> code estimate kh (md-ft)	$k/\Phi$ (md)	Kh (md-ft)	$k/\Phi$ (md)
1	385	5569.2	353.3	5546.6	352.2	5545	352.1
2	192.5	5384	342	5538	351.6	5541	351.8
3	770	5754	365.4	5555.3	352.7	5549	352.36

The feasibility of using the algorithm to perform estimation of multiple variables is again demonstrated.

### 5.6.2 Multiple Well Tests:

To test the approach for multiple wells injecting at multi-rate, more well are introduced. In cases IV and V described in length below, two wells 880ft apart will be injecting CO<sub>2</sub> for two years. It will be tested on different kinds of heterogeneity fields to obtain multiple reservoir parameters.

### 5.6.2.1 Case IV: Multiple wells with heterogeneous block and multiple rate injection

A 3-D CMG-Model was developed with grid size 100\*100\*3 and grid dimensions 50m\*50m\*8m. Two injecting wells Well-1 and Well-2 are present at grid location 45,45,1 and 50,45,1 perforated in all the three layers. As outlined above, the central grid permeability is manually changed in order to reflect heterogeneity in the vicinity of wells with permeability ranging from 1200-1800md while the background grids have constant permeability of 500md. Permeability distribution is shown in Figure 5.11 while the pressure profile and extent of the gas swept region at the end of injection period is shown in Figure 5.12. The gas has migrated more around well-2 as cumulative injection in well-2 is more as compared to well-1. The arithmetic average permeability around well-1 is 1500md and for well-2 is 1490 md based on the extent of the gas swept region.

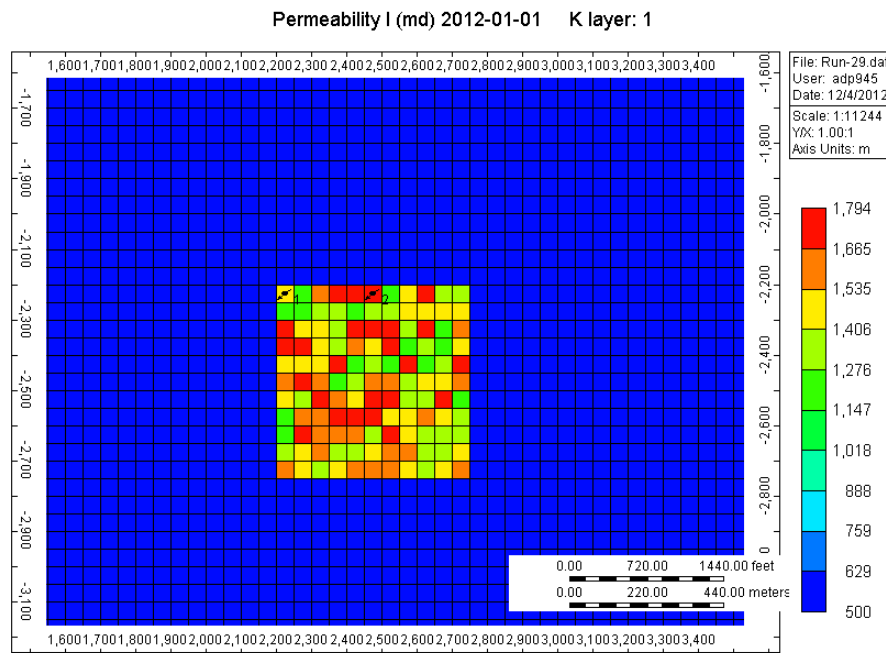


Figure 5.11: Permeability distribution of heterogeneous block

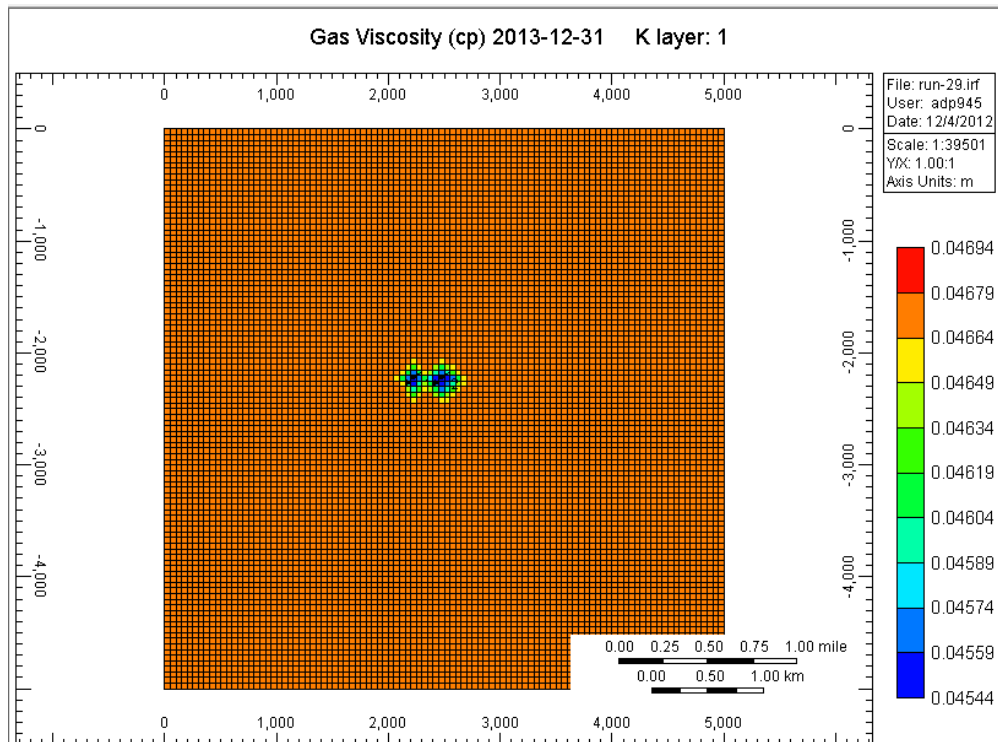
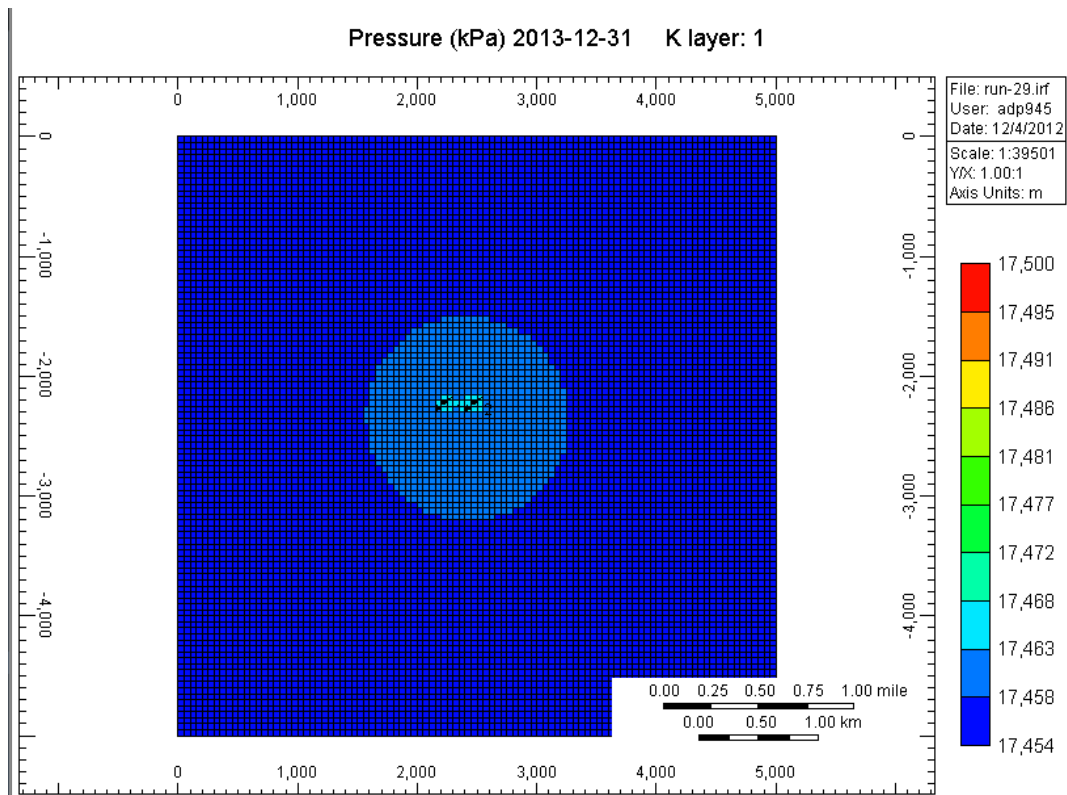


Figure 5.12: Pressure spread and gas viscosity map for multiple well with heterogeneous block at the centre

Parameter estimations:

### 1. Estimation of average permeability

Case #	Unknown Parameter	Initial guess		Actual value (md)	Code output (md)	
	Average Permeability	Porosity $\Phi$	Total thickness H(ft)		@well 1	@well2
1	k	0.2	78.74	1400-1500	1318	1488
2	k	0.4	78.74	1400-1500	1277	1436
3	k	0.1	78.74	1400-1500	1359	1546

Permeability estimates at both the well are close to the correct value. Based on these values, back calculation of porosity will be made to check the correctness of the algorithm.

### 2. Estimation of average porosity using above average permeability

Unknown parameter	Average permeability (md)	Total thickness (ft)	Actual value	Code output
Porosity ( $\Phi$ )	@well 1- 1454	78.74	0.2	@well 1 – 0.202
	@well 2 - 1490			@well 2 – 0.204

The estimate of average porosities in the vicinity of the two wells is close to the reference.

### 3. Estimation of transmissivity

The reference values for this case are  $kh = 118110$  md-ft and  $k/\Phi$  is 7500 md.

From the algorithm estimates, we conclude that for cases of multiple well injecting at variable rate in a heterogeneous medium the estimation of group parameters at well 1 is little underestimated while at well 2 is close to the actual value. Well 1 is present at the corner of the heterogeneous block, implying that the permeability distribution around it is constant = 500md. The underestimation is on the basis of average permeability of the heterogeneous field but if we consider the background permeability then the estimation is correct.

@ Well 1

		Cycle 1		Cycle 2		Cycle 3	
Case #	Initial guess k/Φ (md)	Code estimate kh (md-ft)	Kh/Φh =k/Φ (md)	2 <sup>nd</sup> code estimate kh (md-ft)	k/Φ (md)	Kh (md-ft)	k/Φ (md)
1	7500	104412	6630	103863	6595	103839	6593
2	15000	107499	6826	103992	6603	103844	6594
3	3750	101325	6434	103729	6586	103833	6593

@ Well 2

		Cycle 1		Cycle 2		Cycle 3	
Case #	Initial guess k/Φ (md)	Code estimate kh (md-ft)	Kh/Φh =k/Φ (md)	2 <sup>nd</sup> code estimate kh (md-ft)	k/Φ (md)	Kh (md-ft)	k/Φ (md)
1	7500	121019	7684	121164	7693	121170	7964
2	15000	125142	7946	121363	7706	121181	7695
3	3750	116896	7422	120957	7680	121160	7693

#### 5.6.2.2 Case V: Multiple wells in a heterogeneous field injecting at multiple rate

The final case in this chapter will also have two injecting wells separated 880 ft apart but in a fully heterogeneous field. The permeability distribution has high permeability streaks extending in the NW-SE direction with background grids having varying permeability. These streaks have value ranging between 500-1000md while all the other grid blocks have permeability in the range between 50-100md. Figure 5.4 shows the permeability distribution map for this field. Injection is stopped after two years and gas viscosity map for this case is shown in Figure 5.13. From the gas map, it can be concluded that around well 2 the gas migration is getting influenced by the presence of high permeability streak and is migrating more in the direction of the streak. Based on the extension of gas at the end of two years, the average permeability is calculated to be around 80 md around both the wells.

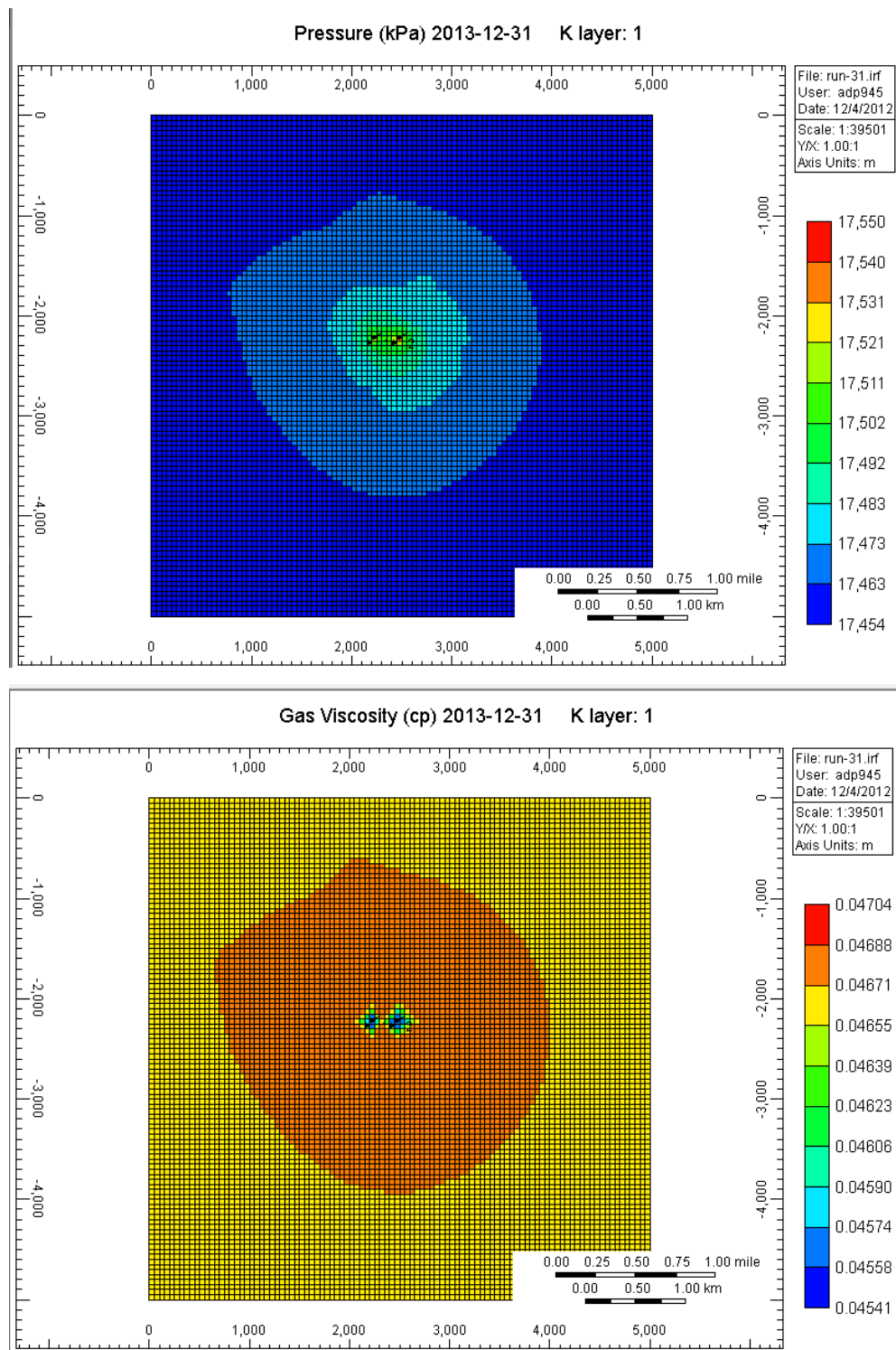


Figure 5.13: Pressure spread and gas viscosity map for fully heterogeneous field with two injection wells



Parameter estimations:

## 2. Estimation of average permeability

Case #	Unknown Parameter	Initial guess		Actual value (md)	Code output (md)	
	Average Permeability	Porosity $\Phi$	Total thickness H(ft)		@ well 1	@ well 2
1	k	0.2	78.74	80	89	86.65
2	k	0.4	78.74	80	86	83
3	k	0.1	78.74	80	90	90.2
Arithmetic average permeability (md)					78	86

The average permeability estimated at both the wells are close to the actual estimate implying that even in highly heterogeneous fields using the injection data and the optimization procedure a correct estimate of permeability can be made.

## 2. Estimation of average porosity using the above values of average permeability

Unknown parameter	Average permeability (md)	Total thickness (ft)	Actual value	Code output
Porosity ( $\Phi$ )	@ well 1- 78	78.74	0.2	@ well 1 – 0.208
	@ well 2 - 86			@ well 2 – 0.202

The average porosity estimated is close to the reference value which confirms the robustness of algorithm.

## 3. Estimation of transmissivity

The reference values for this case are  $kh = 6141$  md-ft and  $k/\Phi$  is 390 md.

The estimation of  $(k/\phi)$  at both the wells is close to the reference value.

@well 1

		Cycle 1		Cycle 2		Cycle 3	
Case #	Initial guess k/Φ (md)	Code estimate kh (md-ft)	Kh/Φh =k/Φ (md)	2 <sup>nd</sup> code estimate kh (md-ft)	k/Φ (md)	Kh (md-ft)	k/Φ (md)
1	390	6977	443	7020	445	7022	445
2	780	7213	458	7032	446	7023	445
3	195	6741	428	7009	445	7022	445

@ well 2

		Cycle 1		Cycle 2		Cycle 3	
Case #	Initial guess k/Φ (md)	Code estimate kh (md-ft)	Kh/Φh =k/Φ (md)	2 <sup>nd</sup> code estimate kh (md-ft)	k/Φ (md)	Kh (md-ft)	k/Φ (md)
1	390	6782	430	6820	433	6822	433
2	780	7052	447	6835	434	6823	433
3	195	6511	413	6804	432	6822	433

## 5.7 Conclusion:

The optimization algorithm developed to estimate reservoir parameters using injection data coupled with well test equations works well for heterogeneous fields. Different kinds of heterogeneity fields were tested in this chapter and the final estimate from the algorithm matches closely to the reference values in all the cases presented. The algorithm predicts the final value of the unknown parameter based on constrained knowledge of geological and well data. The results presented in this chapter also indicate that the pressure response at the injection well is impacted by the heterogeneities in the permeability field and an idea of these heterogeneities can be gained by analyzing the pressure response.. The fast convergence of objective function is observed in almost all the cases implying the robustness of the algorithm.

## CHAPTER 6: CONCLUSION AND RECOMMENDATIONS

The aim of this thesis has been to understand and examine the information contained in the injection data for a wide range of reservoir models demonstrating different heterogeneity and rate fluctuations in order to quantify the uncertainty in the estimation of reservoir parameters to understand its affect on migration of CO<sub>2</sub>. These estimated reservoir parameters or groups of these parameters can then be used to constrain spatial models for thickness, permeability and porosity.

### 6.1 Summary and Conclusions

Several properties of reservoir, fluid and well influence the pressure performance measured during injection of a well. Based on the results described in all the chapters, following conclusions can be made:

- In Chapter 3, we analyzed the effect of different kinds of heterogeneity on the injection performance at the well. Mantilla et al. (2009) and Bhowmik et al (2010) proposed that dynamic measurement of injection rate and pressure in each well can be used to infer the presence the reservoir heterogeneities large enough to affect the overall plume migration. Our approach confirms this hypothesis and concludes that the imprint of presence of nearby heterogeneities can be seen on the pressure profile of wells during the injection period. Specific heterogeneity features like high and low permeability streaks present in the reservoir strongly affects the injection pressure profile during CO<sub>2</sub> injection. Presence of high permeability streaks reduces the injection pressure significantly as compares to the reference case.
- Our approach also demonstrated that the impact of reservoir heterogeneity on the well responses is likely sensitive to the injection rate fluctuations. We studied that when the fluctuations are small (difference between consecutive rate change < 10000 m<sup>3</sup>/d,

Surface condition), the pressure perturbations triggered by permeability contrasts in the reservoir are likely to be dampened as opposed to when the injection rate fluctuations are substantial. Difference in pressure response between reference case and cases with high, low permeability streaks and no streak case was quantified using Discrete Frechet distance (DFD). It was concluded that injection pressure profile respond differently to injection rate fluctuations when high or low permeability streak is present. Hence we conclude that understanding the pressure response behavior to rate fluctuations can provide significant information about permeability heterogeneity present in the reservoir.

- Once it was established that there is an effect of reservoir heterogeneity on the pressure response, the next task was to find out what characteristics of these heterogeneity can be estimated by the assessment of the injection data. In this research, we proposed a method to extract specific characteristics of reservoir heterogeneity like transmissibility ( $kh$ ) and permeability to porosity ratio ( $k/\phi$ ) conditioned to static and dynamic data using inexpensive measurements of injection data (rate and pressure), pressure transient analysis and optimization algorithm. An optimization algorithm called the Dekker-Brent algorithm for is used for the estimation of reservoir parameters in single and multi well fields for single phase of flow of  $CO_2$  in an aquifer. It's a minimization algorithm that finds the minimum of the objective function specified under a tolerance
- Use of pressure transient analysis and optimization algorithm to determine reservoir parameter is an iterative process which requires prior knowledge of heterogeneity distribution. Based on the obtained result from the algorithm, the initial distribution will be updated at each iteration to best match the pressure response.
- Wide ranges of heterogeneity cases were tested in Chapter 5 and for all the cases individual as well as group reservoir parameters were estimated. It was found that

estimated group parameters like transmissibility “kh” and permeability to porosity ratio “ $k/\Phi$ ” were different in different parts of the reservoir implying the presence of heterogeneity. Thus we develop a method to understand and quantify the uncertainty in the spatial distribution of heterogeneities in the formation.

- We conclude that this procedure can help in simultaneous estimation of multiple reservoir parameters that impact the observed pressure response. Application of this approach to reservoirs having injection of CO<sub>2</sub>, yield satisfactory results.
- We remark that one of the advantages of using the Dekker-Brent algorithm is that the convergence is fast and it determines the unknown reservoir parameters satisfactorily.
- In conclusion, reservoir parameters obtained using the pressure transient analysis technique reflects the presence and influence of reservoir heterogeneities at a meter scale. By integrating pressure transient test results with the geological characterization of the reservoir we can obtain a better understanding of how the CO<sub>2</sub> plume will migrate after injection.

## 6.2 Recommendations:

The number of cases discussed in this thesis doesn’t cover the whole spectrum of possible cases. At this point this research project predicts the following future developments:

- **Effect of well location on the results:** In all the single well numerical testing cases we have performed, the well was located at the center of the reservoir. It is, however, worthwhile testing the pressure response if the well is located off-centered positions.

- The optimization algorithm has been applied to field cases to infer large-scale heterogeneity. However real reservoirs have heterogeneity from pore scale to reservoir scale. Therefore there is a need to validate the robustness of the algorithm for cases depicting small scale heterogeneity.
- For all the cases considered in this thesis, analysis was done for single phase models for calculating the reservoir parameters. However, the analysis can be extended to two-phase flow considering the effect of brine in the reservoir.
- We use analytical solutions for radially heterogeneous reservoirs to define an equivalent radial permeability and a corresponding region of investigation. By injection well-test analysis in heterogeneous permeability fields, we determine the arithmetic based average permeability within the radius of investigation. A different averaging model that defines the permeability distribution within the radii of investigation can be developed to check for the final estimation.
- For the reservoir simulations conducted in this research our model was bounded by infinite acting reservoir condition. We can extend this to other boundary conditions, like no flow or constant boundary conditions.

## APPENDIX

### MATLAB code for Dekker-Brent algorithm

```
function [xmin, fmin] = goldensectionmethod(ax, bx, cx, tol)

%GOLDEN    Minimize function of one variable using golden section search
%
%    [xmin, fmin] = golden(f, ax, bx, cx, tol) computes a local minimum
%    of f. xmin is the computed local minimizer of f and fmin is
%    f(xmin). xmin is computed to an relative accuracy of TOL.
%
%    The parameters ax, bx and cx must satisfy the following conditions:
%    ax < bx < cx, f(bx) < f(ax) and f(bx) < f(cx).
%
%    xmin satisfies ax < xmin < cx. golden is guaranteed to succeed if f
%    is continuous between ax and cx
%
%    Roman Geus, ETH Zuerich, 9.12.97

C = (3-sqrt(5))/2;
R = 1-C;

x0 = ax;
x3 = cx;
if (abs(cx-bx) > abs(bx-ax)),
    x1 = bx;
    x2 = bx + C*(cx-bx);
else
    x2 = bx;
    x1 = bx - C*(bx-ax);
end
f1 = Welltest(x1);
f2 = Welltest(x2);

k = 1;
while abs(x3-x0) > tol*(abs(x1)+abs(x2)),
    fprintf(1, 'k=%4d, |a-b|=%e\n', k, abs(x3-x0));
    if f2 < f1,
        x0 = x1;
        x1 = x2;
        x2 = R*x1 + C*x3;    % x2 = x1+c*(x3-x1)
        f1 = f2;
        f2 = Welltest(x2);
    else
        x3 = x2;
        x2 = x1;
        x1 = R*x2 + C*x0;    % x1 = x2+c*(x0-x2)
        f2 = f1;
        f1 = Welltest(x1);
    end
    k = k+1;
end
```

```

if f1 < f2,
    xmin = x1;
    fmin = f1;
else
    xmin = x2;
    fmin = f2;
end

%%%%%%%%%%%%%%%%%%%%%%%%%%%%%%%%%%%%%%%%%%%%%%%%%%%%%%%%%%%%%%%%%%%%%%%%%%%%%%
Pressure Profile solution of a single well in an infinite acting reservoir
injecting at constant rate

function f = singlewellconstrate(Poro)
B=1;
rw = 0.25; %ft
rwsqur = 0.0625; %ft2
h = 78.74; %ft
Pi = 2530.77; %psi
Perm = 800;

f=0;
a = evalin('base', 'q'); % Rate at well 1, STB/d
b = evalin('base', 'BHP'); % psi
c = evalin('base', 'Visg'); % Gas viscosity, cp
d = evalin('base', 'time'); % time,hrs
e = evalin('base', 'ct'); % compressibility, 1/psi

for i = 1:731

    DelP = b(i,1) - Pi;

    %    Any of the below formula can be used

    %    f = f +(DelP -
    (((141.2*a(i,1)*c(i,1))/(k*h))*0.5*(log(((0.0002637*k*d(i,1))/(Poro*c(i,1)*e(
    i,1)*rwsqur))/1)+.80907)))^2;

    f = f+(DelP -
    (((162.6*a(i,1)*c(i,1))/(Perm*h))*((log10((Perm*d(i,1))/(Poro*c(i,1)*e(i,1)*r
    wsqur)))-3.2275)))^2;

end

%%%%%%%%%%%%%%%%%%%%%%%%%%%%%%%%%%%%%%%%%%%%%%%%%%%%%%%%%%%%%%%%%%%%%%%%%%%%%%
Pressure Profile solution of multiple wells in an infinite acting reservoir
injecting at constant rate

function f = welltestmultipleconst(Poro)
B=1;
rw = 0.25; %ft
rwsqur = 0.0625; %ft2
r1 = 17399.28; %ft
r1squr = r1^2;

```



```

r2 = 14786.55;
r2squr = r2^2;
h = 78.74; %ft
Pi = 2542.735; %psi
k = 500;

f=0;
a = evalin('base', 'q1'); % Rate at well 1, STB/d
b = evalin('base', 'q2'); % Rate at well 2, STB/d
c = evalin('base', 'q3'); % Rate at well 3, STB/d
d = evalin('base', 'BHP'); % psi
e = evalin('base', 'Visg'); % Gas viscosity, cp
ff = evalin('base', 'time'); % time,hrs
g = evalin('base', 'ct'); % compressibility, 1/psi

for i = 1:731

    DelP = d(i,1) - Pi;

    f = f + (DelP -
    (((162.6*a(i,1)*e(i,1))/(k*h))*(log10((k*ff(i,1))/(Poros*e(i,1)*g(i,1)*rwsqur
    ))-3.2275)) +
    (((141.2*b(i,1)*e(i,1))/(k*h))*(0.5*expint((r1squr*Poros*e(i,1)*g(i,1))/(0.001
    0548*k*ff(i,1)))))) +
    (((141.2*c(i,1)*e(i,1))/(k*h))*(0.5*expint((r2squr*Poros*e(i,1)*g(i,1))/(0.001
    0548*k*ff(i,1)))))) )^2;

end

%%%%%%%%%%%%%%%%%%%%%%%%%%%%%%%%%%%%%%%%%%%%%%%%%%%%%%%%%%%%%%%%%%%%%%%%%%%%%%
Pressure Profile solution of multiple wells in an infinite acting reservoir
injecting at variable rates

function f = Multirate(k)
B=1;
rw = 0.25; %ft
rwsqur = 0.0625; %ft2
h = 78.74; %ft
Pi = 2542.735; %psi
Poros = 0.2;

f=0;
a = evalin('base', 'q'); % Rate at well 1, STB/d
b = evalin('base', 'BHP'); % Pressure,psi
c = evalin('base', 'Visg'); % Gas Viscosity, cP
d = evalin('base', 'time'); % hours
e = evalin('base', 'ct'); % Gas compressibility, /psi

qfluc=zeros(731,1);
tfluc=zeros(731,1);

qfluc(1,1) =0;
tfluc(1,1) =0;

```

```

qfluc(2,1) =780;

fluc=2;

for i = 1:731

    if a(i,1) ~= qfluc(fluc,1)

        fluc=fluc+1;
        qfluc(fluc,1) = a(i,1);
        tfluc(fluc-1,1) = d(i-1,1);

    end
end

for j = 1:731
    Total = 0;
    t=d(j,1);
    qn = a(j,1);
    for i=1:fluc

        if(a(j,1)==qfluc(i,1))

            no_terms = i; %Number of fluc till "i"
            break;

        end

    end

    no_terms;

    for i=2:no_terms

        Total = Total+(qfluc(i,1)-qfluc(i-1,1))*log10(t-tfluc(i-1,1));

    end
    Sum(j,1) = Total;

    DelP = b(j,1) - Pi;

    f = f+((DelP/qn)-((((162.6*c(j,1))/(k*h))*(Total/qn))+
    (((162.6*c(j,1))/(k*h))*((log10(k/(Poros*c(j,1)*e(j,1)*rwsqr))-3.2275))))^2;
end

%%%%%%%%%%%%%%%%%%%%%%%%%%%%%%%%%%%%%%%%%%%%%%%%%%%%%%%%%%%%%%%%%%%%%%%%

```

## BIBLIOGRAPHY

1. Albert Ofori & Thomas Engler. Effects of CO<sub>2</sub> Sequestration on the Petrophysical Properties of an Aquifer Rock. *Canadian Unconventional Resources Conference*. 147166-MS (2011)
2. Allan Mathieson, John Midgley, Kevin Dodds, Iain Wright, Philip Ringrose & Nabil Saoul. CO<sub>2</sub> sequestration monitoring and verification technologies applied at Krechba, Algeria. *The Leading Edge* (2010)
3. A.M. Aly, W.D. McCain, Jr., N.C. Hill & W.J. Lee. Reservoir Evaluation of a Gas Condensate Reservoir Using Pressure Transient Analysis. *Annual Technical Meeting of The Petroleum Society*. Paper 97-54 (1997)
4. Aminian, K., Ameri, S., Gaines, T.E & Morris, M.E. Semilog Type Curve for Interpretation of Well Test Data. *SPE Eastern Regional Meeting*. 21271-MS (1990)
5. Andrew Cavanagh & Philip Ringrose. Simulation of CO<sub>2</sub> Distribution at the In Salah Storage Site Using High-resolution Field-scale Models
6. Aysegul Dastan & Roland N. Horne. Significant Improvement in the Accuracy of Pressure Transient Analysis Using Total Least Squares. *SPE Annual Technical Conference and Exhibition*. 125099-MS (2009)
7. Best Practices for: Monitoring, Verification and Accounting of CO<sub>2</sub> stored in deep Geologic formations. *National Energy Technology Laboratory*.

8. Bonalde & M. Ramones. A Robust Algorithm for Parameter Estimation in Well Tests. *SPE Advanced Technology Series*, Journal Paper 23656-PA (1994)
9. Brad Bonnell, Chuck Hurich & Rudi Meyer. High Resolution Characterization of Reservoir Heterogeneity with Cross-well Seismic Data – A Feasibility Study. *CSPG-CSEG-CWLS convention* (2006)
10. Chia-Wei Kuo, Jean-Christophe Perrin & Sally M. Benson. Effect of Gravity, Flow Rate, and Small Scale Heterogeneity on Multiphase Flow of CO<sub>2</sub> and Brine. *SPE Western Regional Meeting*. 132607-MS (2010)
11. Cinco-Ley, H., Samaniego-V., F. & Viturat, D. Pressure Transient Analysis for High-Permeability Reservoirs. *SPE Annual Technical Conference and Exhibition*. 14314-MS (1985)
12. C. L. Liner, P. Geng, J., Zeng, H. King & J Li. A CO<sub>2</sub> Sequestration Simulation Case Study at the Dickman Field, Ness Co., Kansas. *SPE Annual Technical Conference and Exhibition*. 145791-MS (2011)
13. D. Jasinge & P.G. Ranjith. Carbon dioxide sequestration in geologic formations with special reference to sequestration in deep coal seams. *American Rock Mechanics Association*. ARMA 11-595 (2011)
14. Dmitriy Silin & George Robin. Combining Step Rate Well Test With Transient-Pressure Test: Is It Possible? *SPE Western Regional Meeting*. 121425-MS (2009)

15. Duy Nghia Nguyen. Carbon Dioxide Geological Sequestration: Technical and Economic Reviews. *SPE/EPA/DOE Exploration and Production Environmental Conference*. 81199-MS (2003)
16. E. Beretta, A. Tiani, G. Lo Presti & F. Verga. Injection Tests as a Reliable Alternative to Conventional Well Testing: A Real Field Experience. *SPE Europec/EAGE Annual Conference and Exhibition*. 100283-MS (2006)
17. Esam Jassim, M.A. Abdi, & Y. Muzychka. A CFD-Based Model to Locate Flow-Restriction Induced Hydrate Deposition in Pipelines. *Offshore Technology Conference*. 19190-MS (2008)
18. Freddy Humberto Escobar, Juan Miguel Navarrete & Hernan Dario Losada. Evaluation of Pressure Derivative Algorithm for Well test Analysis. *SPE International Thermal Operations and Heavy Oil Symposium*. SPE 86936 (2004)
19. F. Zeng & G. Zhao. Well Testing Analysis for Variable Permeability Reservoirs. *Canadian International Petroleum Conference*. Paper 2004-037 (2004)
20. Gringarten, Alain C. Type-Curve Analysis: What It Can and Cannot Do. *Journal of Petroleum Technology*, Journal Paper 16388-PA (1987)
21. James Smith, Sevkett Durucan, Anna Korre, Ji-Quan Shi, Caglar Sinayuc. Assessment of fracture connectivity and potential for CO<sub>2</sub> migration through the reservoir and lower caprock at the In Salah storage site

22. Jean-Pierre Deflandre, Audrey Estublier, Axelle Baroni, Jean-Marc Daniel, Florence Adjémian. In Salah CO<sub>2</sub> injection modelling: a preliminary approach to predict short term reservoir behaviour
23. Johan Zakrisson, Ingrid Edman & Yildiray Cinar. Multiwell Injectivity for CO<sub>2</sub> Storage. *SPE Asia Pacific Oil and Gas Conference and Exhibition*. 116355-MS (2008)
24. Jorge Luis Garduno, Henri Morand, Luke Saugier, W.B Ayers, Jr. & Duane A. McVay. CO<sub>2</sub> Sequestration Potential of Texas Low-Rank Coals. *SPE Annual Technical Conference and Exhibition*. 84154-MS (2003)
25. Iain Wright. CO<sub>2</sub> Geological Storage : Lesson Learned from In-Salah (Algeria). *SBSTA Meeting Bonn* (2006)
26. Iain W. Wright. The In-Salah Gas CO<sub>2</sub> Storage Project. *International Petroleum Technology Conference*. IPTC 11326-MS (2007)
27. Kumar, M. Noh, G.A. Pope, K. Sepehrnoori, S. Bryant & L.W. Lake. Reservoir Simulation of CO<sub>2</sub> Storage in Deep Saline Aquifers. *SPE/DOE Symposium on Improved Oil Recovery*. 89343-MS (2004)
28. Kyung Won Chang & Steven L. Bryant. Dynamics of CO<sub>2</sub> Plumes Encountering a Fault in a Reservoir. *Annual conference on carbon capture and sequestration* (2007)
29. MacAllister, D.J. Pressure Transient Analysis of CO<sub>2</sub> and Enriched-Gas Injection and Production Wells. *SPE Production Operations Symposium*. 16225-MS (1987)

30. Magnus Nnadi & Michael Onyekonwu. Numerical Welltest Analysis. *Nigeria Annual International Conference and Exhibition*. 88876-MS (2004)
31. Massonnat, G.J., Bandiziol, D. & Elf Aquitaine. Interdependence Between Geology and Well Test Interpretation. *SPE Annual Technical Conference and Exhibition*. 22740-MS (1991)
32. M. Carr, F. Sinclair & D. Bruton. Pipeline Walking-Understanding the Field Layout Challenges, and Analytical Solutions Developed for the SAFEBUCK JIP. *Offshore Technology Conference*. 17945-MS (2006)
33. Md. Mohshin & Mohammad Shahedul Hossain. Pressure Transient Analysis, Reservoir Parameters Estimation and Modeling of Kailashtilla Gas Field (Well no: 4). *North Africa Technical Conference and Exhibition*. 150685-MS (2012)
34. Meisam Ashraf, Knut-Andreas Lie, Halvor M. Nilsen, Jan M. Nordbotten & Arne Skorstad. Impact Of Geological Heterogeneity On Early-Stage CO<sub>2</sub> Plume Migration. *International Conference on Water Resources CMWR 2010*
35. M. M. Kamal. The Use of Pressure To Describe Transients Reservoir Heterogeneity. *Journal of Petroleum Technology* (1979)
36. M.M. Kamal. Interference and Pulse Testing-A Review. *Journal of Petroleum Technology* (December 1983)

37. M.M. Kamal, Y. Pan, J.L. Landa & O.O. Thomas. Numerical Well Testing: A Method To Use Transient Testing Results in Reservoir Simulation. *SPE Annual Technical Conference and Exhibition*. 95905-MS (2005)
38. Monitoring Techniques for the Validation Phase Michigan Carbon Dioxide Storage Field Demonstration. *Midwest Regional Carbon Sequestration Partnership* (2010)
39. M. Sengul. CO<sub>2</sub> Sequestration - A Safe Transition Technology. *SPE International Health, Safety & Environment Conference*. 98617-MS (2006)
40. Neil Davis, Fred Riddiford, Clive Bishop, Brian Taylor & Rachid Froukhi. The In Salah Gas Project, Central Algeria: Bringing an Eight Field Gas Development to Sanction. *SPE Middle East Oil Show*. 68180-MS (2011)
41. Philip S. Ringrose, David M. Roberts, Catherine M. Gibson-Poole, Clare Bond, Ruth Wightman, Mark Taylor, Sue Raikes, Martin Iding & Svend Østmo. Characterisation of the Krechba CO<sub>2</sub> storage site: critical elements controlling injection performance
42. P.K. Neog & N.M. Borah. Reservoir Characterization Through Well Test Analysis Assists in Reservoir Simulation - A Case Study. *SPE Asia Pacific Oil and Gas Conference and Exhibition*. 64447-MS (2000)
43. Quanlin Zhou, Jens T. Birkholzer, Edward Mehnert, Yu-Feng Lin & Keni Zhang. Modeling Basin- and Plume-Scale Processes of CO<sub>2</sub> Storage for Full-Scale Deployment. Vol. 48, No. 4-GROUND WATER (2010)



44. Ralf Schulze-Riegert & Shawket Ghedan. Modern Techniques for History Matching. *International Forum On Reservoir Simulation* (2007)
45. R. Cramer, C. Moncur, & L. Berendschot. Well Test Optimization and Automation. *Intelligent Energy Conference and Exhibition*. 99971-MS (2006)
46. Richard Baker. Streamline Technology: Reservoir History Matching and Forecasting = Its Success, Limitations, and Future. *Journal of Canadian Petroleum Technology* (2001)
47. R.K. Sagar, M.G. Kelkar & L.G. Thompson. Reservoir Description by Integrating Well-Test Data and Spatial Statistics. *SPE Formation Evaluation*. Journal Paper 26462-PA (1995)
48. Sally M. Benson & David R. Cole. CO<sub>2</sub> Sequestration in Deep Sedimentary Formations.
49. S. Daungkaew, Walailak U., D.J. Prosser, A. Manescu, & M. Morales. An Illustration of the Information that can be Obtained from Pressure Transient Analysis of Wireline Formation Test Data. *SPE Asia Pacific Oil and Gas Conference and Exhibition*. 88560-MS (2004)
50. Seyed Mohammad Shariatipour, G.E. Pickup, E.J. Mackay & N. Heinemann. Flow simulation of CO<sub>2</sub> storage in saline aquifer using a black oil simulator. *Carbon management technology conference*. CMTC 151042 (2012)
51. Skorstad, M.A. Islam & E. Smørgrav. Conditioning on Effective Permeabilities From Well Tests in Geostatistical Reservoir Characterization: Real Test Case Evaluation. *SPE Annual Technical Conference and Exhibition*. 124280-MS (2009)

52. Smart, C.R. & Walter H. The Well-Site Real-Time Formation Pressure Transient Analysis System. *Permian Basin Oil and Gas Recovery Conference*. 17320-MS (1988)
53. S.-Y. Zheng & P. Corbett. Well Testing Best Practice. *SPE Europec/EAGE Annual Conference*. 93984-MS (2005)
54. Takao Nanba & Roland N. Horne. An Improved Regression Algorithm for Automated Well-Test Analysis. *SPE Formation Evaluation*. (1992)
55. T. Babadagli, A. Al-Bemani & K. Al-Shammakhi. Assessment of Permeability Distribution Through Well Test Analysis. *SPE Asia Pacific Oil and Gas Conference and Exhibition*. 68707-MS (2001)
56. V.A. Kuuskraa, G.J. Koperna & K.C. Schepers. CO<sub>2</sub>-Storage Engineering: Real Solutions to Real Problems. *SPE International Conference on CO<sub>2</sub> Capture, Storage, and Utilization*. 139512-MS (2010)
57. Wright I. W., Mathieson A. S., Riddiford F. & Bishop C. In Salah CO<sub>2</sub> Storage JIP: Site Selection, Management, *Field Development Plan and Monitoring Overview*.
58. Xu, G. Weir, L. Paterson, I. Black & S. Sharma. A CO<sub>2</sub>-RICH GAS WELL TEST AND ANALYSES. *Asia Pacific Oil and Gas Conference and Exhibition*. 109294-MS (2007)
59. Yann Le Gallo, Philippe Couillens & Taoufik Manai. CO<sub>2</sub> Sequestration in Depleted Oil or Gas Reservoirs. *SPE International Conference on Health, Safety and Environment in Oil and Gas Exploration and Production*. 74104-MS (2002)

60. Yusuf Pamukcu, Suzanne Hurter, Laurent Jammes, Dat Vu-Hoang & Larry Pekot. Characterizing and Predicting Short Term Performance for the In Salah Krechba Field CCS Joint Industry Project
61. Yousef Ghomian, Mehmet Urun, Gary A. Pope & Kamy Sepehrnoori. Investigation of Economic Incentives for CO<sub>2</sub> Sequestration. *SPE Annual Technical Conference and Exhibition*. 116717-MS (2008)